Ultimate Temperatures and Stabilities of Steel Frames Subjected to Fire

March 2004

Ruangtananurak Nara

Ultimate Temperatures and Stabilities of Steel Frames Subjected to Fire.

Abstract

When fire takes place in a steel frame, any heated column may buckle at some temperature due to deterioration in both the stiffness and the strength, although the external load to the frame remains unchanged during fire. This column's buckling is likely a main cause of the instability for steel frames subjected to fire. Researches on the high temperature buckling of columns span, in fact, for decades. Culver (1973) was the first to analyze precisely the behavior of the buckling of columns by using finite element analysis. Referring to the experimental studies conducted by Burgess et al.(1992), Franssen has recently made a specific comparison between the test and numerical analysis results (1995,1996).

Although the studies on centrally compressed and simply supported columns provide the basic knowledge on the problem, the behaviors of the heated columns incorporated into the frame are different from those of isolated members. In fact, when fire occurs in a steel frame, the expanded and therefore elongated column is axially restrained by the rest of members, so that thermal compressive force is applied additionally to the heated column (Neves, 1995; Correia Rodrigues et al., 2000). As a result, the buckling temperature of the heated column is lowered due to this thermal stress. On the other hand, since the incorporated column is, at the same time, restrained rotationally at its ends by the neighboring members, the effective length of this column should become shorter than the column height and this raises in turn the buckling temperature of the column.

Another facet of the problem is the overall stability of the frame, when and after the incorporated columns buckle due to fire. Some frames may fall into instability directly after the incorporated column buckle, while the other may remain stable and be able to sustain further increase in member temperature. Once the instability takes place, the former frame cannot maintain static equilibrium any more. This means that, to solve the problem, ordinary *load controlled analysi*s is not applicable in this case, but we need to develop another new numerical method to analyze the unstable frames. For the latter stable frames with heated and buckled columns, on the other hand, stress redistribution capacity of the neighboring members may play an essential role on controlling their ultimate states. Therefore, to clarify the structural performances of the frames with heated and buckled

columns, a special emphasis must be placed on their stabilities as well as their ultimate load carrying characteristics when and after several heated columns buckle. The adopted analysis method must be able to trace these natures of the problem accordingly.

In view of the above observations, the main objectives of this study are to be set as follows:

1. To understand and to clarify the mechanics which control the overall stabilities of steel frames with heated and buckled columns.
2. To develop a numerical analysis program that can solve such stability problems of steel frames subjected to fire.
3. To clarify the buckling temperatures of the incorporated columns as well as the frame's ultimate temperatures.
4. To find the actual ultimate states and the corresponding ultimate temperatures of steel frames subjected to fire.
5. To find the means to prevent the frames subjected to fire from instability.

In order to achieve the above presented objectives, this dissertation is divided into five chapters, which are briefly described below.

Chapter one starts with brief review of previous studies. Fire resistant design of steel structures is reviewed in many relevant aspects, the experimental tests, and numerical analysis. After that, the problem about instability in steel structure that occurred in the collapse of WTC Towers is summarized. This is considered an indispensable background for conceiving the objective of this study, which constitutes the above sections.

In chapter 2, the stabilities and the ultimate behaviors of steel frames after the incorporated heated columns buckle are investigated extensively. If the surrounding members can redistribute the vertical load of the frame which has been carried by the buckled column, it may retain the stability and may not collapse immediately. On the contrary, when the surrounding members are weak, an overall frame will fall into instability directly due to column buckling. This chapter describes and discusses these problems specifically. Furthermore, in this chapter, the development of the numerical analysis method is described specifically, which can simulate both the stable and unstable behaviors of steel frames subjected to fire.

The development is focused on the computational procedure to simulate an unstable and therefore actually a dynamic frame behavior purely by a static means. At the end of this chapter, example numerical solutions solved by the method developed are shown, where complete fire responses and realistic ultimate states due to fire of steel frames are illustrated and discussed extensively.

By using the numerical method whereby the control of the analysis is switched between load and displacement methods, we can examine the behavior of the steel column subjected to fire until it overall collapses. The *load controlled analysis* is the increase-in-temperature method. While the displacement analysis is the analysis that one degree-of-freedom of the unstable member's node is gripped, and it is moved in the direction that the unstable state is growing. The displacement analysis is carried out under the temperature that the structure loses its stability. By using this analysis method to analyze some examples of a steel structure subjected to fire, the following conclusions can be drawn:

● The main unstable condition of a steel structure subjected to fire is the "*snap-through*" process. This snap-through easily occurs in the structure when the post-buckling residual force is low and the stiffness and the strength of the restraining members in the structure are low. That means that the structure's ability to remain stable while the surrounding members restrain the buckling column is intimately connected with the instabilities of the structure itself.

● The collapse of the structure is not decided solely by the buckling of the heated column. The ultimate temperature of the structure's collapse mode varies according to the stress redistribution ability of the surrounding members. If the stress redistribution ability of the surrounding members is low, the structure loses its stability and collapses suddenly after the column buckles. In this case, the ultimate temperature of this kind of structure is lower than the column buckling temperature due to the thermal stress. However, if the stress redistribution ability of the surrounding members is high, the structure still keeps its stability even though the column buckles. The ultimate temperature of this kind of structure is more than the column buckling temperature.

The third chapter clarifies specifically the buckling temperatures of steel columns incorporated into frames. The buckling temperature is defined as the one at which a column begins to show an apparent buckling deformation. The incorporated columns are restrained rotationally by the adjacent members when they buckle. Therefore the effective buckling length of the column is shorter than its

height. In this chapter, simple closed form formulae are presented to estimate both the effective buckling length and the buckling temperature of an incorporated heated column. Finally, comparisons are made between the numerically solved buckling temperatures of incorporated columns and the corresponding theoretical predictions, and the accuracy and the applicability of the formula are discussed in detail.

From the investigated results, the following conclusions can be drawn:

● The rotationally restraining effect of the connecting members has an effect on the column's buckling temperature. However, the thermal expansion of the beam does not have a direct affect on the buckling temperature.

● The exterior column is not axially restrained by the adjacent members during the fire. The lower end of the heated column is rotationally restrained by the unheated connecting members, so its boundary condition can be assumed to be fixed end. On the other hand, for the upper end of the heated column's case, the rotationally restraining effect of the upper-story unheated column can be neglected due to the thermal expansion of the beam. The buckling temperature of the exterior column can be assumed to be the theoretical buckling temperature when the effective length is determined from the proposed equation.

● The interior column is strongly rotationally restrained by the adjacent members, so its effective length is equal to $0.5h$. However, it is also axially restrained by the adjacent members. As a result it buckles at a temperature that is lower than the estimated buckling temperature. In this case, when considering the buckling temperature, the thermal effect should be included.

An incorporated column is not only restrained rotationally as discussed in the previous chapter but, if it is heated, it is also restrained axially by the surrounding members. Chapter 4 clarifies the latter problems specifically. The axial restraint of the surrounding members plays two contrary roles on the stability action of the frame. Firstly, it adds axial compressive force to the incorporated column and so increased compressive force lowers the column's buckling temperature. On the contrary, once the column buckles, the surrounding members turn to work so as to redistribute a part of the axial compressive force carried by the bucked column to other sound columns, which is therefore helps to strengthen the overall stability and to raise the ultimate temperature of the frame. This is called herein stress redistribution effect of the surrounding members. In this chapter, the lowering of the column's buckling temperature and the raise of the frame's ultimate

temperature, which are both brought by the effects of the surrounding members, are formulated respectively in theoretical closed forms. Finally the numerical analysis, which are developed in Chapter 2, are conducted extensively to obtain the realistic column's buckling and the frame's ultimate temperatures of a lot of practical steel frames, which are used to verify the accuracy and the applicability of the above derived formulae. In this chapter, the following conclusions can be drawn:

● The effects of the axially restraining members have two mechanical roles. The first role is to restrain an expanded heated column. As a result of this action, the thermal compressive force is added to the heated column. This causes a drop in buckling temperature of heated columns. On the contrary, the second role is to redistribute a part of the compressive force of the buckled column to other sound columns. As a result of this action, the structure can retain its stability after the column buckles. It causes a rise of the ultimate temperature of a frame. However, if the second stress redistribution ability is not enough, it falls into instability immediately after the heated column buckles. The ultimate temperature for this frame is lower than the theoretical buckling temperature, since the buckling is affected by the first thermal effect.

● Based on the above observation, it is found that a higher ultimate temperature of a frame is obtained if it has higher stress redistribution capacity. A way to improve the fire-resistance capacity of a frame is to install a suitably proportioned hat truss. A hatted frame is found to have definitely an improved redundancy.

● Closed form formulae to predict both the buckling temperature of a heated column and the beam plastified temperature of a frame is presented herein. Conducting the numerical fire response analysis, the predicted temperatures are found to be in good agreement with the numerical results for various structural and heating conditions. The prediction to estimate the improved ultimate temperature of hatted frames is also proposed herein.

In chapter 5, the conclusion of this thesis is drawn:

● The "*snap-through*" phenomenon is the main unstable condition of steel structures subjected to fire. This snap-through easily occurs in the structure when the post-buckling residual force is low and the stiffness and the strength of the restraining members in the structure are low.

● The column's buckling temperature can be estimated by the theoretical buckling temperature when the effective length is determined from the proposed equation. The exterior column's effective length ratio can be calculated from the proposed equation while the interior column's effective length ratio is 0.5.

● In the case that the stress redistribution ability is not enough to retain the stability of the steel frame, the structure falls into the instability state and failure at the buckling temperature under thermal effect. It means the ultimate temperature of that structure is lower than the theoretical buckling temperature. However, in the case that the stress redistribution ability is high, a part of the compressive force of the buckled column is redistributed to other sound columns. As a result the structure can retain its stability after the column buckles.

● The ultimate temperature can be determined by the higher temperature among the bucking temperature under thermal effect and the beam plastified temperature.

● A way to improve the fire-resistance capacity of a steel frame is to increase the redundancy of the axial force to the steel frame.

CONTENTS

Chapter 1

Introduction

1. Introduction

1.1 Brief review of previous studies

1.1.1 Fire resistant design of steel structures

The vulnerability of an unprotected steel structure subjected to fire is deterioration in its material properties. For the ordinary JIS SS400 steel, its strength begins to drop when the temperature reaches 400oC, and loses almost its strength when the temperature is over 800oC (A.I.J, 1999). Furthermore, the thermal force in a restrained heated member is also one of other important problems that should not be missed for investigation by structural designers.

In the past 30 years, the studies about fire resistance of steel structures have rapidly progressed. In 1973, analytical and experimental studies were carried out by Culver et al. on buckling of steel columns under elevated temperatures. However, at that time, they faced significant problems on cost and safety to conduct full-scale experimental works under high temperatures. Thus the models of simply supported columns were experimentally investigated (Stanzak, 1973; Seigel, 1974; Barthelemy, 1976; Kruppa, 1979), but the fire tests on full scale structures could not be carried out in the 1970s.

Alternatively, the fire resistance of structural members was obtained using analytical approaches. Cheng and Mark (1975) proposed an analytical method for the investigation of steel frames at elevated temperatures. In this numerical method, material nonlinearity at elevated temperatures and geometric nonlinearity resulting from large deflections are both considered. In Japan, the numerical studies were first made by Furumura of single-storied and single-spanned steel frames under fire (1981). Furthermore, Furumura et al. (1986) proposed refined stress-strain formulae of structural steel (JIS SS400 and JIS SM490) at elevated temperatures. These formulae are still adopted in many recent researches in Japan.

The Japanese Building Standard Law had prescribed that, to design buildings against fire, surface of steel must not exceed the allowable temperature 350oC during fire. According to this standard, fire protection must be used to keep steel temperatures equal to, or less than this allowable temperature. However, fire protection is vulnerable in that it adds substantially cost of construction as well as length of construction term and it reduces usable interior space.

With rapid advancement of computer technology in the mid-1980s, the

behaviors of multi-storied steel frames have been analyzed by many researchers (Cheat, 1984; Furumura, 1986). From these analyzed results, it has come to be clear that local plastification of individual members never leads to an ultimate collapse of an entire frame. Furthermore, an entire frame remains stable and sustains further developing fire, although the temperature reaches the allowable 350oC prescribed by the Law.

Suzuki (1995) proposed a method to assess the failure temperature of the steel frame based on the simple plastic theory. This predicted failure temperature is the one when a heated part of the frame inside a fire compartment forms a collapse mechanism. In addition, from the study of the effect of creep strain by Suzuki et al. (1992), it was found that the creep strain does not have significant effect on the failure temperature. This indicates that the failure temperature is not time dependent. By comparing the predicted ultimate temperatures with 2-D numerical solutions, the prediction is found accurate in many practical cases of steel frames. However, there are several causes that lower the failure temperature below the above prediction. Flexural or local buckling of heated columns is among such causes. These problems have also been investigated by Suzuki et al.

1.1.2 Problems presented by collapse of the WTC towers

On September 11, 2001, the world was shocked by an atrocity in USA. The two hijacked jetliners were deliberately flown into New York World Trade Center towers (also known as WTC1 and WTC2). Due to this attack, many exterior wall frames and interior columns were destroyed resulting in the overall collapse of the two towers. Several hours later after both towers collapsed, WTC7 also started to fall down and collapsed completely in a short time.

There have been numerous studies (FEMA, 2002; Bazant and Zhou 2002; Usmani et all, 2003.) attempting to explain the collapse since the event. One of the earliest significant works was the study of Bazant and Zhou (2002). In this work, the authors restrict themselves to explain the progressive collapse of the whole structure caused by dynamic overloads from the falling superstructures as a rigid body, once the instability that made the superstructure mobile had already occurred. The analysis is interesting as it shows clearly that once this point is reached, the dynamic overloads will lead to complete collapse. However, the collapse of the WTC1 and WTC2 is the special case of the collapse of the steel structure subjected to fire.

It is because the WTC towers got severely damage due to the attack of the aircraft.

The downward progressive collapse, or pancaking, of the buildings has drawn great attention from scholars. However, it is important that the upward spread of failure which was initiated from the first damaged floors and might be preceding the pancaking must not be neglected. Temperature increase due to intense and/or long lasting fire causes losses of both elastic moduli and strengths of materials and therefore buckling of columns. After buckling of the several columns, if it takes place, the entire frame is highly susceptible to instantaneous upward spreading of failure and therefore to falling into global frame instability. We found sink of the penthouses and kink of the frame on the roof level of WTC7 as shown in Fig. 1.1.1 (FEMA, 2002). Such sink and kink seemed to stem from the far lower floors where fire had long lasted. Buckling and subsequent shortening of several columns or failure of some members carrying vertical load there might have caused partial sinking of all the upper floors resulting in the apparent anomalies of the roof level. After we had seen them, WTC7 soon fell down abruptly and completely as shown in Fig. 1.1.2.

The case of WTC7 is important from the viewpoints of fire resistance engineering, since WTC7 suffered no serious structural damages by the plane attacks but it seemed to collapse primarily due to long lasting fire. From the collapse of WTC7, it can be learned that the extensive failure of interior structural elements leads to the collapse of the overall structure. Moreover, the adequacy of current fire resistance design provisions for the steel structure should also be investigated. However, the bigger and much more important questions for the structural engineering and the fire-resistance engineering are “what led to the instability that initiated the collapse in the first place?” and “how is the structure prevented from this instability process?” There have been fewer attempts to tackle these crucial questions.

Fig. 1.1.1 view from the north of the "kink" or fault developing in WTC7

Fig. 1.1.2 The overall collapse of WTC7

1.1.3 The study about buckling column and stability of steel frames

When fire takes place in a steel frame, any heated column may buckle at some temperature due to deterioration in both the stiffness and the strength, although the external load to the frame remains unchanged during fire. This column's buckling is likely a main cause of the instability for steel frames subjected to fire. Researches on high temperature buckling of columns span, in fact, for decades. Culver (1973) was the first to analyze precisely the behavior of buckling of columns by using finite element analysis. Referring to the experimental studies conducted by Burgess et al.(1992), Franssen has recently made a comparison between the test and numerical analysis results (1995,1996). In Japan, Full-scale tests of steel columns were carried out by Motegi et al. (2000). The 24 specimens of JIS SN400B and SS400 were tested under elevated temperatures .In this research, however, isolated columns were solely examined.

Although the studies on centrally compressed and simply supported columns provide the basic knowledge on the problem, the behaviors of heated columns incorporated into a frame are different from those of isolated members. In fact, when fire occurs in a steel frame, the expanded and therefore elongated column is axially restrained by the rest of members, so that thermal compressive force is induced additionally to the heated column (Neves, 1995; Correia Rodrigues et al., 2000). As a result, the buckling temperature of a heated column is lowered due to this thermal stress. On the other hand, since the incorporated column is, at the same time, restrained rotationally at its ends by the neighboring members, the effective length of this column should become shorter than the column height and this raises in turn the buckling temperature of the column.

This problem has been studied both experimentally and the numerically. A total of 20 tests on steel columns were conducted by Aasen (1985). A specimens were tested using three different support conditions; i.e. unrestrained, rotationally restrained, and axially restrained. The test results show that the axial restraint induces the thermal force as the columns tend to expand, and the failure temperature of the heated column decreases due to this axial restraint. However, since the incorporated column is at the same time restrained rotationally at both ends, this effect in turn makes the column buckling temperature greater than that of the simply supported column. Poh (1995) developed 3-D numerical method to investigate the behavior of axially and rotationally restrained columns under ununiform member temperature distribution.

As for the stability of steel frames subjected to fire, Franssen (2000) has studied numerically buckling of a heated steel column connected by an adjacent member. From the numerical results, he pointed out that, after the heated column buckles, a part of the load that has been formerly supported by this column will be transmitted to the adjacent member, so that the column can retain its stability subsequently after it buckles.

As described above, up till now, the behaviors of the buckling of heated columns have been studied extensively; however, Neither the overall stabilities nor the actual ultimate state of entire steel frames subjected to fire have been studied at all. The collapse of WTC buildings tells us that both the importance and the urgency to solve the problems above are quite high.

1.2 Objective of this study

When a fire occurs in a steel frame, heated members will lose their strength and stiffness. After heated columns buckle, they lose the axial load carrying capacities somewhat or extremely depending on their structural conditions. The problem is the overall stability of the frame, when and after the incorporated columns buckle due to fire. Some frames may fall into instability directly after the incorporated column buckle, while the other may remain stable and be able to sustain further increase in member temperature. Once the instability takes place, the former frame cannot maintain static equilibrium any more. This means that, to solve the problem analytically, ordinary load control analysis is not applicable in this case, but we need to develop another new numerical method to analyze the unstable frames. For the latter stable frames with heated and buckled columns, on the other hand, stress redistribution capacity of the neighboring members may play an essential role on controlling their ultimate states. Therefore, to clarify the structural performances of the frames with heated and buckled columns, a special emphasis must be placed on their stabilities as well as their ultimate load carrying characteristics when and after several heated columns buckle. The analysis method to be adopted must be able to trace these natures of the problem accordingly.

In view of the above observations, the main objectives of this study are to be set as follows:

1. To understand and to clarify the mechanics which control the overall stabilities of steel frames with heated and buckled columns.

2. To develop a numerical analysis program that can solve such stability problems of steel frames subjected to fire.
3. To clarify the buckling temperatures of incorporated columns as well as frame's ultimate temperatures.
4. To find the actual ultimate states and the corresponding ultimate temperatures of steel frames subjected to fire.
5. To find the means to prevent frames subjected to fire from instability.

1.3 Organization of the study

In order to achieve the above presented objectives, this dissertation is divided into five chapters, which are briefly described below.

Chapter one starts with brief review of previous studies. Fire resistant design of steel structures is reviewed in many relevant aspects, the experimental tests, and numerical analysis. After that, the instability problems that occurred in the collapse of WTC Towers are summarized. This is considered an indispensable background for conceiving the objective of this study, which constitutes the above sections.

In chapter 2, the stabilities and the ultimate behaviors of steel frames after the incorporated heated columns buckle are investigated extensively. If the surrounding members can redistribute the vertical load of the frame which has been carried by the buckled column, it may retain the stability and may not collapse immediately. On the contrary, when the surrounding members are weak, an overall frame will fall into instability directly due to column buckling. This chapter describes and discusses these problems specifically. Furthermore, in this chapter, the development of the numerical analysis method is described in detail, which can simulate both the stable and unstable behaviors of steel frames subjected to fire. The development is focused on the computational procedure to simulate unstable and therefore actually dynamic frame behavior purely by static means. At the end of this chapter, example numerical solutions solved by the method developed are shown, where complete fire responses and realistic ultimate states due to fire of steel frames are illustrated and discussed extensively.

The third chapter clarifies specifically the buckling temperatures of steel columns incorporated into frames. The buckling temperature is defined as the one at which a column begins to show an apparent buckling deformation. The incorporated columns are restrained rotationally by the adjacent members when they buckle. Therefore the effective buckling length of the column is shorter than its

height. In this chapter, simple closed form formulae are presented to estimate both the effective buckling length and the buckling temperature of an incorporated heated column. Finally, comparisons are made between the numerically solved buckling temperatures of incorporated columns and the corresponding theoretical predictions, and the accuracy and the applicability of the formulae are discussed in detail.

An incorporated column is not only restrained rotationally as discussed in the previous chapter but, if it is heated, it is also restrained axially by the surrounding members. Chapter 4 clarifies the latter problems specifically. The axial restraint of the surrounding members plays two contrary roles on the stability action of the frame. Firstly, it adds axial compressive force to the incorporated column and so increased compressive force lowers the column's buckling temperature. On the contrary, once the column buckles, the surrounding members turn to work so as to redistribute a part of the axial compressive force carried by the bucked column to other sound columns, which is therefore helps to strengthen the overall stability and to raise the ultimate temperature of the frame. This is called herein stress redistribution effect of the surrounding members. In this chapter, the lowering of the column's buckling temperature and the raise of the frame's ultimate temperature, which are both brought by the effects of the surrounding members, are formulated respectively in theoretical closed forms. Finally the numerical analysis, which are developed in Chapter 2, are conducted extensively to obtain the realistic column's buckling and the frame's ultimate temperatures of a lot of practical steel frames, which are used to verify the accuracy and the applicability of the above derived formulae.

Chapter 5 is the conclusion of this thesis.

Chapter 2

Stability of locally heated steel frames under fire

2. Stability of locally heated steel frames under fire

2.1 Introduction

When fire occurs in a steel-framed structure, heated columns will lose their elastic moduli and strengths of materials, and finally buckle. Column buckling at elevated temperatures is one of the most important modes of collapse for steel frames subjected to fire. In modern fire resistance designs of steel-framed structures, buckling temperatures of columns have come to be specified explicitly as one of the design limits. In Japan, AIJ (1999) has recommended a formula for the buckling temperatures of steel columns. Revised Japanese Building Standard Law has specified an equivalent notification (2000). These critical temperatures have been determined and formulated with respect to heated individual columns.

However, in an ordinary rigidly jointed steel frame such as shown in Fig.2.1.1, buckling of a heated individual column does not necessarily lead to an overall collapse of the structure. It is possible that, after the heated column has buckled and its strength has deteriorated, a part of the load which has formerly been carried by the buckled column could now be redistributed to other sound load carrying elements with the help of the surrounding beams, if the beams have enough stiffnesses and strengths to do so. In such cases, although the frame moves appreciably to a different position of equilibrium due to column buckling, it does not necessarily indicate that the frame loses stability. To analyze the fire response of the structure under stable process, the frame is subjected to constant overall load and increasing member temperature. This fire analysis is called *load controlled analysis*. This *load controlled analysis* is continued as far as the structure can retain its stability.

On the other hand, if the surrounding beams and other load carrying elements are less stiff or weaker, the frame now becomes highly susceptible to an overall structural instability due to column buckling. In this case, the *load controlled analysis* cannot trace the fire response of the structure beyond its instability point. In order to solve this problem, the *displacement controlled analysis* is adopted in this study. This *displacement controlled analysis* is the analysis that one degree-of-freedom of the unstable member's node is gripped, and it is moved in the direction that the unstable deformation is growing. The *displacement controlled analysis* is carried out under the suspended member temperature at which the structure loses its stability.

In this chapter, a theoretical study will first be made on the stabilities and overall behaviors of simple steel frame models after the incorporated heated columns buckle. Three stable and unstable processes will be identified on the behavior of the model frame; i.e. stable process of the frame with an elastic beam, unstable one with an inelastic beam, and unstable one with an inelastic beam.

A new procedure will next be developed and incorporated into the existing nonlinear finite element analysis code which enables one to analyze all stable, unstable and ultimate behaviors of frames subjected to fire. This is called the *Alternate Control Method* of analysis whereby the control is switched between load and displacement depending on the frame's stable and unstable processes, respectively.

In the end of this chapter, two numerical examples solved by this method will be shown to illustrate the full behavior from beginning of heating to final overall collapse of steel frames subjected to fire.

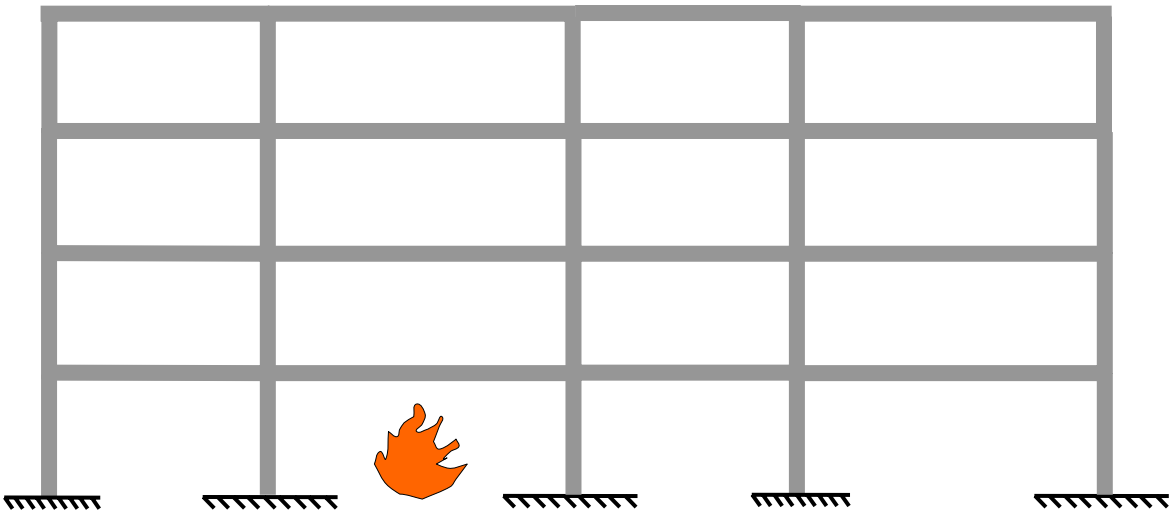

Fig.2.1.1 A steel frame subjected to fire

2.2 The buckling temperature of steel columns

When subjected to fire, an unprotected steel structure will lose its stiffness and strength as a result of deterioration in its material properties. The Stress-Strain relationships of heated JIS SS400 steel are shown in Fig. 2.2.1 (Furumura et al., 1986; Suzuki, 1995; Suzuki and Nakagawa, 2000). These were obtained from coupon tests under various constant steel temperatures.

As seen in the figure, the strength of the steel starts to decrease when the temperature is more than 400oC; it weakens to half of its strength under room temperature when the temperature reaches 600oC. At 800oC, the strength of the heated steel falls to around 1/10 of the strength at room temperature. Reductions in both tangent modulus and strength of the heated material occur according to the compressive strengths of the steel columns under high temperatures, since the buckling strength of a uniformly heated column may be evaluated by the following theoretical formula.

$$\lambda_e^2 = \frac{\pi^2 E_t\left(T_{cr}, \bar{p}\bar{\sigma}_y\right)}{\bar{p}\bar{\sigma}_y} \qquad (2.2.1)$$

This equation demonstrates the relation between the effective slenderness factor λ_e, the existing compressive stress $\bar{p}\bar{\sigma}_y$, and the critical member temperature T_{cr} of a column, where $\bar{\sigma}_y$ is the yield stress at room temperature of the material. $E_t(T_{cr}, \bar{p}\bar{\sigma}_y)$ expresses the tangent modulus of the material subject to the stress $\bar{p}\bar{\sigma}_y$ at temperature T_{cr}. $\bar{p}$ is the ratio of applied compressive force to the column to its yield strength and is referred to hereafter as *axial force ratio.*

Figure 2.2.2 illustrates the theoretical buckling temperatures of columns with various slenderness factors and subject to various compressions, which is obtained by applying Eq. (2.2.1) to columns made of the same material as shown in Fig. 2.2.1. From the figure we can see that the buckling temperature of the heated column can be easily determined when the effective slenderness ratio λ_e of the column and the axial load ratio acting on the column are known. (A curve in Fig. 2.2.2 will be used in later discussion). However, to determine precisely the buckling temperature by this tangent modulus method, we need to know the accurate effective slenderness ratio of columns for under various structural and heating conditions. This problem will be studied in detail in the next chapter.

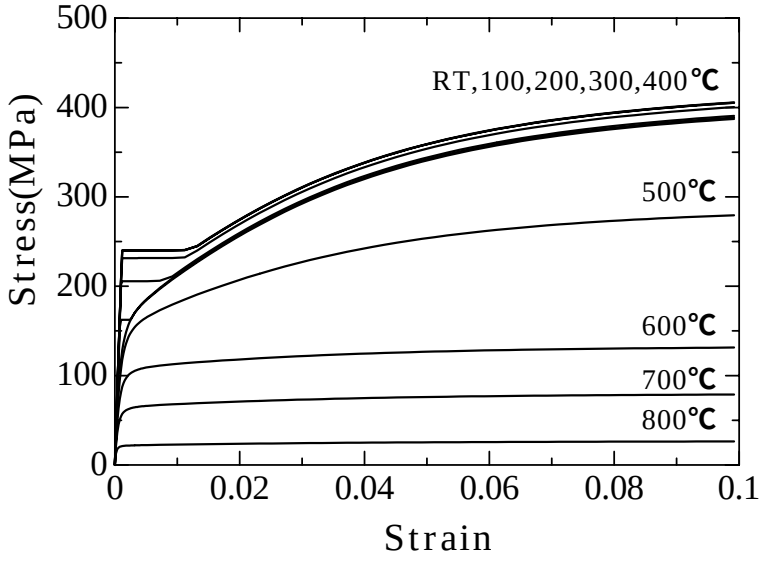

Fig. 2.2.1 Stress-Strain relationships of JIS SS400 steel under various member temperatures.

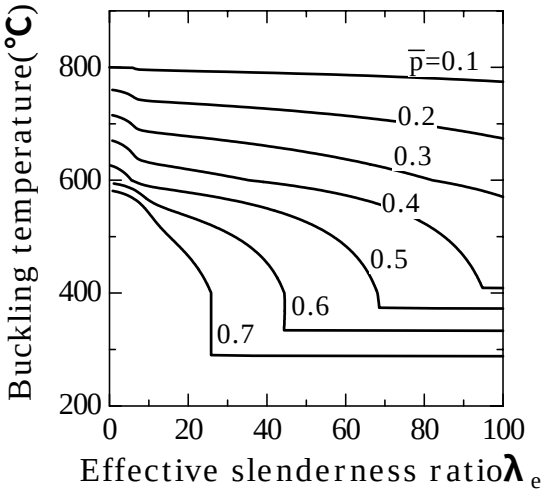

Fig. 2.2.2 Buckling temperatures of SS400 steel columns.

2.3 Schematic view of the unstable behavior of a locally heated steel frame

To study what happens to a frame after a constituent column buckles, a simple model frame shown in Fig. (2.3.1) was proposed. The model frame is a single-storied two-spanned steel frame. The interior column is to be heated uniformly, while the rigid exterior columns and the elastic beam are kept at room temperature. Pin supports at both ends are assumed at the interior column for brevity. As shown in the figure, the interior column is to carry the weight with mass M, whose downward displacement is denoted by x (positive). The resisting force of the beam supporting the mass is denoted by $Q(x)$. When the temperature is increased, the heated interior column expands longitudinally due to thermal expansion. Therefore, the net contraction of the height of the heated interior column is $x + \alpha hT$, where α is the material's coefficient of the thermal expansion, while T and h are the temperature and the initial length of the interior column, respectively. The axial force N represents the pre-post buckling resistance of the column. This axial force is a function of the net contraction of the height of the interior column. So the equation representing the motion of the mass M is expressed as follows:

$$M\ddot{x} = Mg - Q(x) - N(x + h\alpha T) \tag{2.3.1}$$

The dot on a variable represents its time derivative. The right-hand side of Eq. (2.3.1) is the downward resulting force acting on the mass (see Fig 2.3.1(b)), while the resistance of the structure can be represented by $Q(x) + N(x + h\alpha T)$. If the right-hand side of Eq. (2.3.1) is vanished, the model stays in static equilibrium. On the other hand, if this is positive, it means the system falls into the unstable process. So from Eq. (2.3.1), we can explicitly explain the stable-unstable behaviors of a locally heated steel frame.

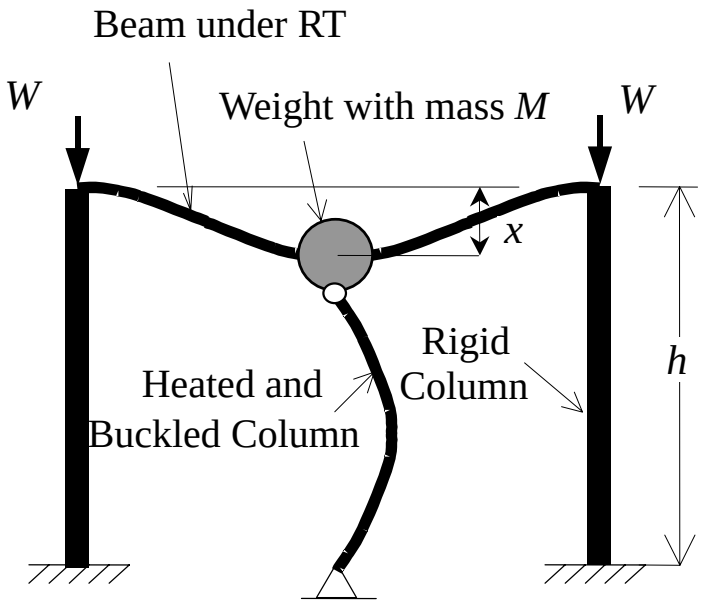

(a) A model frame

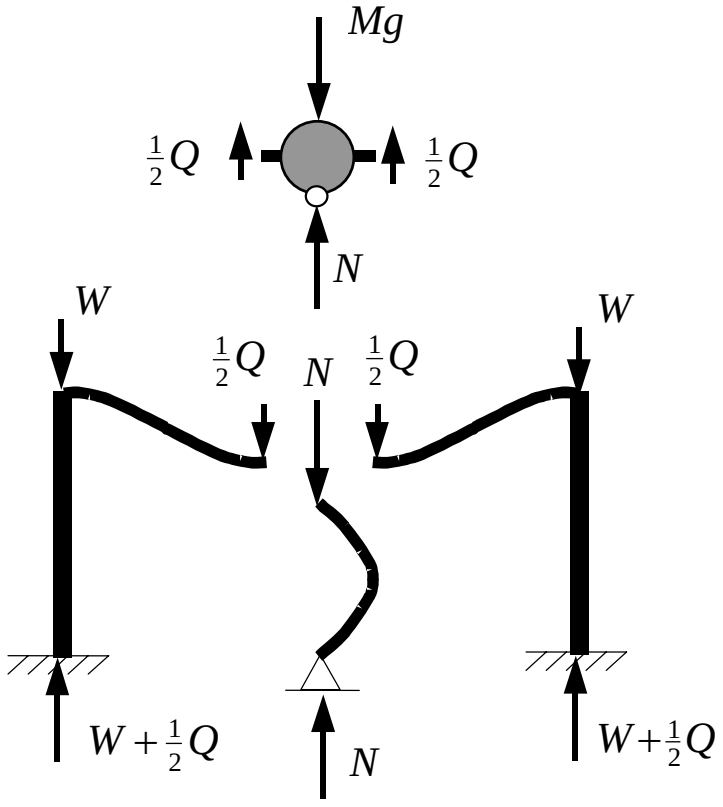

(b) Vertical forces acting on the mass and the individual members

Fig. 2.3.1 A model frame with a heated and buckled column

2.3.1 Stability of the frame with an elastic beam

The relationships of the relevant quantities of Eq. (2.3.1) are depicted in Fig. 2.3.2. The horizontal axis shows the axial deformation of the column, while the vertical axis shows the vertical force acting on the mass. The $N\sim x$ curves in the figure represent the resistances of the interior column under three different constant temperatures: T_1, T_2, and T_3, respectively. We suppose $T_1 > T_2 > T_3$. Because of thermal deformation, the respective curves do not start from the origin. The $N\sim x$ curve of T_3, for example, starts at $x = -\alpha h T_3$, where α is the thermal expansion coefficient of steel. The top of the each curve shows the buckling strength at each temperature. The post buckling behaviors of the column are indicated by the descending parts of the respective curves. The straight line IJ represents the resistance of the beam, assuming it behaves elastically according to $y = -kx + mg$, where k denotes elastic stiffness of the beam. The distance from the horizontal axis to the straight horizontal line XY shows gravitational force of the mass, while the distance from the horizontal axis to the straight line IJ represents the total load acting on the heated column. The equation of equilibrium at state I can be written as the following expression:

$$Mg - kx_1 - N(x_1 + \alpha h T_1) = 0 \qquad (2.3.2)$$

As shown in this equation, the force acting on the heated column, i.e. $Mg - kx_1$ is greater than Mg, since x_1 is negative. The additive $|kx_1|$ occurs due to axial restraint by the spring. This force is called the "*thermal force*". As can be seen, the column strength decreases from the state I and this indicates this column starts to buckle at temperature T_1. However, if the stiffness is very small, $k \approx 0$, this column would buckle at state K on the curve at temperature T_2. As T_2 is greater than T_1, this indicates that the buckling temperature of the heated column decreases due to the axially restrained effect of the spring.

In these cases where the beam and the heated column behave respectively such as shown in the figure, all the forces acting on the mass continue to be in equilibrium after the heated column buckles. The equilibrium at state A for example is represented generically by the following expression:

$$Mg - kx_3 - N(x_3 + \alpha h T_3) = 0 \qquad (2.3.3)$$

This equation indicates that the structure is still stable although the column buckles. The figure illustrates that, as the temperatures increase from $T_1, T_2,$ to T_3, the deformations of the column also increase from x_1, x_2 to x_3 progressively after the heated column buckles. Therefore, for this system, although the column strength deteriorates because of buckling, the system can still retain stability in the process of gradual increase of the temperature of the buckled column. It must however be noted that the displacement of the heated column cannot increase unless the member's temperature increases in the stable process, and therefore the $N \sim x$ curves of each member's temperature exist only at the point where the curved lines intersect with the straight line IJ.

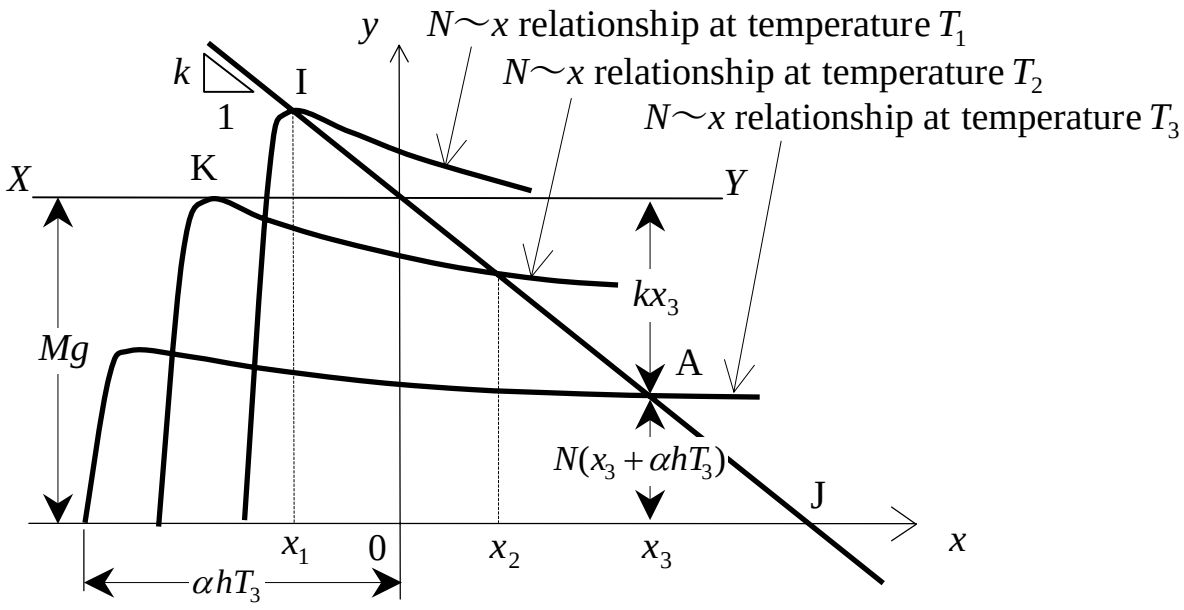

Fig. 2.3.2 Stability of the model with an elastic beam

2.3.2 Instability of the frame with an elastic beam

The figure 2.3.3 shows the behavior of the model frame similar to Fig 2.3.1(b). Similar as before, the beam is assumed to be elastic, and the resistance of this beam is to be represented by the straight line $y = -kx + mg$. However, in this case, one $N \sim x$ curve touches the bottom of the straight line $y = -kx + mg$. Point B at temperature T_4 represents such state in the figure. In explaining the behavior of the system from now on, the temperature of the heated column is assumed to be constant at T_4. Looking at the state U with increasing deformation of the system, the corresponding resistance of the system [$(kx_U + N(x_U + \alpha hT_4))$] does not reach the weight of the mass Mg [i.e. $Mg - kx_U - N(x_U + \alpha hT_4) > 0$]. This indicates that the acceleration of the system cannot be vanished in view of Eq. (2.3.1) and therefore the system must fall into a dynamic state. The term $\ddot{x}$ is positive, so in fact, the column dynamically deforms from state B to state U. That means this system starts to become unstable once the state B is reached. Since the dynamic motion is rapid compared to increase in member temperature, the unstable motion so generated may be performed under the suspended member temperature T_4. This motion continues until the system recovers the static equilibrium at state C. The phenomenon in which the static equilibrium of the system jumps from one state (state B) to another (state C) is known as "*snap-through*" phenomenon. After the motion reaches state C, the system recovers stability and it comes to bear again further increasing member temperatures. The figure illustrates that, when temperature rises to T_5, the column deformation increases from x_5 to x_6.

However, if the beam is not strong enough in the above unstable motion of the system, it may be plastified fully during the dynamic motion. In such cases the system could not recover stability and the system could not bear the temperature beyond the buckling temperature of the heated column.

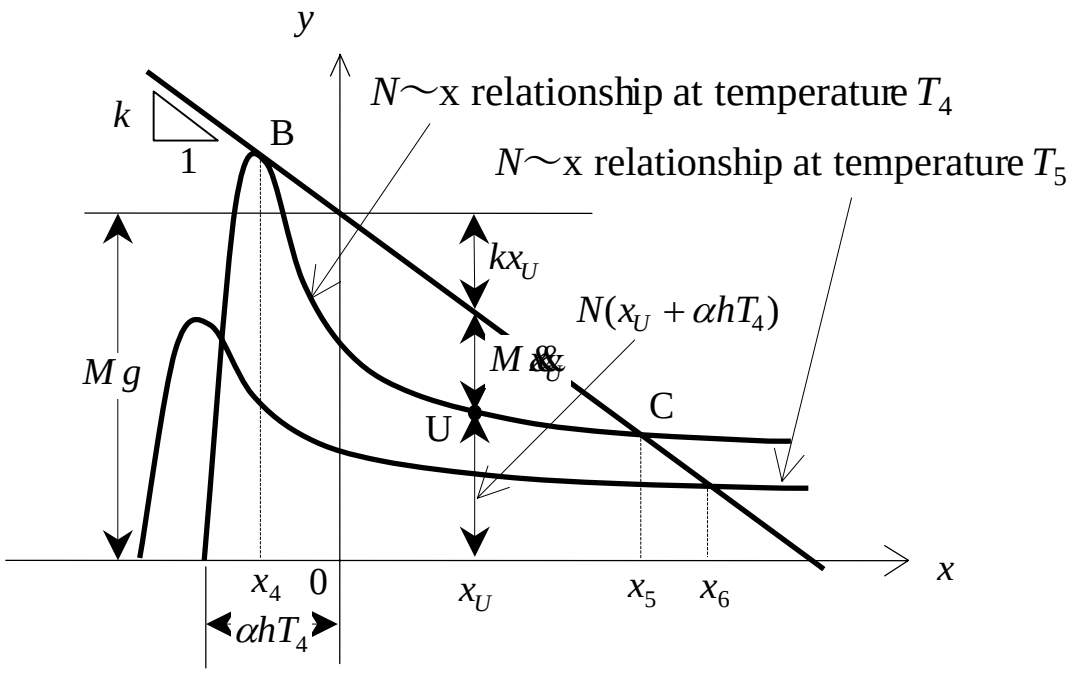

Fig. 2.3.3 The instability of the model with an elastic beam

2.3.3 Instability of the frame with an inelastic beam

As expected from the discussion of section 2.3.2, a frame may more likely fall into instability as the neighboring beam becomes less stiff, or the elastic stiffness k becomes smaller. This implies that any plastification of the beam may increase susceptibility to loss of stability.

The figure 2.3.4 shows a graphical illustration of Eq. (2.3.1) for a frame with an inelastic beam. At state E in the figure, the $N\sim x$ curve of the interior column with temperature T_6 comes in contact with the upper curve DEFG, which defines the resistance $Q(x)$ of the inelastic beam. This indicates that the frame falls into instability at state E exactly due to plastification of the beam, since it would have remained stable if the beam had been kept elastic as shown by the extended dotted line in the figure.

The figure further shows that subsequent gradual hardening of $Q(x)$ helps the frame to recover stability at state G. The hardening may result from the growth of catenary action of the finitely bent beam after initial yielding. Similar as before, such snap-through action as the equilibrium jumps from state E to G takes place in this case also. However, the needed displacement x_8 to recover stability may be too large in this case for practical use.

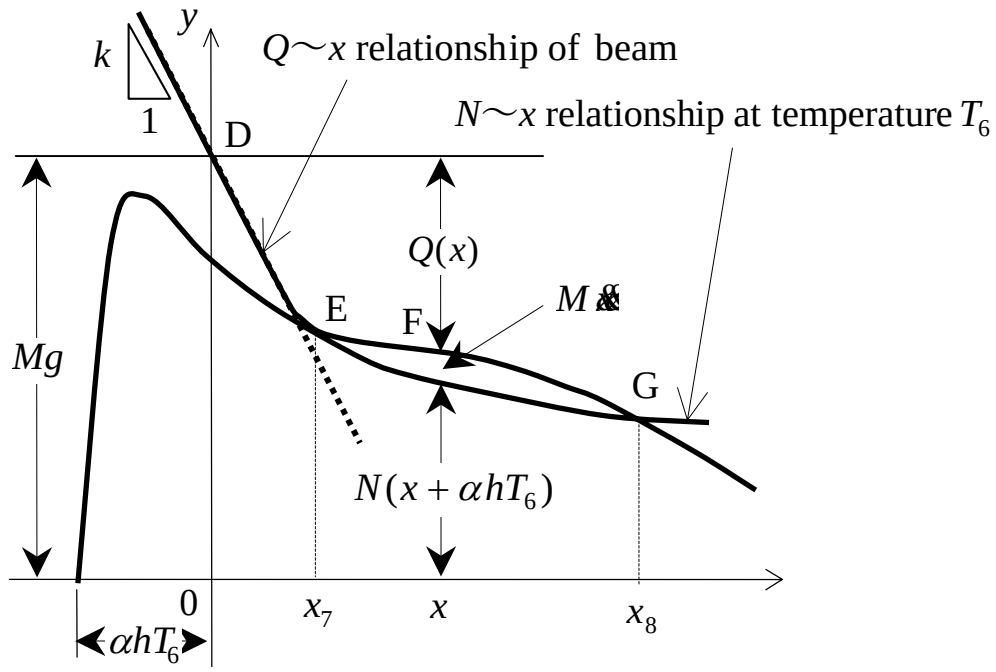

Fig. 2.3.4 The stability of the model with an inelastic beam.

2.3.4 Unstable motion of steel frames from dynamical point of view

In Figures 2.3.3 and 2.3.4, the points C and G are presumably the end point of the unstable motion of the frame from the viewpoint of static. However, taking dynamics in consideration, they are not actual end points of frame's motion, since, at these points, the velocity of the mass still exists. Davies and Neal (1963) studied extensively the dynamical aspects of the "*snap-through*" phenomenon in truss frameworks at room temperature. Based on their study, the dynamic behavior of the "*snap-through*" action is described below for the same heated frame as shown in Fig. 2.3.1(a). The same curves for the heated interior column and the beam as in Fig. 2.3.3 are depicted again respectively in Fig. 2.3.5(a). Point B is the starting point of snap-through action of the frame similar as before. Since the dynamic snap-through action is very rapid, it can be assumed that this action is to be performed under the suspended member temperature.

The energy of the system can be determined by the energy integral of the equation of motion Eq. (2.3.1) as in the following expression:

$$\frac{1}{2}Mv^2 = \int_{x1}^{x}\left[Mg - k\xi - N(\xi + \alpha Th)\right]d\xi \qquad (2.3.4)$$

where x_1 denotes the vertical displacement of the mass at state B, while x and v are the subsequent vertical displacement and the velocity of the mass, respectively.

Equation (2.3.4) expresses the kinetic energy of the mass during the snap-through action. As shown in Fig. 2.3.5(a), this kinetic energy can be represented directly by the area S enclosed by the three lines—the straight line $y = -kx + Mg$, the curved line $N \sim x$, and the vertical line that parallels with y axis and intersects x axis at x. When the displacement x increases, the area S is found to increase if the straight line $y = -kx + Mg$ situates over the curved line $N \sim x$, while it decreases if the line $y = -kx + Mg$ situates below the curve $N \sim x$.

As seen in Fig. 2.3.5(b), the displacement of the mass exceeds point C although the equilibrium of the force is achieved at this point. This is due to the fact that, at point C, the velocity of the mass continues to exist. The velocity of the mass becomes 0 at point D because the velocity of the mass v returns to 0 as the area S reaches 0. However, at point D, the equilibrium of force is now not achieved causing reversal of the direction of motion. The subsequent velocity of the

mass v can be determined by the integral Eq. (2.3.4) in which, in this case, the integral interval begins with the displacement of point D in place of x_1.

As the direction of motion of the mass reverses, the column becomes now unloaded elastically. As a result, the load-displacement relationships of the column change from the curved line $N \sim x$ to the straight line DE as shown in Fig. 2.3.5(c) and the column will deform up to point E where the velocity of the mass becomes 0 again. Then the direction of motion of the mass reverses once more. If the system does not possess damping property, it will vibrate between points D and E harmonically and endlessly. However, due to the fact that there are damping properties in most structures, the motion of the system would finally rest at point F. Therefore, point F is the actual end point of the "*snap-through*" action of the frame. At this point, the frame gets more severely damaged than at state C.

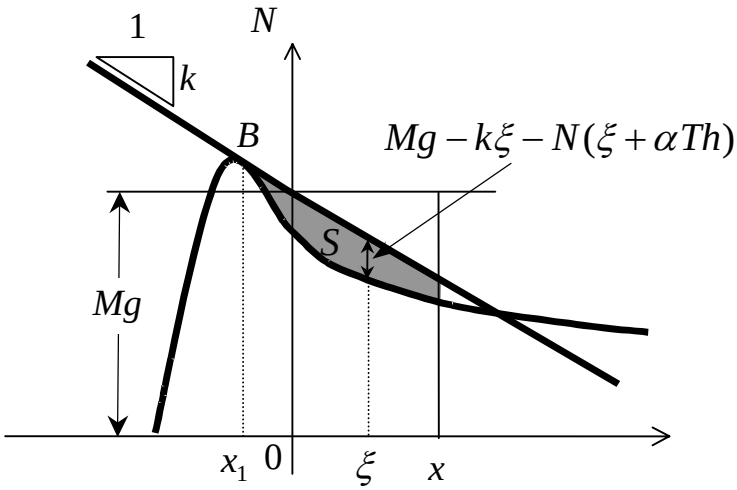

(a) The kinetic energy of the system, when deformed until x, is equal to area S

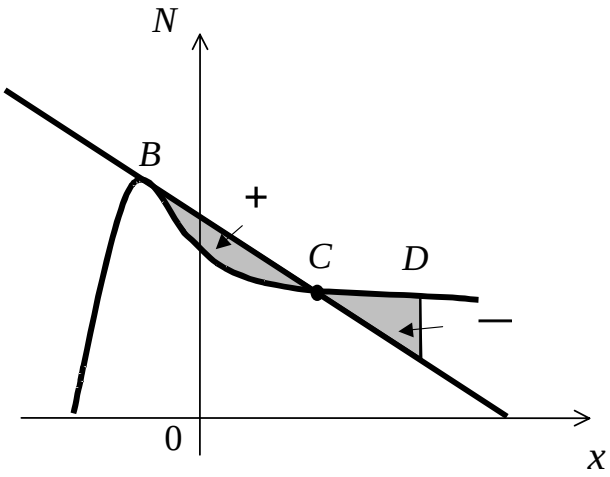

(b) The direction of motion turns back at the point D that the area S becomes 0

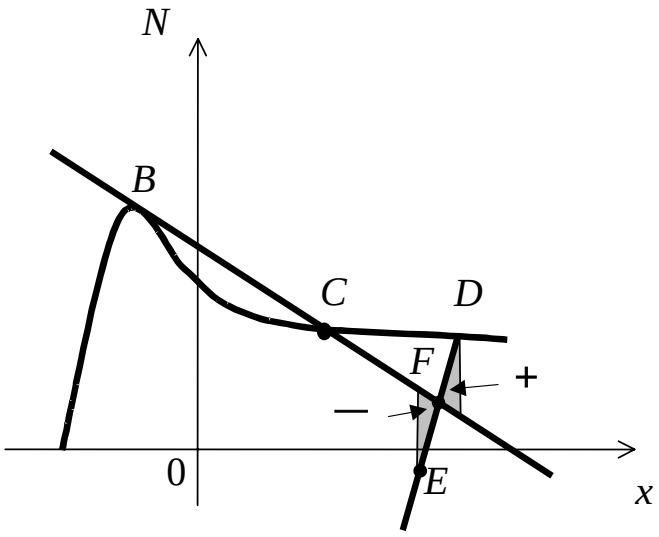

(c) The movement of system ends at the state of point F for the structures have damping properties

Fig. 2.3.5 The actual dynamic behavior of the frame

2.4 Fire response analysis of structures containing unstable processes

This section is intended to develop a numerical solution method that enables one to analyze refined fire responses of steel frames including "*snap-through*" phenomena. The finite element analysis is used to reach this goal.

However, once a heated frame falls into instability, it behaves in fact dynamically. Several studies have in the past been made of analyzing similar instability problems of steel members and steel trusses as actually dynamical problems, all of which are however subjected to ordinary temperatures. In this research, the aforementioned unstable process is treated as a quasi-static process, which is shown at length in the following.

Fire response analysis is usually a *load controlled analysis* which is performed under the condition that the frame is subjected to constant overall load and increasing member temperatures. In fact, the frame behaves almost statically under increasing temperatures as far as it remains stable in the sense of section 2.3.1. According to this fact, it is adequate that this process may be solved with the usual *load controlled analysis*.

In this research, this is the nonlinear finite element analysis which considers material nonlinearities due to elasto-plasticity and thermal expansion of heated steel as well as geometrical nonlinearities due to finite member displacement. The following three basic assumptions are further supposed in the analysis.

1. Only the plannar displacement within the plane of the plannar frame is considered. The members are to deform so that plane sections remains plane.
2. Shear strains are neglected.
3. The member temperature is to distribute uniformly throughout the respective individual members.

The geometrical nonlinearities are evaluated in terms of the Total Lagrangian Formulation. The controlling equations for the discretized system of a frame are derived based on the displacement method of the structural mechanics. Step by step scheme with Newton-Raphson iteration is used to solve the derived nonlinear equations. The recurrent and linearized algebraic equations of the system are expressed in the following matrix form.

$$\left\{\overline{\mathbf{P}}^{t+\Delta t} - \mathbf{P}^{t}\right\} = \left[\mathbf{K}^{t}\right]\{\Delta \mathbf{u}\} \qquad (2.4.1)$$

The terms with the superscript t denote the values at the temperature step of time t, or the approximated solution that was obtained before getting the exact solution. The term with superscript $t+\Delta t$ denotes the quantity that is the exact solution at the temperature step of time $t+\Delta t$ or the next approximated one during iterative procedure. The term with an upper-bar shows the one that has been prescribed or controlled, while the terms with no bar and no superscript is the solution for each temperature step. Thus, $\left\{\overline{\mathbf{P}}^{t+\Delta t}\right\}$ is the external load set for the next step, and is constant over all the temperature steps. $\left\{\mathbf{P}^{t}\right\}$ represents the nodal forces and $\left[\mathbf{K}^{t}\right]$ is the tangent stiffness matrix. $\{\Delta \mathbf{u}\}$ is an unknown in this equation. It is the incremental nodal displacement from time t to time $t+\Delta t$.

Solving this equation, the displacement $\left\{\mathbf{u}^{t+\Delta t}\right\} = \left\{\mathbf{u}^{t}\right\} + \{\Delta \mathbf{u}\}$ can be determined for the given $\left\{\overline{\mathbf{P}}^{t+\Delta t}\right\}$. Next, the stress distribution and the nodal force vector equivalent to this stress field are computed according to the solved displacement field. To get the convergent solution of the next time step $t+\Delta t$, the above procedure may be repeated iteratively until the evaluated $\left\{\mathbf{P}^{t}\right\}$ approaches the given $\left\{\overline{\mathbf{P}}^{t+\Delta t}\right\}$, which indicates the left hand side of Eq.(2.4.1) becomes vanished.

If, in the process of the above *load controlled analysis*, column buckling or some other local instability takes place at a specific member temperature, such numerical difficulty may often be encountered that the member temperature cannot be increased any more subsequently.

This is because, beyond the attained temperature range, the static equilibrated solution does not exist anymore, even if the temperature increment is infinitely small. Mathematically, such loss of equilibrium results from the fact that the stiffness matrix of the system is no longer definitely positive.

Physically, it means that, without lowering the member temperature, no stress distribution which satisfies equilibrium condition can be found at the neighborhood of the attained stress state.

This state is similar to the beginning of the "*snap-through*" action,(i.e, state B as explained in section 2.3.2.) The frame subsequently falls into an unstable mode, and unstable motion would start.

When this state has been reached, at first, the increase of temperature is temporarily suspended at the temperature at which the unstable state occurs.

Next, one degree-of-freedom of the unstable member's node will be gripped, and the analysis is changed to the "*displacement control*" method. In this method, the gripped degree-of-freedom is moved in the direction that the unstable state is growing.

As described above, this *displacement controlled analysis* progresses under constant temperature conditions. For flexibility of the analysis, the gripped degree-of-freedoms and the directions of the movement will be decided manually. For example, in the case where the analysis cannot progress after the conditions occur in which the column reaches its buckling limit; the control of the analysis is changed to displacement. In this case, the translational vertical degree-of-freedom of the node on the top of the buckled column is gripped, and it is gradually moved downward. The equilibrium equation of this displacement control analysis can be expressed as the following equation:

$$\begin{Bmatrix} \overline{\mathbf{P}}^{t+\Delta t} + R_m^t \overline{\mathbf{b}} - \overline{\mathbf{P}} \\ \overline{u}_m^{t+\Delta t} - u_m^t \end{Bmatrix} = \begin{bmatrix} \mathbf{K}^t & \overline{\mathbf{b}} \\ {}^{\mathrm{T}}\overline{\mathbf{b}} & 0 \end{bmatrix} \begin{Bmatrix} \Delta \mathbf{u} \\ -\Delta R_m \end{Bmatrix} \qquad (2.4.2)$$

where $\overline{u}_m^{t+\Delta t}$ is the controlled displacement of the gripped degree-of-freedom at time $t+\Delta t$. This $\overline{u}_m^{t+\Delta t}$ is controlled by the user. The subscript m denotes the number of this degree of freedom in the unknown vector. $\{\overline{\mathbf{b}}\}$ is the vector where the m th element is 1 and the other elements are 0. $\{{}^{\mathrm{T}}\overline{\mathbf{b}}\}$ is the transpose of $\{\overline{\mathbf{b}}\}$. As seen in Eq. (2.4.2), a single unknown ΔR_m is added to the original equation according to adding a single equation to $\overline{u}_m^{t+\Delta t} - u_m^t = \Delta u_m$.

Thus, the unknown $u_m^{t+\Delta t}$ is solved so that it coincides correctly with the controlled quantity $\overline{u}_m^{t+\Delta t}$, while ΔR_m solved simultaneously is an increment of the reactive force which must work to constrain the conjugate displacement to have the just controlled value.

Total reactive force is obtained by summing up every obtained increment; i.e. $R_m^{t+\Delta t} = R_m^t + \Delta R_m$, which is initialized to zero at the instant when the control changes from load to displacement. The term $\{\overline{\mathbf{P}}^{t+\Delta t} + R_m^t \overline{\mathbf{b}}\}$ on the left hand side of Eq. (2.4.2) represents the actual external force plus the generated reactive force, which is considered an effective external force term in the form of equation. As with the load control analysis, Newton-Raphson procedure will be repeated until the left-hand side of equation approaches 0.

The frame becomes in fact unstable under the given external force $\{\overline{\mathbf{P}}^{t+\Delta t}\}$,

if the direction of the reactive force $R_m^{t+\Delta t}$ is opposite in sign to the processing direction of the controlled displacement $\overline{u}_m^{t+\Delta t}$, because this solved reactive force works in this case so as to prevent the growth of the unstable deformation.

This unstable process and the according *displacement control analysis* must continue under the constant suspended member temperature, as far as the above condition is met. If this process continues endlessly, then the frame would not be able to support the given load anymore at this member temperature and would collapse directly with the growth of the unstable motion.

On the contrary, if the reactive force turns back to 0, this indicates the frame recovers its static and stable equilibrium. This state may correspond to the state C, the end point of snap-through action, in Fig. 2.3.2. The displacement control analysis is then quitted. The previous load control analysis is to restart subsequently again under the constant external load and increasing member temperature. The frame may bear further increasing member temperatures stably.

However, it is possible another "*snap-through*" action may occur again. In this case, we may repeat the above procedure. The analysis methods whereby the control is switched between load and displacement is called the "*Alternate Control Method*".

The appeared reactive force is physically an inertial force with the unstable dynamic motion of the frame. This is specifically a concentric inertial force in this case which works along the direction according to that of gripped DOF.

This indicates that the analysis neglects other inertial effects. Therefore, the above analysis cannot trace the correct unstable behavior of the frame completely, since masses may be distributed over the frame.

Moreover, from the viewpoint of dynamics, as described in section 2.3.4, the above computed end point of instability is not an actual end point of motion of the frame, since the frame has kinetic energy at this point and therefore the motion never be ceased then. As a result, in the case where the kinetic movement is severe (the structure that the snap-through easily occurs), the accumulated kinetic energy of the system also increases. Therefore, the actual end-point of the instability process is the point of the displacement that is larger than point *C* in Fig. 2.3.5 (b). This means, the structure gets damaged and deformed greater than the state at point *C* where the reactive force turns back to 0.

Note that in the case where the kinetic movement is severe, the needed displacement to regain stability may also be too large. Consequently, the state of the structure at the starting point of the "*snap-through*" —for example point *E* in

Fig. 2.3.4—can be determined as the practically-collapsed state of the whole structure. On the other hand, in the case where the kinetic movement is small, the kinetic energy of the system is insignificant. Accordingly, the point that the reactive force turns back to 0 is considered close to an actual end point of motion. So the both points can be assumed as the same point.

The above-developed method, the *alternate control method*, asserts that high temperature frame instability can be analyzed statically, if such dynamical natures of the problem are neglected. This is the very feature of the present analysis.

The objectives of the following sections are to verify the existence of snap-through phenomena for practical steel frames subjected to fire, to observe their realistic behavioral natures, to understand the importance of this problem both in structural and fire resistance engineering, and to try to improve the high temperature stability of steel frames. The method developed is said to be a basic analysis tool to investigate these problems.

2.5 The numerical analysis of locally heated steel frames under fire

In this section, realistic stable and/or unstable behaviors of locally heated steel frames are reviewed. A series of fire response analysis results are presented, with emphasis on the ultimate structural performances of frames and their stabilities after the constituent heated columns buckle.

Two normal rigidly-joined frames are analyzed in the section. The first model is a three-spanned and 2-storied structure as shown in Fig. 2.5.1(a). For this model, the sum of the beam strengths is low; thus the frame would collapse and fall into an unstable state after the column buckle. The second model is a three-spanned and six-storied structure as shown in Fig. 2.5.1(b). For this case, the stress redistribution ability of the beams could be anticipated, so the structure can keep its stability even through the column buckle. As explained in section 2.3.2, the structure would collapse at a temperature that is higher than the column buckling temperature.

In the analysis models, only on the beams of the second floor, the vertical load $20kN/m$ is distributed uniformly. Vertically concentric forces also act on the tops of the columns at the roof level, so that the axial force ratios $\bar{p}$ of the lowest portions of the interior and exterior columns become 0.4 and 0.2, respectively. A fire compartment is set in the entire space inside the center span of the lowest floor for each case. Accordingly, the interior columns and the center beam of the lowest floor are assumed to undergo a uniform increase of member temperature (marked by dark lines in the figures). The figures illustrate the left half of a symmetrical frame, which is perfectly suited to this fire response analysis.

The nonlinear finite element analysis that was proposed in the last section is adopted to obtain refined fire responses for the frames above (Suzuki, 1993; Suzuki, 1995). The local buckling of the column is not considered in this analysis.

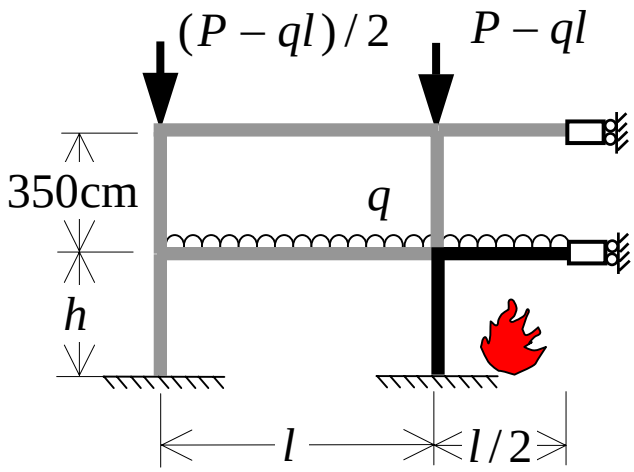

(a) two-storied and three-spanned structure

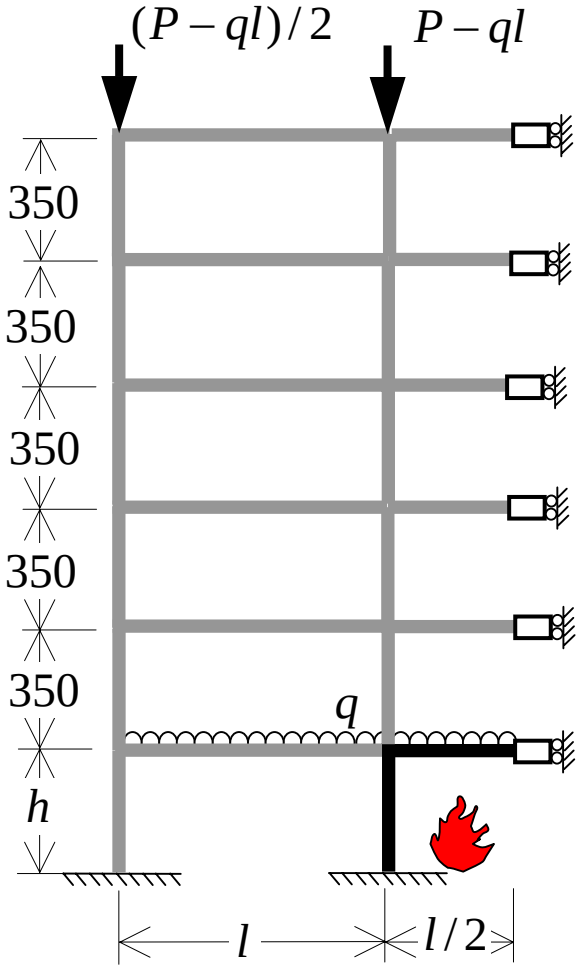

Column:Box-350x350x16

Beam:H-600x200x10x15

Column axial load ratio $\overline{p} = 0.4$

Beam distributed load q = 20 kN/m

Span length l = 700cm

(b) six-storied and three-spanned structure

Fig. 2.5.1 The analysis model

2.5.1 Analysis of the frame where the stress redistribution effect to the surrounding members is low

The numerical results of the two-storied frame are summarized below. This analyzed model is the representation of the frame where the stress redistribution effect to the surrounding member is low. Figures 2.5.2 shows the change of states of deformation for the two-storied frame while Figures 2.5.3 shows summaries of analysis for the two-storied frame.

1. The temperature of the heated column is increased to the temperature of 598oC. From Fig. 2.5.3(a), the heated column expands due to the thermal expansion when the temperature increases. However, the expansion is axially restrained by the upper unheated beams; it causes the force acting on the heated column increase as shown in Fig. 2.5.3(b). At a temperature of 598oC, the force acting on the top of the heated column increases to $0.45\overline{P}_y$. And the heated column buckles at this temperature. This state is shown in Fig. 2.5.2(a) which lengthening of the heated interior column shifts shortening as shown in Fig. 2.5.3(a) The temperature of 598oC is a little lower than the theoretical buckling temperature 623oC which is predictable if a half of the story height of the first floor is taken as the effective length (λ_e = 18.3) and the axial load ratio $\overline{p}$ = 0.4 for the interior column applied to the curve in Fig. 2.2.1. For the analysis aspect, the analysis begins with controlling the load, where the dead load to the frame is controlled to be constant and the temperature of the specified members are to increase step wisely at every updated of the solutions. This *load controlled analysis* is successful as far as the frame keeps its stable state. For this frame, the strength of the surrounding member is not enough to retain the frame's stability, thus the frame starts to fall into an unstable state (as shown the state B in Fig. 2.3.4). With the load control, the analysis cannot continue beyond this temperature, because the equilibrium has existed no more.

2. To continue the analysis, the control of analysis is changed from load to displacement. The system falls into unstable state causes the buckle of the heated column. So the vertical degree-of-freedom of the upper end of the buckled column is gripped and moved downward forcible and statically instead of dynamically. Since this process is dynamic in fact and therefore very rapid, we suspend increase of temperature throughout the *displacement controlled analysis*. This *displacement*

controlled analysis for an unstable process is now preceded for the stepwise increment of the forced downward displacement under a suspended member temperature. The reactive force that conjugate to the controlled displacement control analysis is then induced accordingly. This vertical reaction is computed under the condition that it makes the controlled displacement take just a prescribed value. This *displacement controlled analysis* continues as far as the vertical reaction so computed acts upward, since this indicates the instability of the system. By changing the control of analysis to displacement, the behavior of the structure after the heated column buckle can be expressed. As can be seen in Fig. 2.5.3(a), the heated column subsides continuously while the temperature of the column is constant at the temperature of 598oC. The axial force of the column also decreases continuously as shown in Fig. 2.5.3(b), because this buckled column cannot sustain the load anymore. The part of load that cannot be supported by the buckled column will be transferred to the sound exterior column through the surrounding beams. In this example, the stress redistributing ability of this structure is too small, thus the frame cannot recover its stability. Fig. 2.5.2(b) shows the collapsed of this structure. In this case, the temperature of 598oC is the ultimate temperature of this structure.

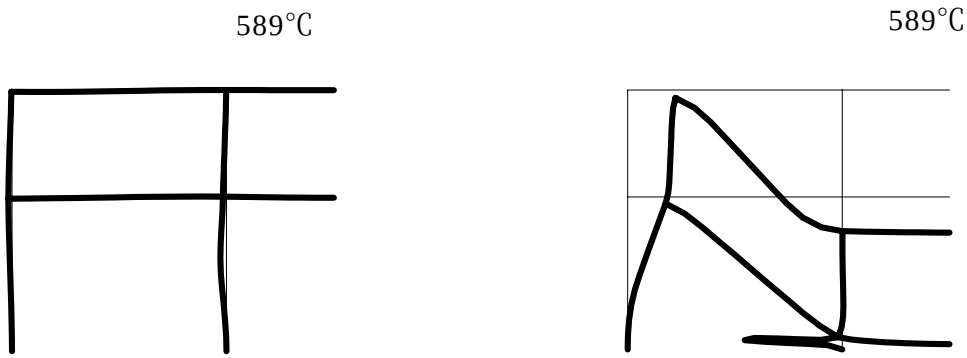

(a) Column buckled

(b) Collapsed

Fig. 2.5.2 Change of states of deformation for the two-storied frame

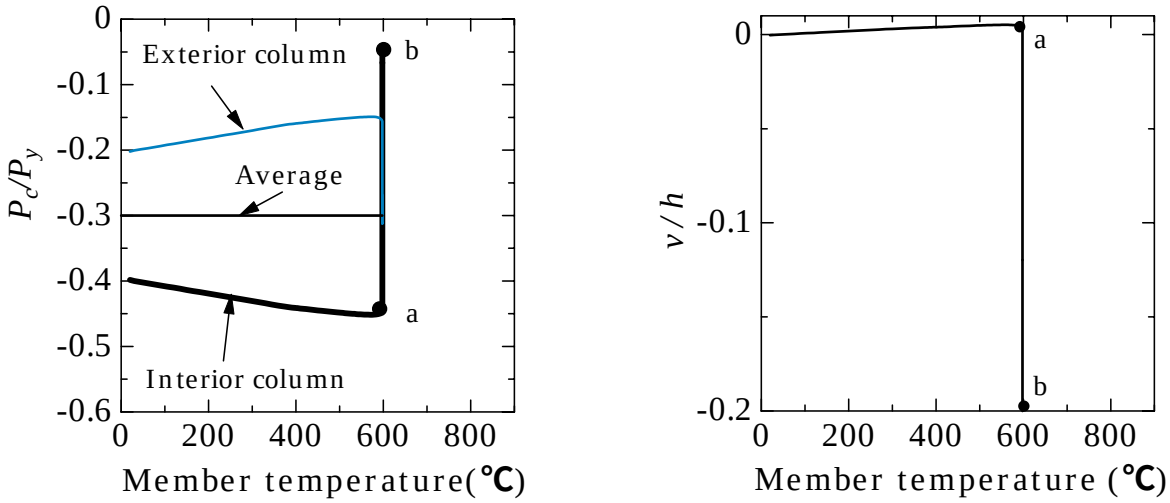

(a) Axial forces of the columns

(b) Vertical displacement of the head of the heated column

P_C : Axial forces of the columns

v : Vertical displacement of the head of the first floor interior column

h : Height of the first floor

Fig. 2.5.3 Summaries of analysis for the two-storied frame

2.5.2 Analysis of a frame where the stress redistribution effect to the surrounding members is high

The following example is a six-storied frame in which the strength of the surrounding members is higher than in the previous example. In this case, as explained in section 2.3.1, the part of load that cannot be supported by the buckled column would be redistributed to the other sound member. We can further investigate the behavior of a frame after heated columns buckle. All the numerical results for this frame are summarized in Figures 2.5.4 and 2.5.5.

1. The heated column of this frame buckled at temperature of 580oC (as shown in Fig. 2.5.4(a)). As in the previous example, the temperatures of the heated members are to increase stepwisely from the temperature of 0oC. As seen in Fig. 2.5.5(a) and 2.5.5(b), the heated column expands relative to the increasing temperature. However, the expanded column is axially restrained by the unheated surrounding beams. So the force acting on the heated column also increases relative to the expansion of the heated column.

From Fig. 2.5.5(b), we can see that the axial force acting on the heated column is more than $0.5\overline{P}_y$, when the column buckles at a temperature of 580oC. As shown in Fig. 2.5.5(a) and (b), the head of the heated column starts to subside and the compressive axial force acting on the column decreases at this temperature

It was stated that this temperature of 580oC is the buckling temperature of this six-storied frame. This buckling temperature is lower than the buckling temperature of the previous example of 598oC and also is lower than the theoretical buckling temperature of 623oC. This temperature lowering is due to the greater thermal stress that is induced by the restraining effect of the beams. However, in contrast to the previous example, in this case, after the heated column buckled, the axial strength of the buckled column deteriorates continuously with its continuing collapse - but the frame does not fall into an unstable state. This is due to the stress redistribution effect onto the surrounding beams, as shown in state I in Fig. 2.3.2. Thus the member temperature can increase statically, although the column buckled (this corresponds to the shift from state I to state A in Fig. 2.3.2)

2. At 694oC, the frame falls into instability due to full plastification of all the beams in the outer spans. As seen in Fig. 2.5.4(b) of this state, both ends of all the

beams have been plastified significantly in the outer span before state (b) was reached. The mechanical situation here is similar to state E in Fig. 2.3.4. In the analysis, the occurrence of instability can be inferred when the *load controlled analysis* fails with the smallest temperature increases. So, in this state, the control of the analysis changes to displacement.

3. By using displacement control, the state of the frame after the formation of the unstable state can be analyzed. From state (b) to state (c) [as shown in Figures 2.5.4(b) and (c)], the heated column subsides greatly during the unstable process, and the outer-span beams bent greatly in a way that corresponds to the subsidence of the column. The bent beams start to act as catenary and suspend the buckled column; this is called the stress redistribution effect. As can be seen in Fig. 2.5.5(c), the axial force on the second floor beam in the outer span changes from compressive force to tensile force during the change from state (b) to state (c). In this case, the stress redistribution effect on the beams is large enough; thus, the reactive force returns from acting upward to zero. The frame recovers at state (c) as shown in Fig. 2.5.4(c). It now can be seen that the change from state (b) to state (c) is an unstable process for this frame. The process may therefore be called a snap-through phenomenon of this frame, in which the stable equilibrium of the frame jumps from state (b) to state (c).

4. We now change the control of analysis to load and increase the member temperature again, since the frame has recovered its stability at state (c). From state (c) at a temperature of 694oC in Fig. 2.5.4(c), the temperatures of the specified members increase to 759oC. The beams in the outer span act as the tensile members to suspend the part of load that cannot be supported by the buckled column. This is different from the behavior of the same beams transforming from state (a) to state (b), when they acted as bent members to suspend a part of the load.

As shown in Fig. 2.5.4(d), the frame deforms throughout to a great extent during this process. In fact, Fig. 2.5.4(c) and Fig. 2.5.5(b) tell us that the interior column has failed extensively, that all the beams in the outer span have deformed greatly, and that sinking of the roof has developed by as much as 2 m. locally before state (c) is reached. It can be said that the failure, which was triggered by the buckling of the heated interior column, has spread upward throughout the frame in a short time. Since that damage in state (c) is large-scale, state (b) may be the

practical ultimate state in this case. However, we have continued the analysis further.

5. The frame loses stability again, since the low part of the exterior columns fail, which are being pulled inward by tension from the suspended beams. We again change the control of analysis to displacement, in which the same displacement is controlled as before. State (e), obtained by the *displacement controlled analysis*, is the one forming during the subsequent unstable process. The frame never recovers stability subsequently. In this case, the temperature of 759oC is the structurally ultimate temperature of this frame.

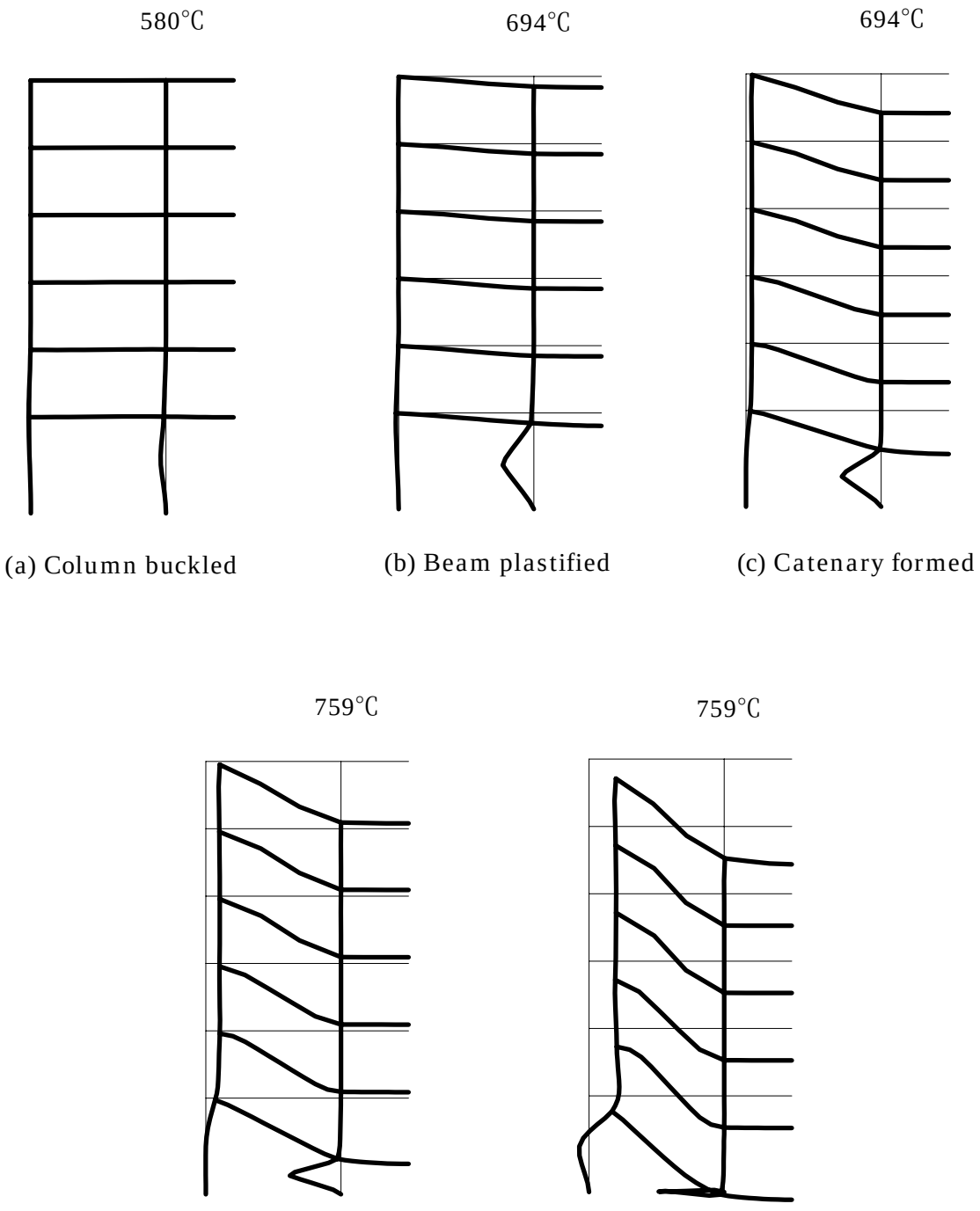

Fig. 2.5.4 Change of states of deformation for the six-storied frame

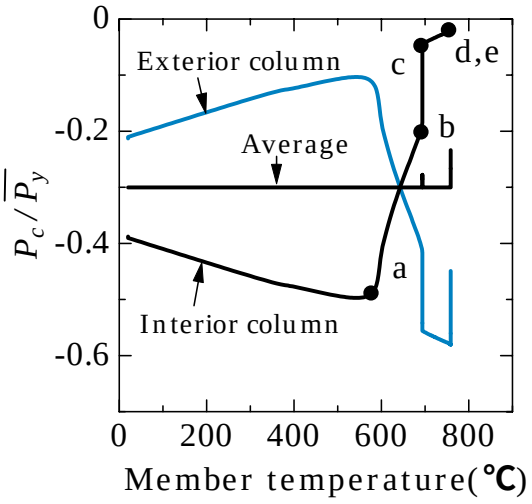

(a) Axial forces of the columns

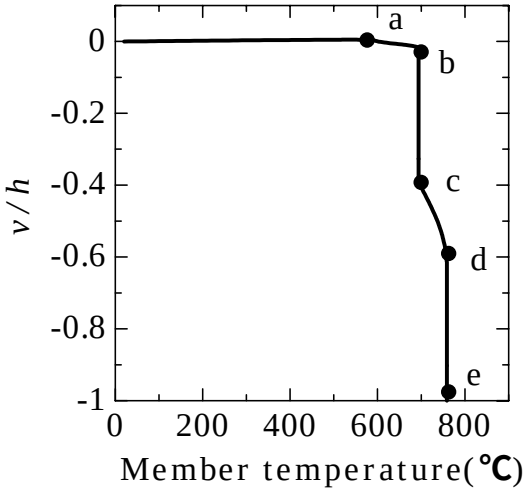

(b) Vertical displacement of the head of the heated column

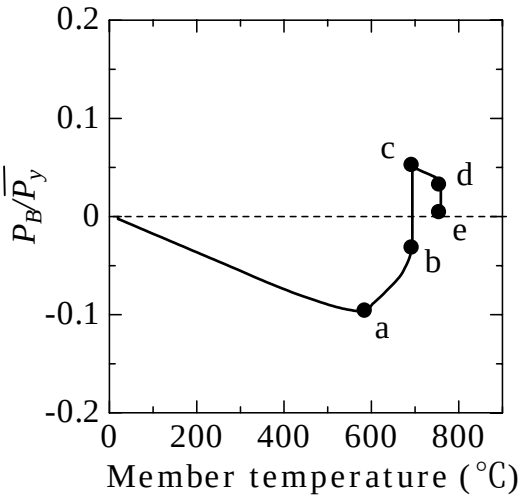

(c) Axial force of the beam

P_C : Axial forces of the columns

P_B : Axial force of the second floor beam in the outer span

v : Vertical displacement of the head of the first floor interior column

h : Height of the first floor

Fig. 2.5.5 Summaries of analysis for the six-storied frame

2.6 Conclusions

After a column of a steel-frame structure is heated from fire occurring in a part of the structure, it is improbable for the entire structure to fall into an unstable state due to only a buckling column. To investigate this condition, a structure solution method that can analyze the fire response of a steel-framed structure, including the unstable processes occurring, was developed. By using this analysis method to analyze some examples of a steel structure subjected to fire, the following conclusions can be drawn:

◆ The main unstable condition of a steel structure subjected to fire is the "*snap-through*" process. This snap-through easily occurs in the structure when the post-buckling residual resistance is low, and the stiffness and the strength of the restraining members are low. That means that the structure's ability to remain stable, while the surrounding members restrain the buckled column, is intimately connected with the instabilities of the structure itself.

◆ The collapse of a structure is not decided solely by the buckling of the heated column. The ultimate temperature of the structure's collapse mode varies according to the stress redistribution ability of the surrounding members. If the stress redistribution ability of the surrounding members is low, the structure loses its stability and collapses suddenly after the column buckle. In this case, the ultimate temperature of this kind of structure is lower than the column buckling temperature (due to thermal stress). However, if the stress redistribution ability of the surrounding members is high, the structure still keeps its stability even though the column buckles. The ultimate temperature of this kind of structure is more than the column buckling temperature.

Chapter 3

The buckling temperature of steel columns

3. The buckling temperature of steel columns

3.1 Introduction

It is recognized that after a heated column buckles during fire, the buckled column is axially restrained by surrounding members; as a result a structure does not collapse directly due to buckling of one column. However, for the structure for which the stress redistribution effect is not enough, it collapses at the same time when the column buckles. In this case, the ultimate temperature of the structure is equal to the column buckling temperature. From the previous discussion, it is clear that buckling of columns is a main cause of the collapse of steel-framed structures. Therefore, it is necessary to understand more about the buckling temperature of heated columns.

Buckling of a column during fire has been studied from many perspectives (Burgess et al., 1992; Franssen, 1995, 1996, 1998; Talamona, 1997). Studies on isolated columns with axial loads have in the past been carried out and used to make design specifications centering on the buckling temperature of heated columns. However, in fact, when a fire occurs in a steel frame, the heated column is rotationally restrained by adjacent members. Thus, the effective length of the buckling column should be shorter than the height of the heated column. The results of many studies support the conclusion of a reduction in the column buckling length in fire.

In addition, for the case where an exterior column is heated, the exterior column is displaced laterally due to thermal expansion of beams during fire. This will likely cause a drop of the buckling temperature (Bailey, 2000). However, in fact, an increase in length of an adjacent beam would also lead to a decrease in the rotational restraint of the adjacent beam. Thus, it is not clear which is the cause of the drop of the buckling temperature in this case. It is thus imperative that the behavior of all columns during fire should be clearly understood.

In this chapter, the main objective is to investigate the influence of the rotational restraint of the adjacent members on the buckling temperature of a column during fire, and to investigate the influence of thermal expansion of beams at the same time. Therefore, three types of columns are herein investigated respectively; i.e. simply supported columns, exterior columns, and interior columns.

In evaluating the column's buckling temperature, the mathematical formulae pertaining to the theoretical buckling temperature are proposed. The tangent

modulus theory is applied to predict the bucking temperature in this chapter. In order to use the proposed formulae to estimate accurately the buckling temperature it is needed to realize the precise effective-length of the buckled column, therefore, this chapter also proposes the equation to provide the effective length of the buckled column. Finally, the numerical method proposed in the previous chapter is used to verify the applicability of both proposed equations.

3.2 The theoretical buckling temperature

In section 2.2, the theoretical buckling temperature of a heated column was briefly introduced. In this section, this is studied more specifically.

As seen in section 2.2, the buckling temperature of a column subjected to fire can be predicted based on the tangent modulus theory as shown in the following expression:

$$\lambda_e^2 = \frac{\pi^2 E_t\left(T_{cr}, \overline{p}\overline{\sigma}_y\right)}{\overline{p}\overline{\sigma}_y} \tag{3.2.1}$$

where λ_e is the effective slenderness ratio of the heated column, $\overline{p}\overline{\sigma}_y$ is the existing compressive force, and T_{cr} is the column's critical temperature. $\overline{\sigma}_y$ is the yield stress at room temperature of the material. $E_t(T_{cr}, \overline{p}\overline{\sigma}_y)$ represents the tangent modulus of the material subjected to the stress $\overline{p}\overline{\sigma}_y$ and the temperature T_{cr}, and $\overline{p}$ is the axial force ratio. The graphic representation of Eq. (3.2.1) of JIS SS400 steel (as shown in Fig. 2.2.1) is depicted again in Fig. 3.2.1. In this figure, the axial force ratio of a column varies from 0.1 to 0.7, while the column's effective slenderness ratio varies between 0 and 100. This is the workable range of an ordinary steel-framed structure's column. As seen in this figure, the buckling temperature of the column T_{cr} can be easily found if the compressive stress $\overline{p}\overline{\sigma}_y$ and the column's effective slenderness are known. Any theoretical buckling temperature curve of any other material may be constructed in the same manner if the stress-strain relationships of the material are known.

As seen in Fig. 3.2.1, for the axial force ratio $\overline{p}$ = 0.1, change in buckling temperature remains quite slight at a high temperature (around 830oC) as the effective slenderness increases. However, for the larger axial force ratio, the buckling temperature decreases more severely as the effective slenderness ratio of column increases. This decrease becomes more significant as the axial force ratio becomes larger. For example, when $\overline{p}$ = 0.5, the buckling temperature falls steeply when the effective slenderness ratio approaches to 70. In this case, the columns with λ_e of the range between about 70 to 100 has the identical buckling temperature about 380℃ as seen in the same figure. This means the critical stresses of all these columns are equal to the same yield strength of the material at this temperature

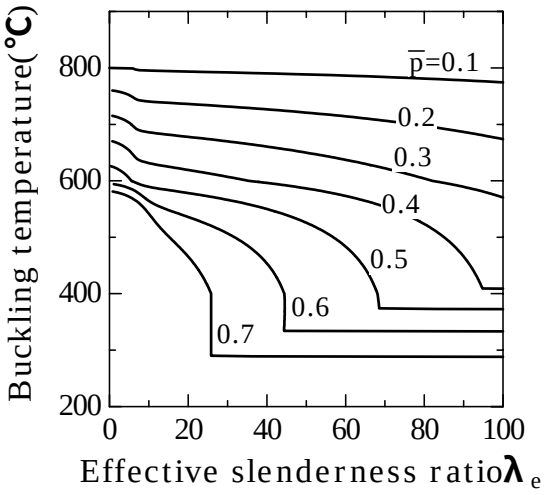

Fig. 3.2.1 Buckling temperatures of SS400 steel columns.

At this point, we wish to examine the accuracy of the theoretical buckling temperatures that may be obtained by Eq. 3.2.1. The plotted points ● and ○ in Fig. 3.2.3 show examples of the buckling temperatures that are obtained by the numerical analysis. The ○ represents the buckling temperatures of the heated columns incorporated in the frame shown in Fig.3.2.2 (a), while the ● represents those in Fig. 3.2.2 (b). The size of the beam and columns and other parameters are shown in Fig. 3.2.2. The heated columns have slenderness ratios of 25.6, 51.3, 78.6, 102.6, and 128.2. The columns' length is handled to control the slenderness ratios. The black solid lines in the figure represent the above mentioned theoretical buckling temperatures of the heated member.

From the boundary conditions of both analyzed models as shown in Fig. 3.2.2, thermal stress would not be generated while the heated columns undergo thermal expansion. The vertical loads acting on the head of the columns are assumed to be constant while the column's temperature is progressively increased. In this analysis, this entire frame falls into an unstable state and collapses after the heated column has buckled. That is, in this case, the ultimate temperature of the structure is equal to the buckling temperature of the column.

In Fig. 3.2.2, the lower end of the heated column is fixed, while the upper end is rotationally restrained by either the heated beam for the model shown in Fig. 3.2.2(a,) or the unheated upper column for the model shown in Fig. 3.2.2(b). Therefore, the effective length ratio of the buckling column would vary between 0.5

(for the column fixed at both ends) and 0.7 (for the one fixed-end and another pinned-end column). In this section, assuming the effective length of $0.5h$ the points ●, ○ are plotted in Fig. 3.2.3 under this assumption.

It is clear that the numerical buckling temperatures are lower than the theoretical buckling temperatures. This implies that the effective length of the heated column in numerical model shown in Fig. 3.2.2 is longer than $0.5h$.

However, it was also noticed that, as shown in Fig. 3.2.3, the numerical buckling temperatures of the model frame of Fig. 3.2.2(a) are nearly equal to those of the frame of Fig. 3.2.2(b).

The above numerical results seem quite suggestive to considering the restraining effects of the adjacent members, since the numerical buckling temperatures are almost the same for both frames although the latter with the unheated upper column should have restrained the lower column much more than the former frame with only a heated beam does. It is thus likely that the upper story unheated column does not effectively rotationally restrain the heated column. This observation will be investigated more thoroughly in section 3.4.2.

The way to predict the effective length of the buckled column will be presented specifically in the next section.

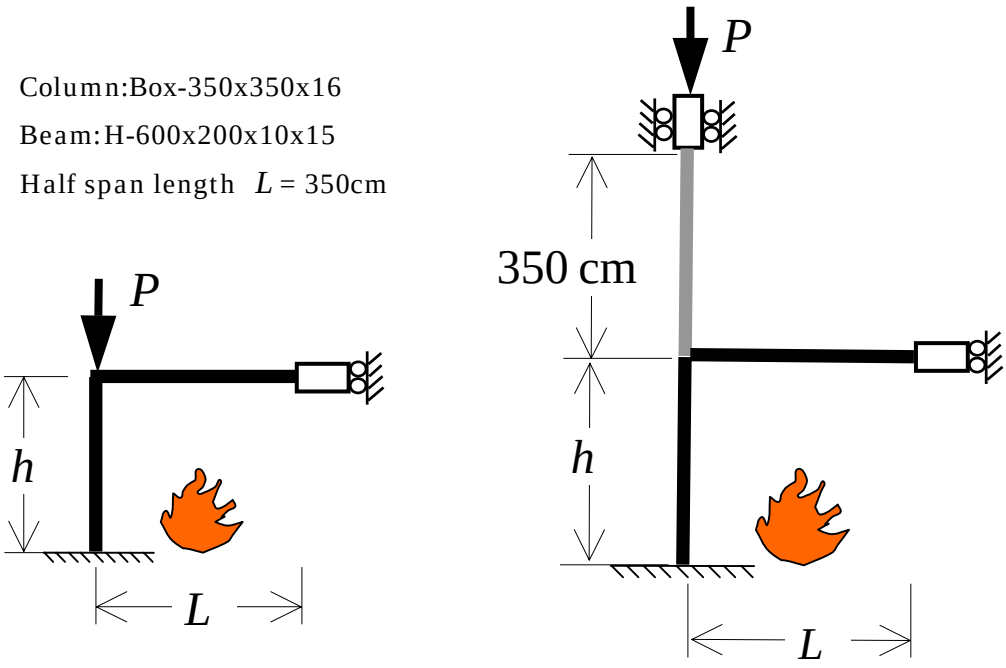

(a) A single storied frame (b) A two-storied frame

Fig. 3.2.2 The analysis models

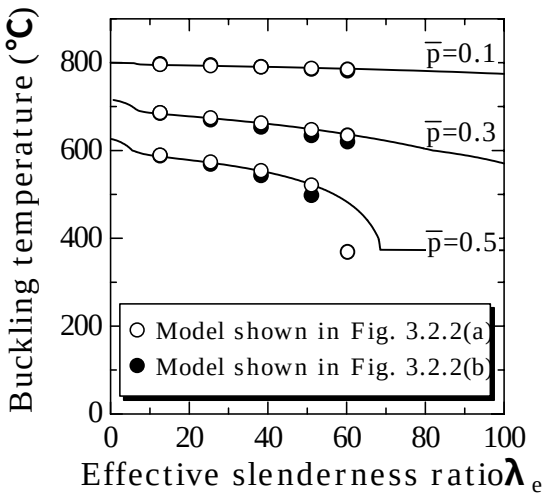

Fig. 3.2.3 Numerically analyzed buckling temperatures

3.3 The evaluation of the effective length of heated columns

When fire occurs in a structure as shown in Fig. 3.3.1, the behavior of a heated column incorporated into a structure is not always the same as that of an isolated column, even though the initial loading is the same at room temperature. For an incorporated column, both ends of the column are rotationally restrained by the surrounding members and therefore the effective length of the heated column should be shorter than the height of the story subjected to fire. In this section, a formula for predicting the effective length ratio of a heated column γ will be proposed, where the extent of the rotational restraint of the surrounding members are to be specifically taken into account.

Fig. 3.3.1(b) shows an extracted sub-structure that represents the heated portion of an entire frame of Fig. 3.3.1(a). In the figure, the fire occurs only in one part of the structure, so the unheated members will prevent these heated buckling columns from lateral sway. The Young's modulus of the unheated members at room temperature $\overline{E}$ are much larger than the tangent modulus of the heated members at the high temperature E_t. Therefore, in Fig. 3.3.1(a), the lower end of the heated column is only barely to rotate, being restrained largely by the unheated beam and column of the lower story. The lower end of the heated column is therefore assumed to be fixed.

At the upper end, due to the thermal expansion of the heated beam, the unheated column of the upper story is pushed out, while rotation of the node and the moment of the upper end of the heated column also increase. Because of this rotation, the heated column is bowed before it buckles. This is what probably causes the drop of the column buckling temperature although it was strongly rotationally restrained by the unheated column. Due to the both positive and negative effects on the buckled column, the rotationally restraining effect of the upper-story is supposed to be neglected. The numerical buckling temperature as shown in Fig. 3.2.1 also affirms this analytical approach.

Fig. 3.3.1(c) shows the symmetric mode of the buckling. To determine the average rotational restraint of the heated beam, a non-rotated and non-sway roller supports are set at the center of the span. In the case where both columns buckle at the same time, both columns can be combined into a single column, as shown in Fig. 3.3.1(d). The combined column's moment of inertia is equal to $\sum_{i\in\text{columns}} I_{Ci}$. The rotational restraint of the heated beam is represented by a rotating spring. The stiffness of this rotating spring K_B can be evaluated by $E\sum_{i\in\text{beams}}(I_{Bi}/L_i)$.

The general differential equation for the column shown in Fig. 3.3.1(d), when the lateral load vanishes, is

$$EI\frac{d^4y}{dx^4}+P\frac{d^2y}{dx^2}=0 \tag{3.3.1}$$

This can be rewritten as

$$\frac{d^4y}{dx^4}+k^2\frac{d^2y}{dx^2}=0 \tag{3.3.2}$$

where $k^2=P/EI$

The general solution of this equation is

$$y=A\sin kx+B\cos kx+Cx+D \tag{3.3.3}$$

The boundary conditions for this column are

$$y=0, \qquad \frac{dy}{dx}=0 \qquad \text{at} \quad x=0 \tag{3.3.4}$$

$$y=0, \qquad hK_C\frac{d^2y}{dx^2}+K_B\frac{dy}{dx}=0 \qquad \text{at} \quad x=h \tag{3.3.5}$$

Using these conditions with the general solutions Eq.(3.3.3) yields the following equations for the constants

$$B+D=0 \tag{a}$$

$$kA+C=0 \tag{b}$$

$$A\sin kh+B\cos kh+Ch+D=0 \tag{c}$$

$$-Ak^2\sin kh-Bk^2\cos kh+\frac{K_B}{hK_C}(Ak\cos kh-Bk\sin kh+C)=0 \tag{d}$$

Investigating the possibility of curved forms of equilibrium, we observe that the only way to have a nontrivial solution of these four equations is to have the determinant of the coefficients equal to zero, i.e.

$$\begin{vmatrix} 0 & 1 & 0 & 1 \\ k & 0 & 1 & 0 \\ \sin kh & \cos kh & h & 1 \\ k^2 \sin kh + \dfrac{K_B}{hK_C} k \cos kh & -k^2 \cos kh - \dfrac{K_B}{hK_C} \sin kh & \dfrac{K_B}{hK_C} & 0 \end{vmatrix} = 0 \qquad (3.3.6)$$

and the following equation is obtained.

$$k^2 h^2 \cos kh + kh \frac{K_B}{K_C} \sin kh - kh \sin kh + 2 \frac{K_B}{K_C} (\cos kh - 1) = 0 \qquad (3.3.7)$$

Due to restraint of surrounding columns, an axial compressive force also develops in the heated beam. In this study, therefore, the stiffness of the beam and the column are assumed to be the tangent modulus at the elevated temperature E_t. Eq. (3.3.7) can be rewritten in the form:

$$K = \frac{X(-X \sin X + \cos X)}{2(1 - \cos X) - X \sin X} \qquad (3.3.8)$$

Where $K = \dfrac{\sum_{i \in \text{beam}} (I_{Bi} / L_i)}{\sum_{i \in \text{column}} (I_{Ci} / h)}$, and $X = \dfrac{\pi}{\gamma}$

the effective length ratio γ can be determined directly from Eq. (3.3.8).

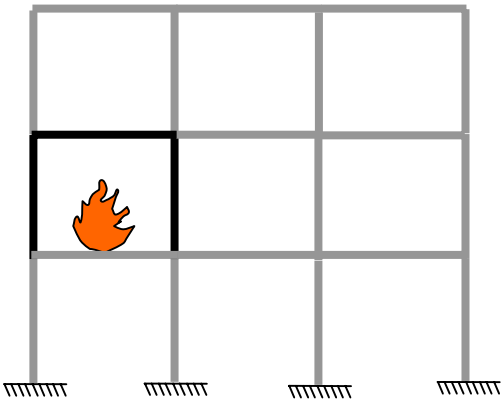

(a) A steel frame subjected to fire

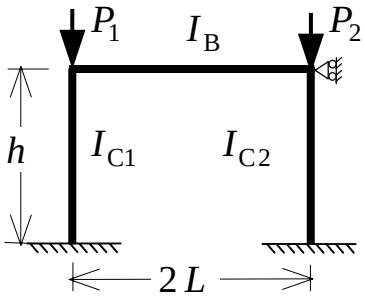

(b) The extracted fire compartment

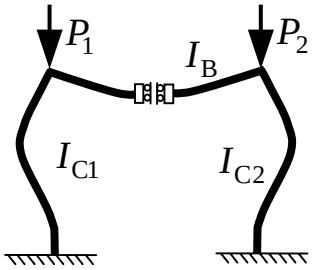

(c) Buckling mode of a non-sway structure

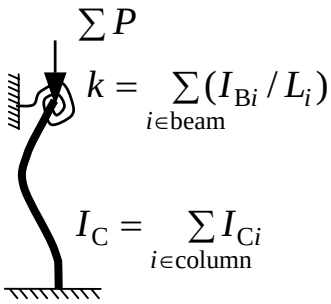

(d) Buckling mode of the combined columns

Fig. 3.3.1 Buckling mode of a non-sway column

3.4 Results of analysis and discussion

The rotational restraining effect of adjacent members is investigated in this section. In addition, the accuracy and the applicability of the theoretical buckling temperatures (Eq. (3.2.1)), and the proposed estimation for the effective length ratio (Eq. (3.3.8)) are also examined by comparing the predictions with a series of numerical results. .

The *alternate controlled analysis* method that was proposed in the previous chapter is used to get numerically the column's buckling temperature and the ultimate temperature of steel frames. In this study, the local buckling of the heated member is not considered.

The computer program in this thesis is based on the one developed by Suzuki and Iwai (1993). In this program, one steel member is divided into 10 sub-elements, where a member indicates a beam type member placed from one connection to another. Moreover, in one sub-element, the integral points are set to be 3 points along the length of the elements and 7 points along the cross-section. The Gauss quadrature is applied to compute relevant integrals over an element. From Suzuki's study, sufficiently accurate results can be obtained from this discretization refinement.

The coefficient of thermal expansion of steel is assumed to be constant regardless of change in temperature and is set to be $12.0\times10^{-6}\mathrm{K}^{-1}$. JIS SS400 steel is taken as the material.

In this section, the study is divided into three types of columns, shown as follows:

1. Simply supported columns
2. Exterior columns
3. Interior columns

The definitions for the variables used in this section are shown below:

$\bar{p}$ the axial force ratio = $P/\overline{P}_y$

q the load distributed uniformly on the beam (kN/m)

λ_e the column's effective slenderness ratio = $\gamma\lambda$

γ the effective length ratio

P the axial compressive force acting on the heated column at room

temperature (kN)

$\overline{P}_y$ the yield force of the column at room temperature (kN)

λ the column's slenderness ratio

h the height of the heated column

l the length of the beam.

L the half- span length of the beam

3.4.1 Simply supported columns

To investigate the accuracy of the proposed theoretical buckling temperature (Eq. (3.2.1)), simply supported columns as shown in Fig. 3.4.1 are analyzed. As seen in the figure, the lower end is pin supported, while the upper end is a roller free to displace vertically. In this case, the effective length is equal to the column length h. Moreover, a constant axial compression P applies through the upper end of the column. In addition, a little transverse initial irregular force is provided at the center of the column. The size of the analyzed column is Box-350x350x16. The analysis parameters are shown in Table 3.4.1.

Table 3.4.1 The analysis parameters of the simply supported column.

Effective slenderness ratios λ_e	10-80
Axial load ratios $\overline{p}$	0.1, 0.3, 0.5, 0.7

3.4.1.1 Results and discussion

Fig. 3.4.2 compares the numerical buckling temperatures with the theoretical buckling temperatures. The solid lines represent the theoretical buckling temperatures that are obtained from Eq. 3.2.1, while the ● shows the numerical buckling temperature.

In the numerical analysis, the member temperature is increased stepwisely until the heated column buckles. In the analysis, an equilibrium solution could become no longer be found once the column buckles. This means the control of the analysis have to be changed subsequently to displacement. However, in some cases where the effective slenderness ratio and axial force ratio are large (λ_e and $\overline{p}$ are more than 40, 0.5 respectively) and when the column's strength reaches the yield point, the tangent modulus of the steel become close to 0. At this temperature, the equilibrium solution does not temporarily exist. However this temperature is not the actual buckling temperature of the column. In this case, the analysis is continued with switching the control to *displacement controlled analysis* until the stabilities of the column are recovered subsequently. Thereafter temperature is increased again until the column buckles finally. By using the *alternate controlled analysis* method, the accurate buckling temperature can be determined by means of

the above procedure.

As seen in Fig. 3.4.2, the column buckling temperature decreases when the effective slenderness ratio and the axial force ratio increase. In general the heated columns have been plastified before the column buckles. However, for the case where the buckling temperature is on the straight line (for example, $\overline{p}$ = 0.7 and λ_e > 25), the heated columns buckle at the temperature where the heated column's stress reaches the yield stress of the steel. From the figure, the numerical buckling temperature is in good agreement with the theoretical buckling temperature. That is, the theoretical buckling temperature from the proposed formula is appropriate.

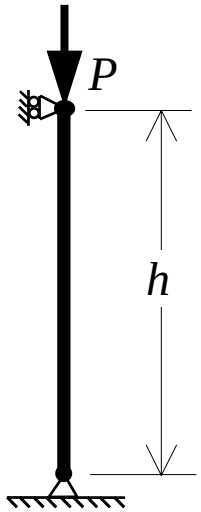

Fig. 3.4.1 A simply supported column

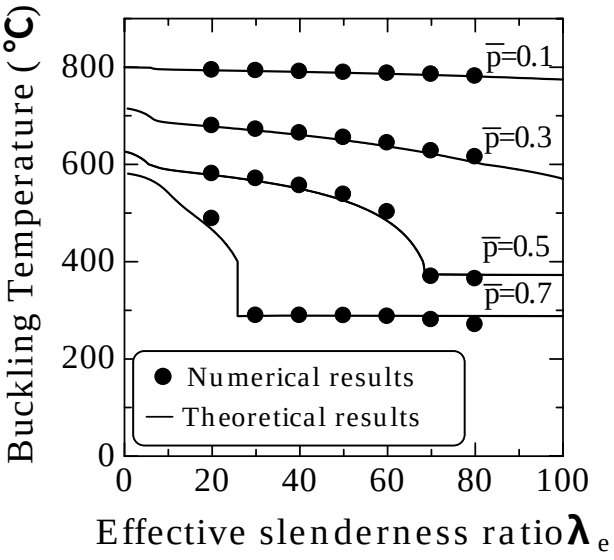

Fig. 3.4.2 Numerically analyzed buckling temperature of the simply supported column

3.4.2 Exterior columns

When fire occurs in a steel frame as shown in Fig. 3.4.3, both heated columns in the fire compartment expand due to thermal expansion. In this case, as opposed to the heated interior column, the heated exterior column is not axially restrained by the adjacent heated beam, but it is rotationally restrained by the connecting members. Furthermore, due to thermal expansion of the heated beam, an upper end of the heated column is laterally displaced, and a bending moment is induced onto the column. Thus the column is subjected severely to anti-symmetric bending moment and acts as a beam-column member in the earlier stages of fire. However, as the member temperature increases close to the buckling temperature, this bending action tends to vanish and subsequently the bending moment of the upper end of heated column changes its direction. Finally the buckling of the column takes place and it leads to the failure of the frame.

The effect of the thermal expansion of the heated beam on the buckling temperature is the first problem that we have to study in this section. In fact, this gives rise to $P-\delta$ effect on the heated column. As noted above, the heated exterior column's upper end is laterally displaced and is subjected to large bending moment caused by the expansion of the connecting beams during fire. This is what probably causes some drop of the column buckling temperature.

To investigate the $P-\delta$ effect, a frame shown in Fig. 3.4.3(a) is used as the model for analysis. The column size is shown in Fig. 3.4.3, and the beam in this model is considered to be rigid. This indicates that, however long the beam is, the effective length ratio of the column is always equal to 0.5. In addition, the temperature increase in the beam is to be as the same rate as in the column. As seen in the figure, the axial compression and the distributed load are applied through the top of the column and onto the beam, respectively. The axial force ratio $\overline{p}$, the column effective slenderness ratio λ_e, and the beam's half span length L parameters are shown in table. 3.4.2

Next, in order to clarify the effective buckling length of the column and to examine the accuracy of its estimation with Eq. (3.3.8), we have to study the rotationally restraining effect of the adjacent member on the heated column.

The models used for numerical analysis are the single-storied and three-storied steel frames as shown in Fig. 3.4.3(a) and (b), respectively. The black solid lines in the figures represent the heated members, while the other members are at room temperature. That means the upper end of the heated column in Fig.

3.4.3(a) is rotationally restrained by only the heated beam, while in Fig. 3.4.3(b)'s case, the rotational restraining members are the heated beam and the upper floor unheated column. The analysis parameters are shown in Table. 3.4.3.

Table 3.4.2 The analysis parameters of the exterior column - effect of the expansion of the heated beam

Axial load ratios $\bar{p}$	0.1, 0.3, 0.5
Effective slenderness ratios λ_e	51.3, 102.6
Half span lengths of the beam L (m)	3.5, 7.0, 10.5, 14.0
Beam type	Solid beam

Table 3.4.3 The analysis parameters of the exterior column - effect of the beam size

Axial load ratios $\bar{p}$	0.1, 0.3, 0.5
Slenderness ratios λ	25.6, 51.3, 78.6, 102.6, 115.4, 128.2
Half span lengths of the beam L (m)	3.5, 10.5
Beam size	H-200x100x5.5x8 H-600x200x10x15 H-900x300x18x26

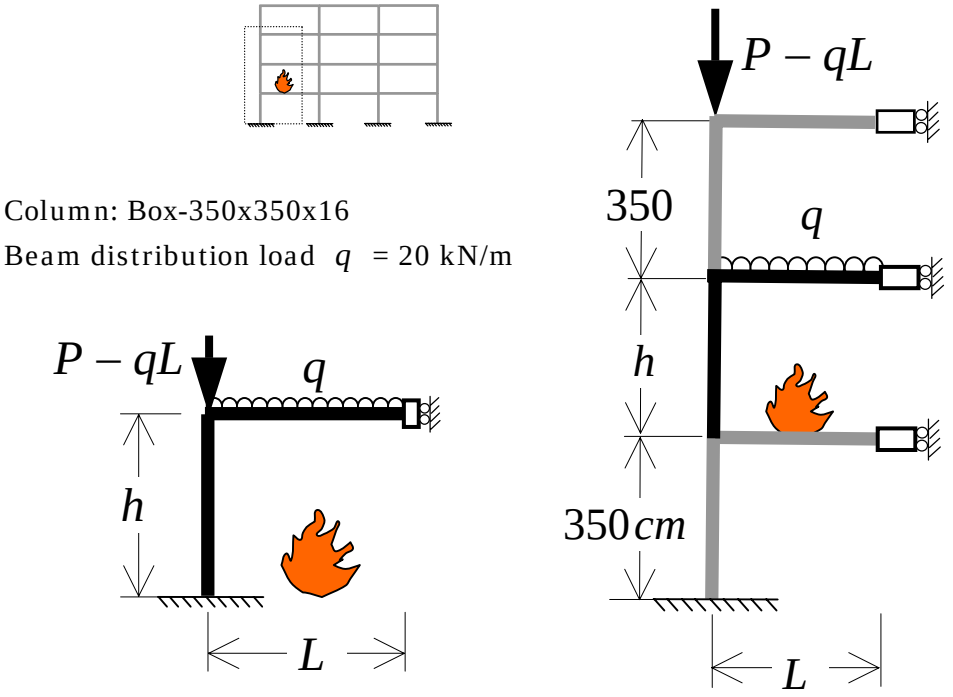

(a) one-storied frame (b) three-storied frame

Fig. 3.4.3 The analysis models of a steel frame which the exterior column is heated

3.4.2.1 The behavior of the exterior column during fire

To investigate and to grasp the behaviors of steel frames subjected to fire and buckling of the heated column, the example of the numerical analysis result as shown in Fig. 3.4.4 is discussed here. The numerical analysis model is the steel frame as shown in Fig. 3.4.3(b) in which $\overline{p}$ is equal to 0.5 and λ is equal to 25.6. The distributed load on the beam is set to $10\,\mathrm{kN/m}$. Fig. 3.4.4(a) shows the histories of the end bending moments of the heated column, the heated beam, and the upper-floor unheated column at the connection.

The figures 3.4.4(b), and (c) show the displacement and the bending moment of the frame during fire, respectively. As seen in Fig. 3.4.4(a), under the temperature between 0 and 200, both columns connected to the heated beam are pushed outward due to the thermally expanded beam. Thus, the resistant bending moment of the heated column's upper end and the unheated column's lower-end are increasing continuously.

However, after the member temperature exceeds 200oC, the upper end of the heated column starts to be plastified , therefore the bending moment of this member decreases although the expansion of the heated beam have still increased. When the temperature of the column exceed 500oC, as seen in Fig. 3.4.4(b), the heated column starts to bend clearly, and as in Fig. 3.4.4(a), the resistant bending moment decreases clearly. The top of the heated column sinks continuously according to temperature increase as shown in Fig. 3.4.4(b).

Finally, the heated column buckles at the temperature of 586oC. From Fig. 3.4.4(a), we can see that the direction of the bending moment of the heated column's upper end reverses from the direction before buckling. Because, when the column buckles, the upper end of the heated column is rotationally restrained by the adjacent members. And as seen from Fig. 3.4.4(a), the bending moment of the heated column decreases abruptly and changes in sign at the temperature of 586oC. Since the member temperature cannot increase anymore, this means the attained temperature is not only the buckling temperature of this column but also the ultimate temperature of the frame.

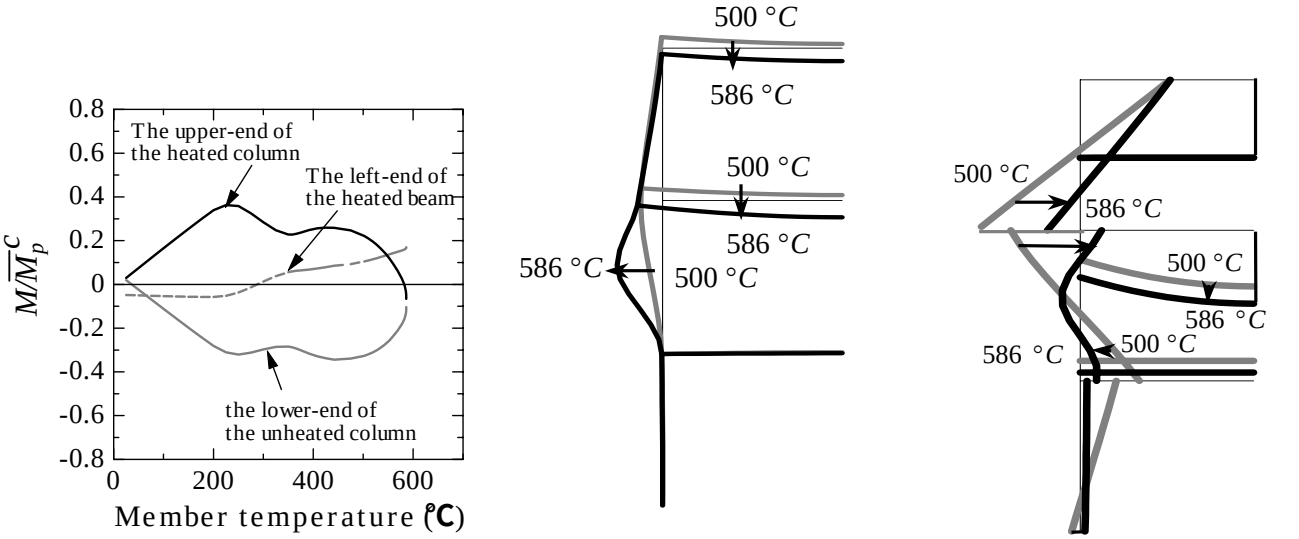

(a) The bending moments of each member at the connecting node

(b) The deformation of the frame at bucking temperature

(c) The bending moment at buckling temperature

M : The bending moment
$\overline{M}_P^C$: The full plastic moment of the heated column

Fig. 3.4.4 The numerically analyzed results of the frames shown in Fig. 3.4.3(b) (λ =25.6, L =3.5 m, $\overline{p}$ = 0.5, Beam: H-600x200x10x15)

3.4.2.2 Effect of the thermal expansion of the heated beam

The figure 3.4.5 shows the numerical buckling temperatures of the frames shown in Fig. 3.4.3(a) for varying the span length of the beam. In general, the magnitude of rotational restraint of the beam varies according to sectional stiffness and span length of the beam. In these cases, the beams are assumed to be rigid. That indicates the column is rotationally restrained by the heated beam perfectly, so the effective length ratio of the column is equal to 0.5 although the span length increases. We can say that, in this case, the column buckling temperature is only the function of the thermal expansion of the heated beam.

Increase in length of the beam is to cause the increase in the thermal expansion. As a result, the lateral displacement of the upper end of the heated column δ increases, so the buckling temperature of the column should drop due to the $P-\delta$ effect. However, as can be seen in Fig. 3.4.5, the heated column with λ_e = 25.5 and $\overline{p}$ = 0.3 buckles at the temperature around 680oC regardless of

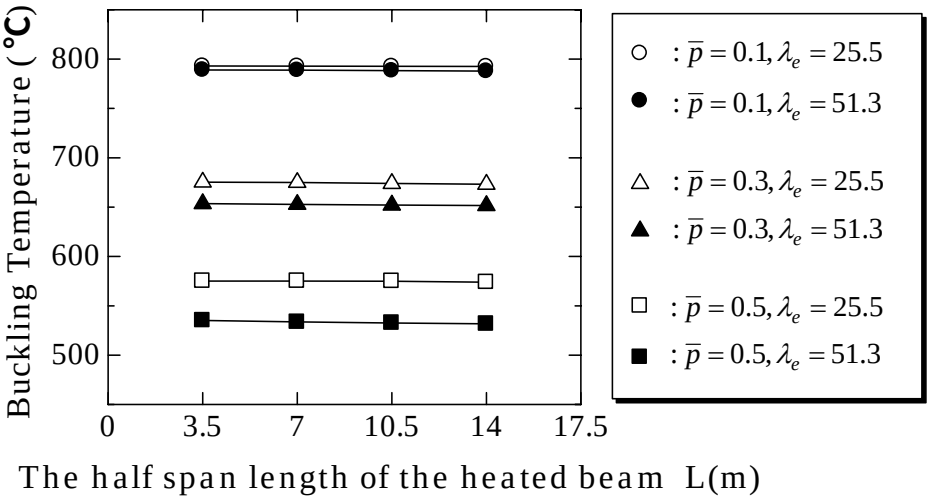

Fig. 3.4.5 The numerically analyzed buckling temperature
- effect of the thermal expansion of the heated beam

changing the span length of the beam. Other cases tell also the same results as seen in the figure; i.e. the buckling temperatures do not decrease nevertheless the thermal expansion increases. From these results it can be concluded that the thermal expansion of the heated beam has not any direct effect on the buckling temperature of the column.

3.4.2.3 Effect of the beam size

To investigate the effect of the rotational restraint of beams, beam sizes of H-600x200x10x15, H-900x300x16x28, and H-200x100x5.5x8 are used as the analysis parameters. Figures 3.4.6 show the numerical buckling temperatures of the heated columns as shown in Fig. 3.4.3 (a), and (b). Fig. 3.4.6(a), (b) and (c) represent the results of the model frames for which the beam sizes are H-600x200x10x15, H-900x300x16x28, and H-200x100x5.5x8, respectively. L is set to be 3.5 m commonly for all the models.

The mark △ in the figures represents the column buckling temperatures of the frames shown in Fig. 3.4.3 (a), in which the upper end of the heated column is rotationally restrained only by the heated beam. On the other hand, the ● shows the column buckling temperatures of the frames shown in Fig. 3.4.3(b) in which the heated beam and the unheated column of the upper floor are the rotationally restraining members. All of the numerical buckling temperatures are plotted taking the effective buckling length ratios γ to the abscissa which is evaluated by the

proposed Eq. (3.3.8). If the proposed effective length ratio is appropriate, the numerical buckling temperatures should be in good agreement with the theoretical buckling temperature.

Since, as described in section 3.3, the rotationally restraining effect of the upper-floor unheated column is neglected Eq. (3.3.8), the effective length ratio γ s of the heated columns of the both frames shown in Fig. 3.4.3(a) and in Fig. 3.4.3 (b) result identical, if the framing of the floor in fire is identically proportion. As seen in the evaluated effective length ratio γ in each figure, the effective length ratio γ decreases when the column slenderness ratio increases. This is because larger slenderness ratio of the column indicates simply a longer column length and a smaller column stiffness $(K_C = I_C / h)$ in this case and therefore we obtain a smaller γ when the corresponding larger K is substituted in Eq. (3.3.8).

From the results, it can be seen that the numerical buckling temperatures of the frame shown in Fig. 3.4.3(a) are in good agreement with the theoretical results. Therefore, it can be concluded that the buckling temperature of the exterior column can be estimated by the effective length ratio γ and the theoretical buckling temperature that are calculated from the proposed expressions.

For the column buckling temperature of the three-storied frame shown in Fig. 3.4.3(b), it can be seen that the column buckling temperatures where the beam size is H-900x300x16x28 and γ is equal closely to 0.5, are in good agreement with the theoretical buckling temperatures. Since the heated column is strongly rotationally restrained by the adjacent members in these cases, the boundary conditions of both ends can be assumed to be fixed. For the results of the frames in which the beam size is H-600x200x10x15, the numerical buckling temperatures are also in good agreement with the theoretical predictions.

The numerical buckling temperature of the frame, in which the beam size is H-200x100x5.5x8, is higher than the theoretical buckling temperature estimated by the effective length ratio $\gamma \approx 0.7$. However, in fact, the upper-end of the heated column in both cases is rotationally restrained by the upper floor unheated column. Thus its boundary condition should be approximately fixed end, and the effective length ratio γ should also be close to 0.5. But, from the numerical analysis results, it is found that the numerical buckling temperatures of the columns, with the beam sizes H-600x200x10x15 and H-200x100x5.5x8, are lower than the theoretical buckling temperature estimated by the effective length ratio $\gamma \approx 0.5$. This indicates that the effective length ratio γ of both cases is higher than 0.5, and the rotationally restraining unheated column of the upper floor does not strongly affect

the buckling temperature of a column.

From the above results, it can be concluded that increasing the size of the connecting beam has the effect of increasing the buckling temperature of the column which can be estimated quantitatively by Eq. (3.3.8).

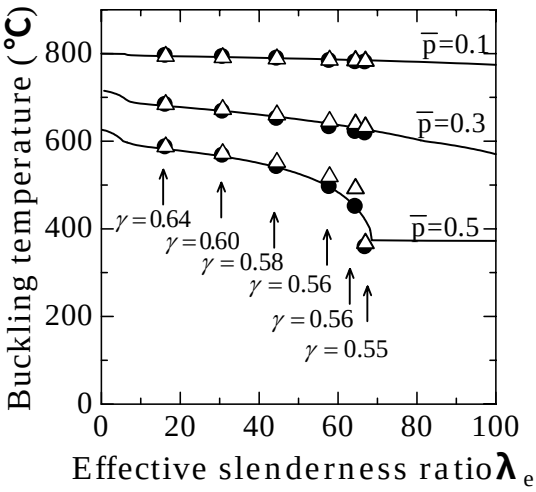

(a) Beam size : H-600x200x10x15

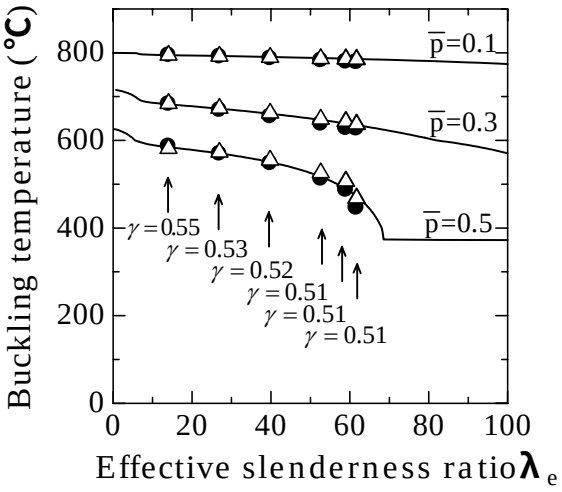

(b) Beam size : H-900x300x18x26

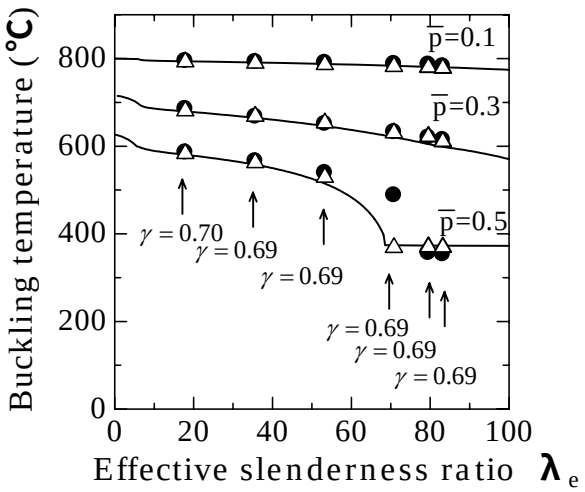

(c) Beam size : H-200x100x5.5x8

— The theoretical buckling temperature calculated from Eq. (3.2.1)

Numerical results

△ The column buckling temperature of the frame shown in Fig. 3.4.3(a)

● The column buckling temperature of the frame shown in Fig. 3.4.3(b)

Fig. 3.4.6 The numerically analyzed buckling temperature - effect or the beam size

3.4.2.4 Effect of the beam span length

Table 3.4.4 The analysis parameters of the exterior column- effect of the span length

Axial force ratios $\overline{p}$	0.3, 0.5
Slenderness ratios λ	25.6, 51.3, 78.6, 102.6
Half span lengths of the beam L (m)	3.5, 7.0, 10.5
Beam size	H-600x200x10x15

The analysis conditions and parameters are shown in table 3.4.4 to see the effect of the beam span length. Figures 3.4.7 show the column buckling temperatures of the frames shown in Fig. 3.4.3(a) and (b). All of the numerical results are plotted taking the effective length ratio γ to the abscissa evaluated by the proposed Eq. (3.3.8). Table 3.4.5 shows the evaluated effective length ratios γ. Since an increase in the span length of the beam leads to a decrease in the rotational stiffness of the beam $(K_B = I_B / L)$, the resulting effective length ratio γ becomes greater.

Table 3.4.5 The effective length ratios of the exterior columns – effect of the beam span length

The column slenderness ratio λ	The effective length ratio γ		
	L = 3.5 m	L = 7.0 m	L = 10.5 m
25.6	0.636	0.662	0.673
51.3	0.600	0.636	0.652
78.6	0.578	0.616	0.636
102.6	0.564	0.600	0.622

As shown in Fig. 3.4.7, the column buckling temperatures decreases when the span lengths of the beams increase. As discussed above, an increase in the span length of the beam leads to a decrease in the stiffness of the beam, which gives rise to a decrease in the rotationally restraining effect.

It can be seen that the numerical buckling temperatures of the frames shown in Fig. 3.4.7 are in fairly good agreement with the theoretical results. However, the numerical buckling temperatures of the frames shown in Fig. 3.4.3(b) with $\overline{p}$ = 0.3, λ = 102.6 and L = 7, 10.5 m is lower than the theoretical results. That means the theoretical buckling temperatures that are estimated by the proposed effective length ratio γ (as expressed in Eq. (3.3.8)) provide unsafe estimations. However, it

is found that these steel frame conditions will not be used in practice because the column's effective slenderness ratio λ_e and the span length $2L$ of the beam are too large.

It is noticed that the numerical buckling temperatures of the columns of Fig. 3.4.3(b) is lower than the results of the columns of Fig. 3.4.3(a), even if both frames are under identical mechanical and thermal conditions for the heated members. As seen in Fig. 3.4.3, it is found that the upper end of the heated column of Fig. 3.4.3(a) is rotationally restrained by only the heated connecting beam, while, for the case of the frame of Fig. 3.4.3(b), not only the heated beam but also the unheated column of the upper floor should restrain strongly the heated column. Therefore the column's effective length of the former frame should have been longer than that of the latter model resulting in a lower buckling temperature.

However the numerical results show different facts from the above thought. It is likely that the unheated column of the upper story has no rotationally restraining effect on the heated column. This observation will be investigated below.

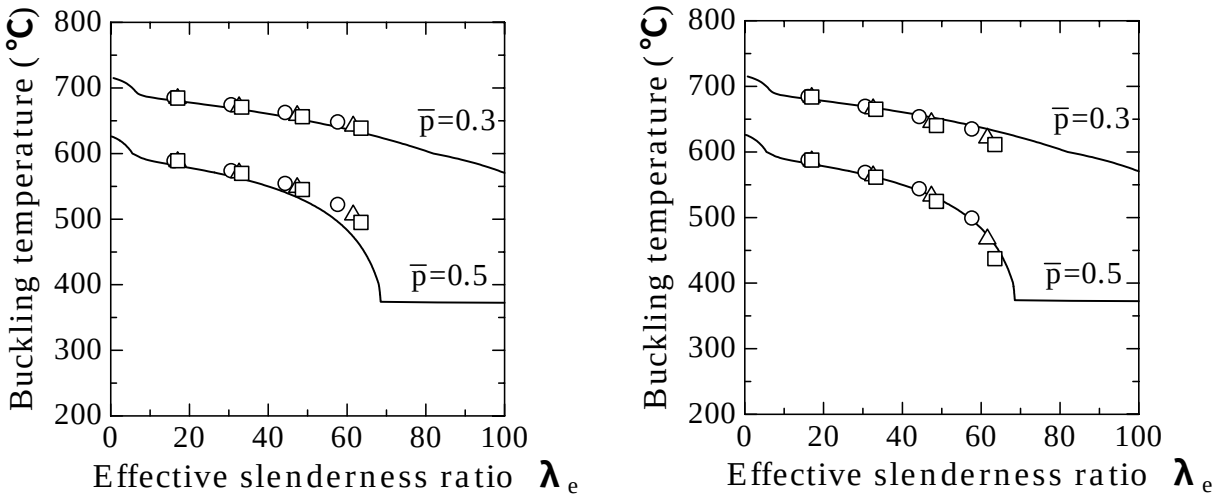

(a) The model frame shown in Fig. 3.4.3(a) (b) The model frame shown in Fig. 3.4.3(b)

— The theoretical buckling temperature calculated from Eq. (3.2.1)

Numerical results

○ The half span length L =3.5 m △ The half span length L = 7.0 m

□ The half span length L = 10.5 m

Fig. 3.4.7 The numerically analyzed buckling temperature - effect or the span length of the beam

3.4.2.5 Rotationally restraining effect of the unheated column of the upper floor

As seen above, we found that the rotationally restraining effect of the unheated column of the upper floor is not clear. To investigate this problem in more detail, the steel frames of Fig. 3.4.3(a) and (b) are again examined for the numerical study, where the analysis parameters in Table. 3.4.6 are taken now. Herein, the axial load ratio $\bar{p}$ is to be 0.5 and the column's slenderness ratio λ = 103.

Table 3.4.6 The analysis parameters - rotationally restraining effect of the unheated column of the upper story

Case 1	L = 3.5 m, Beam:H-450x200x10x14
Case 2	L = 7.0 m, Beam:H-600x200x10x15
Case 3	L = 10.5 m, Beam:H-650x240x13x15

Fig. 3.4.8 shows the numerical analysis results. Fig. 3.4.8 (a) is the numerical column buckling temperatures of the steel frames shown in Figs. 3.4.3(a) and (b), respectively. Fig. 3.4.8(b) shows the rotation of the node of the heated column's upper end. The rotational stiffness of the beam $(K_B = I_B / L)$ is identical for all the cases, thus the evaluated effective length ratio γ of all models is equal to 0.6. This means the theoretical buckling temperature determined by this γ is equal to 473oC that is represented by the solid line in Fig. 3.4.8(a).

It can be seen in Fig. 3.4.8(a) that the numerical buckling temperatures of the frame of Fig. 3.4.3(a) are almost the same for all beam span lengths. It is observed that the numerical buckling temperature is a little higher than the estimated solid line. In estimating γ, as previously mentioned, both the heated column and the beam have the common tangent modulus E_t of steel at elevated temperature. It may however be unlikely that the heated beam plastifies fully due to the axial restraint of the heated column. The heated beam's stiffness is rather close to the Young's modulus at elevated temperature E for these frames of 3.4.3(a). Thus the actual effective length ratio γ may become smaller than the estimated value, and this may be the reason why the numerical buckling temperatures in these cases exceed the estimated value.

On the other hand, the numerical buckling temperatures of the frames of Fig. 3.4.3(b) decrease slightly due to an increase of the span length of the beam. It is

found also in the figure that all the buckling temperatures are lower significantly than 543oC which is obtained by using $\gamma = 0.5$ in Eq. (3.2.1), where this factor must in fact be taken if the upper column works fully to restrain the rotation of the heated lower column.

It is now pointed out that the decrease in the buckling temperature is somewhat sensitive to the increase in the nodal rotation of the heated column's upper end. As seen in Fig. 3.4.8(b), for all the frames of Fig. 3.4.3(a), these nodal rotations are found very small. On the contrary, for the frames of Fig. 3.4.3(b), the increase in the span length of the beam is found to give rise to a significant increase in the rotation.

When the member temperature increases, the exterior column is pushed out by the thermal expansion of the heated beam. Since, the unheated upper column is much stiffer than the lower heated column when both are pushed out, the resulting deformation concentrates into the heated column as shown in Fig. 3.4.4(b). The above nodal rotation results therefore from this deformational concentration of the heated column. The more both columns are pushed out by a longer heated beam, the more the nodal rotation results. This rotational displacement increases when the temperature increases. Due to this rotational displacement, the heated column is bent before it buckles. It causes likely the damage of the heated column. As a result, the column buckles at a lower temperature although it was strongly rotationally restrained by the unheated upper column. But, the heated adjacent beam also works to restrain the heated column from rotation at the upper end.

From the above discussion, we find that the rotationally restraining unheated column has both positive and negative effects on the buckled column. However, this rotational displacement is not generated in such frames as in Fig. 3.4.3(a), because forcible end rotation does not takes place for the buckled column in these frames.

As discussed above, the rotationally restraining effect of the upper-floor unheated column can be neglected when determining the effective length of the exterior column. Therefore the combining use of the theoretical buckling temperature (Eq. (3.2.1)) and the proposed effective length ratio γ (Eq. (3.3.8)), which is formulated neglecting all the effect of the upper stories is appropriate for estimating the buckling temperature of the exterior column.

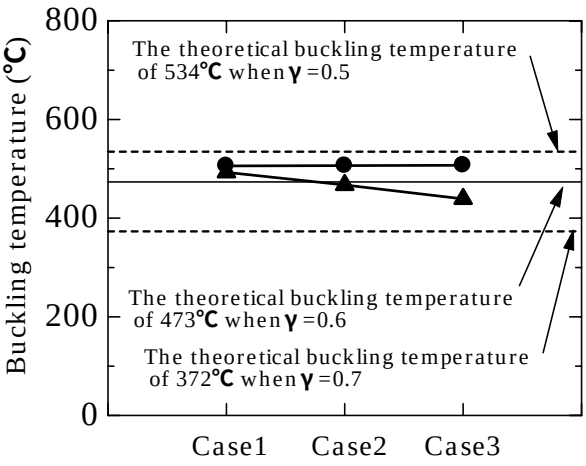

(a) The buckling temperature

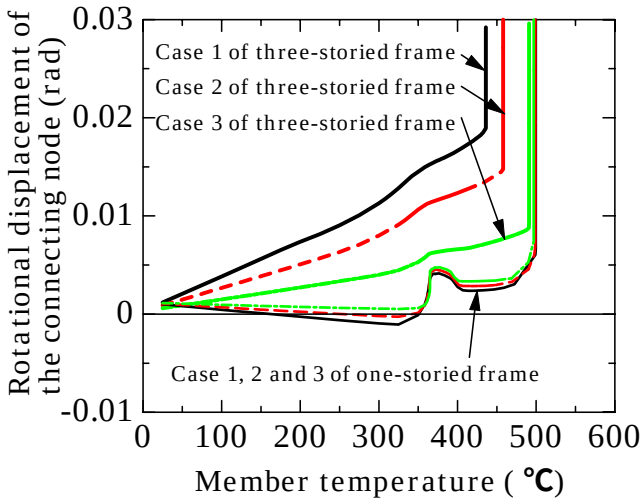

(b) The rotational displacement

Case1: L = 3.5 m, Beam:H-450x200x10x14	Case2: L = 7.0 m, Beam:H-600x200x10x15
Case3: L = 10.5 m, Beam:H-650x240x13x15	

Fig. 3.4.8 The numerically analyzed results, rotationally restrained effect of the unheated column of the upper story (λ =103, $\overline{p}$ = 0.5)

3.4.3 Interior column

When interior columns are subjected to fire, its behavior during fire is different from that of the exterior column as discussed in the last section. The upper end of a heated interior column is more largely restrained rotationally by unheated beams. On the other hand, expanding heated interior columns are axially restrained by adjacent beams placed within the next span or spans as shown in Fig. 3.4.9. Therefore the restrained interior columns are subjected to an additional compressive force which is a thermal force. This thermal force causes a drop in the buckling temperature of the columns. However, as described in section 2.5.2, after the buckled column loses its strength, these same beams turn to play a role to redistribute a part of the axial force to other sound columns which were carried by the buckled column before it buckles.

To investigate the effective length of interior columns, frames shown in Fig. 3.4.9(a) are used as the numerical analysis model. In the figure the black marked members are to be heated. From the boundary conditions of this model, the heated column is not axially restrained by the adjacent members and therefore thermal compressive force does not occur in the heated column. The constant vertical load P is applied downward to the top of heated column. The analysis parameters are shown in Table 3.4.7.

For purpose of comparison, general regular multi-storied frames are also considered. The analysis model in this case is a sub-structure extracted from the original frame which constitutes a multi-storied 3-spanned frame and includes the leftmost two spans of the original frame as shown in Fig. 3.4.9(b). The analysis parameters are shown in Table 3.4.8.

As anticipated, the interior column is strongly restrained rotationally by the adjacent unheated beams. In fact, since the constant K of Eq. (3.3.8) in this case can be expressed as

$$K = \frac{(\bar{E}I_B / L) + (E_t I_B / L)}{E_t I_C / h} \qquad (3.4.1)$$

, we can see that the numerator is much larger than the denominator in the equation. This K is large enough to assume that the effective length ratio of the interior column is 0.5.

Table 3.4.7 The analysis parameters of the interior column – effective length ratio

Axial load ratios $\bar{p}$	0.1, 0.3, 0.5
Slenderness ratios λ	25.6, 51.3, 78.6, 102.6, 128.2, 153.8

Table 3.4.8 The analysis parameters of the interior column – effect of slenderness ratio and the number of story

Axial load ratios $\bar{p}$	0.1, 0.3, 0.5
Slenderness ratios λ	25.6, 51.3, 78.6, 102.6, 128.2, 153.8
Number of story	4, 6

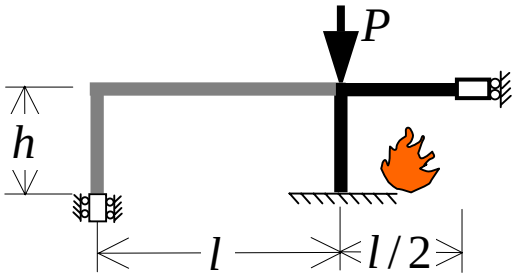

(a) A single-storied and three-spanned steel frame

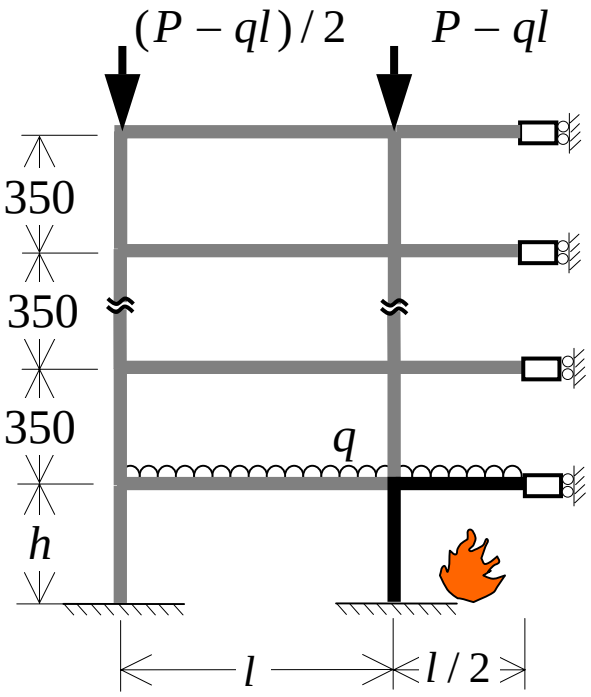

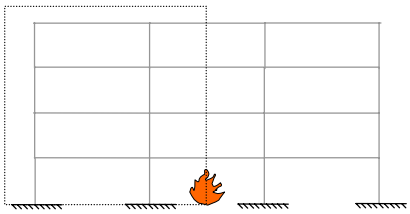

Column:Box-350x350x16

Beam:H-600x200x10x15

Beam distributed load q = 20 kN/m

Span length l = 700cm

(b) A multi-storied and three-spanned steel frame

Fig.3.4.9 The analysis models of a steel frame which the interior column is heated

3.4.3.1 The effective length ratio of the interior column

Fig. 3.4.10 shows the numerical buckling temperature of the frame shown in Fig. 3.4.9(a). The solid line represents the theoretical buckling temperature calculated from Eq. (3.2.1), while the ● represents the numerical buckling temperature of the column. The column's effective length ratios are very close to 0.5 for all the cases.

Since, for the frame shown in Fig. 3.4.9(a), the exterior column's lower end is a vertically movable roller, the heated column is not axially restrained. This indicates the load supported by the buckled column is not redistributed. In this case the ultimate temperature of the frame is equal to the column buckling temperature.

As seen in the figure, the numerical buckling temperatures of the columns are in good agreement with the theoretical buckling temperature for all the cases. It is therefore clear that the effective length ratio γ of the interior column is equal to 0.5.

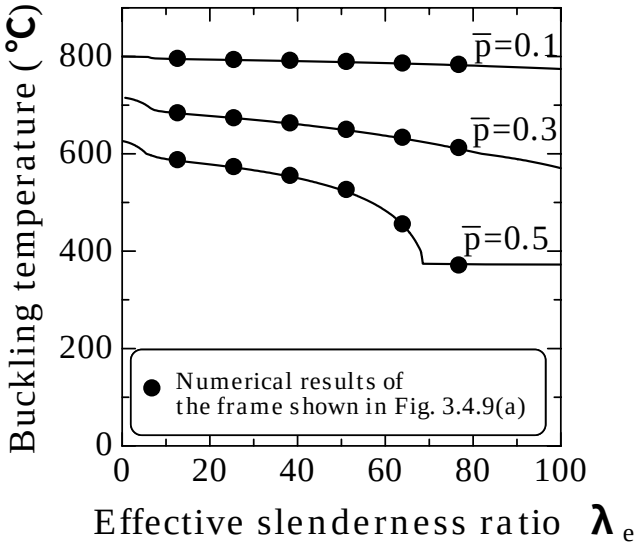

Fig.3.4.10 Numerically analyzed buckling temperatures of the interior column

3.4.3.2 Effect of the slenderness ratio

The figures 3.4.11 (a) and (b) show the axial force versus shortening relationships of the heated column of the frame with λ_e = 25.6 and $\bar{p}$ = 0.3. The numerical column buckling temperatures and the numerical ultimate temperatures of various multi-storied frames shown in Fig. 3.4.6(b) are shown in Fig. 3.4.12. The figures 3.4.12(a), (b), and (c) show the numerical results of the frames with the axial force ratios of 0.1, 0.3, and 0.5, respectively. The results of a four-storied and a six-storied frame are plotted in each figure. The solid lines represent the theoretical buckling temperature.

As discussed in section 2.3.1, a frame with high stress redistribution ability can keep stability after the interior column buckles, whose behavior can therefore be traced using the *load controlled analysis*. Thus such frames do not fall into instability although the heated columns buckle. In this case, the numerical buckling temperature is difficult to determine. In this study, the buckling temperature of the heated column is defined as the temperature at which the rate of the column shortening becomes the maximum with respect to temperature increment. In the above example, the point a in Fig. 3.4.11(b) corresponds to the state of buckling in view of the definition.

It is the matter of course that the column buckling temperature decreases according to the increase in the column slenderness ratio. However, as seen in Fig. 3.4.12(a), it is notable that the numerical ultimate temperatures of the frames with $\bar{p}$ = 0.1 is almost equal to 830oC regardless of changing column slenderness ratios.

On the other hand, observing the ultimate buckling temperatures of the four-storied frames with $\bar{p}$ = 0.3 in Fig. 3.4.12(b), it is contrastive that the numerical ultimate temperature of the frame decreases when the column slenderness ratio increases. The difference between the two cases results from the different manner in stress redistribution in both cases. A smaller axial forces carried by the buckled column may be fully redistributed by the surrounding beams. This corresponds to the cases of $\bar{p}$ = 0.1 in the above. This is also approximately the case of the above 6-storied frames with $\bar{p}$ = 0.3 (see Fig. 3.4.12(b)).

For all these frames, since all the axial forces initially carried by the buckled columns are fully redistributed, the resulting mode of collapse of the frame is, instead of column buckling, excessive hanging deformation of the heated beams at temperatures nearly equal to 830oC. On the other hand, for the above 4-storied frame cases with $\bar{p}$ = 0.3, the stress redistribution cannot be fully performed, since

the strength capacities of the surrounding beams are not enough to redistribute the axial force. The mode of collapse for these cases is buckling of heated interior columns. The according ultimate temperatures become the smaller significantly below 830oC with the larger slenderness of the buckled column. This topic will be considered in detail in the next chapter.

3.4.3.3 Effect of the number of floors of the frame

As seen in Fig. 3.4.12, the column buckling temperatures of the four-storied and six-storied frames are lower than their theoretical buckling temperature, and the column buckling temperature of the six-storied frame is lower than that of the four-storied frame. This is because the axial restraining effect on column buckling of the six-storied frame is greater than that of the four-storied frame.

The larger restraining effect gives the larger compressive force to the heated column as shown in Fig.3.4.11, where thermal compression grows up faster for the four-storied frames than for the six-storied cases. In fact, the axial force of the column for the four-storied frame increases up to $0.4\overline{P}_y$, while up to $0.45\overline{P}_y$ for the six-storied frame. Note that both columns were subjected to $0.3\overline{P}_y$ equally at initial room temperature.

On the other hand, it is found that the ultimate temperature of the six-storied frame is higher than that of the four-storied frame. This indicates that the stress redistribution ability is greater for the former frame than for the latter.

However, for some frames in Figs. 3.4.12(b) and (c), the ultimate temperatures are found to be lower than the theoretical buckling temperature. For example, four-storied frames of $\overline{p} = 0.3$, $\lambda_e > 30$ and those of $\overline{p} = 0.5$, $\lambda_e > 20$ are such cases.

The frames whose ultimate state are almost coincident with the column buckling in Fig. 3.4.12, are found to fall always in instability with snap-through action once the heated columns buckle. Such frames have necessarily either weaker columns with poor post-buckling strengths or less stiff and/or weaker beams.

From these results, it can be concluded that the buckling temperature of the heated column undergoing a thermal stress cannot be evaluated by only the theoretical buckling temperature calculated from Eq. (3.2.1).

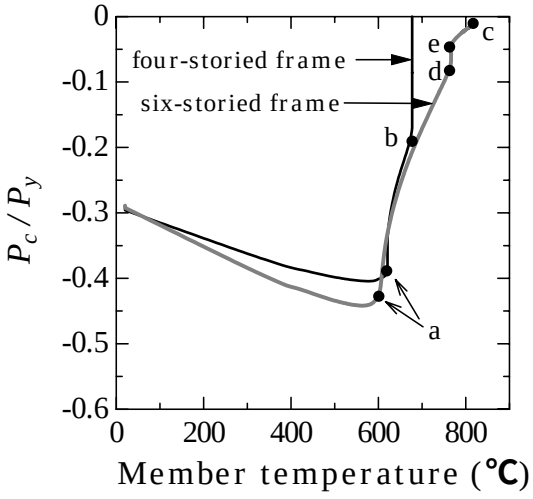

(a) Axial forces of the columns

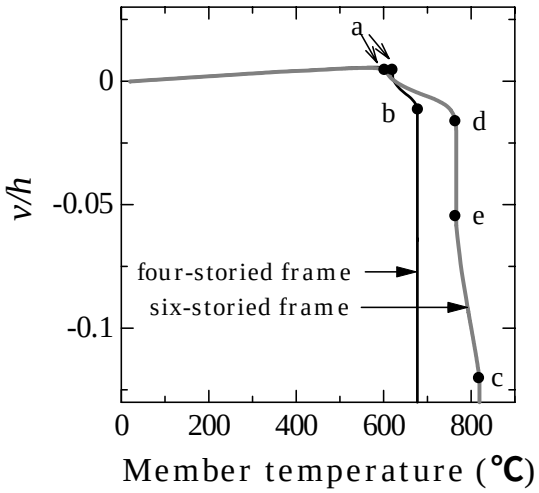

(b) Vertical displacement of the head of the heated column

P_C : Axial forces of the columns

v : Vertical displacement of the head of the first floor interior column

h : Height of the first floor

Fig. 3.4.11 Summaries of analysis for steel frames which the interior column is heated

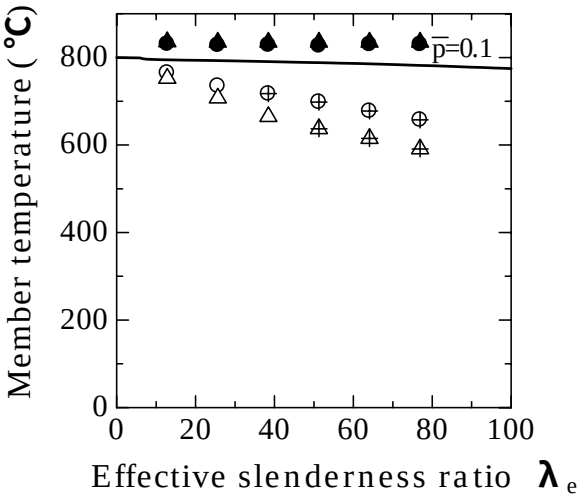

(a) The axial load ratio $\bar{p}$ = 0.1

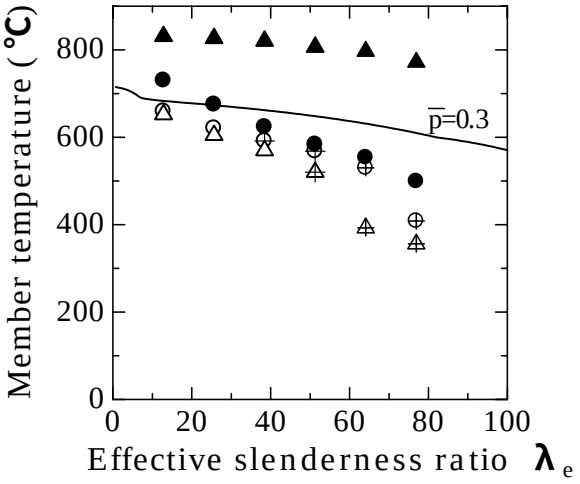

(b) The axial load ratio $\bar{p}$ = 0.3

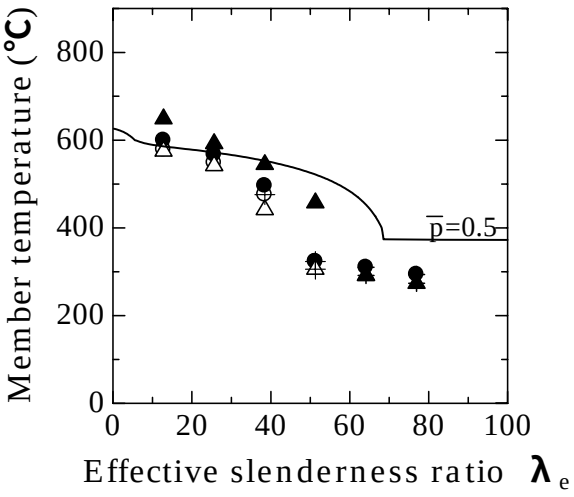

(c) The axial load ratio $\bar{p}$ = 0.5

Numerical results

○ Buckling temperature of four-storied frame ● Ultimate temperature of four-storied frame

△ Buckling temperature of six-storied frame ▲ Ultimate temperature of six-storied frame

+ Temperature that “Snap through” phenomenon occurred

Fig. 3.4.12 The numerically analyzed buckling temperature of interior column and ultimate temperature of the steel frame shown in Fig. 3.4.9(b)

3.5 Conclusion

In this chapter, the buckling temperature of the columns subjected to fire is extensively investigated. The following conclusions can be drawn:

◆ The rotationally restraining effect of the connecting members has an effect on the column buckling temperature. However, the thermal expansion of the beam does not have a direct affect on the buckling temperature

◆ The exterior column is not axially restrained by the adjacent members during fire. The lower end of the heated column is rotationally restrained by the unheated connecting members, so its boundary condition can be assumed to be fixed end. On the other hand, for the upper end of the heated column's case, the rotationally restraining effect of the upper-story unheated column can be neglected due to the thermal expansion of the beam. The buckling temperature of the exterior column can be assumed to be the theoretical buckling temperature (Eq. (3.2.1)) when the effective length is determined from the proposed equation (Eq. (3.3.8))

◆ The interior column is strongly rotationally restrained by the adjacent members, so its effective length is equal to $0.5h$. However, it is also axially restrained by the adjacent members. As a result it buckles at a temperature that is lower than the estimated buckling temperature. In this case, when considering the buckling temperature, the thermal effect should be included.

Chapter 4

The ultimate temperature of steel frames subjected to fire

4. The ultimate temperatures of steel frames subjected to fire

4.1 Introduction

It is one of the most important findings in the previous chapter that not only rotational but also axial restraining effects of the surrounding members affect the behavior of a steel structure with heated and buckled columns. The effective length of a heated column is affected by rotationally restraining beams that are connected to the heated column and the higher buckling temperature results for columns with shorter effective buckling lengths. On the other hand, since the surrounding members restrain simultaneously the axial lengthening of the heated column, the thermal compressive force is induced in the column in addition to the existing compressive force. This lowers the buckling temperature of a restrained column. However, after the heated column buckles, the same surrounding members turn to work to redistribute a part of the compressive force which was carried initially by the buckled column to other sound columns. By means of this action, a lot of steel frames subjected to fire do not collapse directly due to buckling of heated columns and therefore the ultimate temperatures of these frames are greater than the initial buckling temperature of the local component.

From the above discussion, the surrounding members are found to provide two conflicting effects to the failure of a steel frame subjected to fire. One effect of the surrounding members is to restrain the thermal elongation of the heated column and therefore to increase its compressive force resulting in lowering its buckling temperature. The other effect is to redistribute the compressive force of a buckled column and therefore to heighten the ultimate temperature of the entire frame. The first effect has been studied and reported in many papers but all researches covered only the member level. On the other hand, Jean-Marc (2000) also researched about the redistribution effect of beams. That paper also proposed an analytical method for the failure temperature of columns, and discussed that the overall structure does not collapse down although the axially restrained column buckled early. However, the way to evaluate the ultimate temperature of frames did not expressed at all.

In this chapter both effects of the axial restraint of the surrounding members are studied extensively in the structure level. Furthermore a way to evaluate and formulate both the buckling temperature under thermal effects and the ultimate temperature of frames are proposed. Rigidly connected regular steel frames and

hatted frames are considered herein, where fire is to occur inside an inner or outer span of some single floor. The parametric studies using the proposed *alternate control analysis* are adopted to study these effects. Comparing the numerical results with the predicted buckling and ultimate temperatures obtained by the proposed formulae, the accuracy and applicability of the formulae are verified in detail. In the end of this chapter, an introduction is made how to prevent a structure from fatal instability when it is subjected to fire.

4.2 The buckling temperature of heated columns under thermal effect

For such a frame as shown in Fig 4.2.1, due to restraint of thermal elongation provided by adjacent members, the axial force of a heated column will increase during fire. This increase is a function of the stiffness of the adjacent beams and thermal elongation of the heated column. For analysis, a structure may generally be represented by a simple system shown in Fig.4.2.2. In this system, a longitudinal spring is connected to a buckled column so as to represent the effect of the rest of the structure on the column. If the action of the spring is assumed to be linear, the longitudinal thermal force at temperature T is written as the following.

$$Q = \frac{K_S K_C}{K_S + K_C} \alpha T h \tag{4.2.1}$$

where K_S is the stiffness of the spring, K_C is the stiffness of the column varying as function of time, α is the thermal expansion coefficient, T is the column temperature, and h is the height of the column.

From Eq. (3.2.1) and Eq. (4.2.1), the buckling temperature of the column under the thermal effect can be evaluated from the following equation.

$$\lambda_e = \sqrt{\frac{\pi^2 E_t(T_{cr,}\, \bar{p}\bar{\sigma}_y + \sigma_{th}(T_{cr}))}{\bar{p}\bar{\sigma}_y + \sigma_{th}(T_{cr})}} \tag{4.2.2}$$

where $\sigma_{th} = Q/A$, σ_{th} is the thermal stress, and A is the cross-sectional area of the heated column.

To calculate the theoretical buckling temperature of a column without a spring, as seen previously in section 3.2, Eq. (3.2.1) gives an explicit solution for the slenderness ratio of the column if its buckling temperature and its axial force ratio are given. On the other hand, for a column with a spring, Eq. (4.2.1) is not explicit with respect to λ_e, since σ_{th} on the right hand side is a function of unknown λ_e. An approximate solution for this problem is proposed below.

As shown in Fig. 4.2.1(b), the members restraining the heated column are unheated beams placed inside the spans next to the fire compartment. As the heated column expands, all such beams become bent almost anti-symmetrically and

the corresponding restraining force increases. Finally, as seen in Fig. 4.2.3, Plastic hinges may be formed at both ends of all the individual beams. Therefore the restraining effect of these beams is maximized when full formation of the plastic hinges on all these beams. In the case of a frame shown in Fig. 4.2.3, for example, the maximum restraining force acting on the buckling column is written as follows:

$$Q_p = \frac{2nM_p^b}{l} \tag{4.2.3}$$

where M_p^b is the full plastic moment of the unheated beam, n is the number of the beam placed in the outer span, and l is the outer span length. It is assumed herein that the restraining effect of the adjacent members can be evaluated by the above maximized and constant Q_p instead of Q which changes according to temperature increase of the column. This means the buckling temperature of the column under thermal effect can be easily evaluated from Eq. (4.2.2) when $\sigma_{th} = Q_P / A$ are substituted. So the buckling temperature of the column under thermal effect can be evaluated from the expression as follow:

$$\lambda_e = \sqrt{\frac{\pi^2 E_t (T_{cr,}\, \overline{p}\overline{\sigma}_y + \sigma_{th})}{\overline{p}\overline{\sigma}_y + \sigma_{th}}} \tag{4.2.4}$$

However, the buckling of the column does not necessarily occur when the thermal stress in column reaches its maximum value. In fact, the slenderness ratios of columns of general steel-framed buildings are less than 40. In these cases, an increase in thermal elongation is not very severe. So the heated column, in most cases, buckles before the both ends of the beams become inelastic. Nevertheless, Eq. 4.2.3 is more appropriate than Eq.4.2.1 because it is just a function of M_p^b, n and l, thus, it is not temperature dependent. This Q_p is the upper limit of the thermal force, so the buckling temperature under thermal effect calculated from Eq. (4.2.4), is conservative. The accuracy of this approximation will be verified in detail in section 4.5.

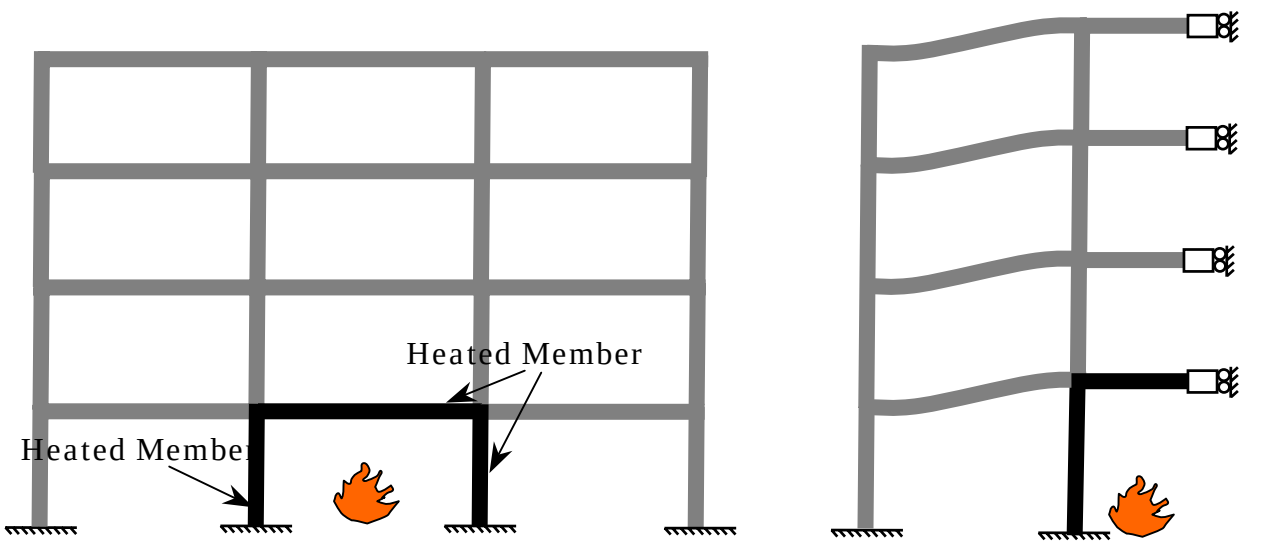

(a) A steel frame

(b). The heated steel column restrained by the surrounding member

Fig. 4.2.1 A steel structure subjected to fire

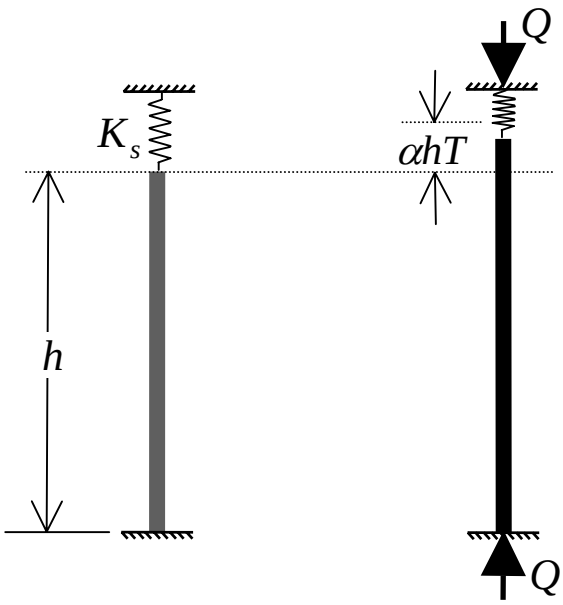

(a) A steel column at room temperature

(b) An axial compression due to the thermal expansion

Fig. 4.2.2 Simple model of a restrained column

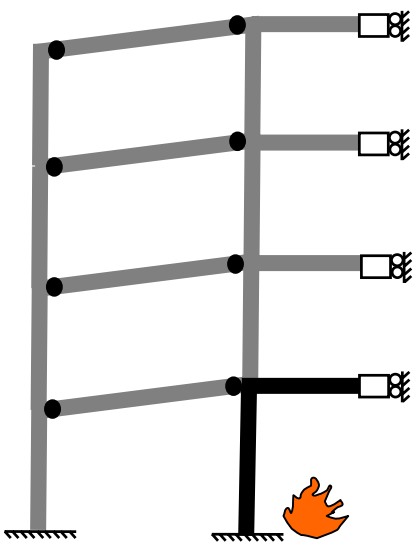

Fig. 4.2.3 The plastified surrounding beam due to the column's thermal expansion

4.3 The residual resisting force of a buckled column

It was discussed in section 2.5.2 and 3.4.3 that not only the strength of surrounding members but also the residual strength of buckled columns play important roles to prevent a frame under fire from falling into instability. Therefore, it is necessary to evaluate the post-buckling load-axial deformation relationships of a buckled column.

In 1954, Paris proposed load-axial deformation relationships for long compression members. For a long column, after the mid-span of the column becomes plastified, the column suddenly falls into buckling. So, Paris assumed that the plastic hinge is formed at the mid-span section of the column. In his study, the axial deformation of a column in the plastic range was calculated from the sum of two causes, i.e. the shortening due to elastic deformation and the shortening due to flexure. The author has shown that the load-axial deformation relationships calculated from proposed equation is in good agreement with the test results of the columns with the effective slenderness ratio of 76.3, 118, and 159, respectively. It has however been found that, for the shorter column with the effective slenderness ratio of 34.6, the proposed load-axial deformation relationship is found to be lower than the test result.

Concerning this problem, Katoh et al. (1975) presented an equation to calculate load-axial deformation relationships of short columns. A short column, although the axial load reaches the yield strength, does not buckle suddenly and the inelastic range spreads longitudinally from the mid-span as the loading proceeds. Thus, the shortening due to plastic deformation is added to the Paris's equation in their studies. The resulting load-axial deformation relationships are in good agreement with all length range of columns. However their proposing equations are too complicated to handle intuitively. Furthermore, the above studies are limited to columns under room temperatures. The load-axial deformation relationships of the column under elevated temperature are not clearly studied to date. Therefore in this study, the load-axial deformation relationships of a buckled column at elevated temperatures are proposed. These relations will be used to consider the *beam plastified temperature* in the next section.

A simply supported and centrally compressed column is shown in Fig.4.3.1. To make the equation simplified and practical, the cross section of the column is assumed to be a two-flange section. Therefore, the moment-curvature relationships of a beam with an identical cross-section are similar to its stress-strain

relationships. This study focuses on the high temperature behavior, thus the bilinear stress-strain relationships were adopted for steel. Fig.4.3.2 shows the moment-curvature relationships under a temperature T. E is Young modulus, while E_t is a tangent modulus of the plastic steel at temperature T. The interaction function of a two-flange section can be written as $M/M_P = 1-(P/P_y)$. So the solid line shown in Fig.4.3.2 represents the moment-curvature relationships of the column with applied axial force ratio $\overline{p}$.

As the column shortens after it buckles, the plastic range spreads longitudinally from the mid-span of the column. As shown in Fig 4.3.1(b), the interval bc is assumed to be still elastic, while the interval ab is assumed to reach elastic-plastic state. The strain distributions of both states are shown in Fig 4.3.3. The deflection of the buckled column is assumed to be a sine curve as the following.

$$y = \delta \sin \frac{\pi x}{2h} \tag{4.3.1}$$

where δ is the deflection at mid-span. Therefore, the moment at point a and b can be calculated from

$$N\delta \sin \frac{\pi l_1}{2l} = M_p^c = M_{po}^c \cdot (1-\frac{N}{P_y^c}) \tag{4.3.2}$$

$$N\delta = M_p^c + 2E_t I_c (\phi - \phi_y) \tag{4.3.3}$$

respectively, where M_{p0}^c is the full plastic moment, M_p^c is the full plastic moment when load N is applied, P_y^c is yield strength of the column, I_c is the moment of inertia, and $\phi_y = 2\varepsilon_y / d$ is the yield curvature, respectively of the cross section.

Substituting $y''(l) = \phi = \delta \cdot (\pi / 2h)^2$ into and assuming $\phi >> \phi_y$ in Eq. (4.3.3), we have

$$\delta = \frac{M_p^c}{N - 2P_t} \tag{4.3.4}$$

where $P_t = E_t I_c \left(\frac{\pi}{2h} \right)^2$ (4.3.5)

Substituting Eq. (4.3.4) into Eq. (4.3.2) yields

$$\sin \frac{\pi h_1}{2h} = 1 - \frac{2P_t}{N} \tag{4.3.6}$$

h_1 can be determined by solving the above equation.

The axial shortening deformation of a buckled column can be calculated as follows:

$$\Delta = y_e + y_p + y_g \tag{4.3.7}$$

where y_e, y_p, y_g are elastic shortening, plastic shortening, and shortening due to flexure, respectively. So the load-axial deformation of the buckled column is written in the following form.

$$\Delta = \frac{1}{2} \int_0^h (y')^2 dx + \int_{h_1}^h (\varepsilon_0) dx + \frac{Nh}{EA} \tag{4.3.8}$$

where $\varepsilon_0 = \frac{d_c}{2} \phi = \frac{d_c}{2} y''$. Therefore, Eq. (4.3.8) can be rewritten as follows:

$$\Delta = \frac{(\delta \pi)^2}{16h} + \frac{\delta \pi d_c}{4h} \left(\sqrt{1 - \left(1 - \frac{2P_t}{N} \right)^2} \right) + \frac{Nh}{EA_c} \tag{4.3.9}$$

If the column length is H ,Eq. (4.3.9) can be rearranged as follow

$$\Delta = \frac{(\delta \pi)^2}{4H} + \frac{\delta \pi d_c}{H} \left(\sqrt{1 - \left(1 - \frac{2P_t}{N} \right)^2} \right) + \frac{NH}{EA_c} \tag{4.3.10}$$

where $P_t = E_t I_c \left(\frac{\pi}{H} \right)^2$

The full plastic moment M_{p0}^c and the yield strength P_y^c at elevated temperatures are functions of the temperature, i.e. M_{p0}^c and P_y^c decrease according to increase in temperature and represented as follows:

$$M_p^c = \kappa(T) \cdot \overline{M}_{p0}^c \qquad (4.3.a)$$

$$P^c = \kappa(T) \cdot \overline{P}_{y0}^c \qquad (4.3.b)$$

where $\overline{M}_{p0}^c$ and $\overline{P}_{y0}^c$ are the full plastic moment and the yield strength of the column section at ambient temperature, respectively. $\kappa(T)$ is the reduction ratio of the strength of material at elevated temperature. This $\kappa(T)$ can be obtained as follows:

$$\kappa(T) = \begin{cases} 1 & ;(RT \le T < 400) \\ 1 - \frac{0.9}{400}(T - 400) & ; \quad T > 400 \end{cases} \qquad (4.3.c)$$

In this study, JIS SS400 steel is taken as the testing material. The stress-strain relationships of the heated steel propose by Furumura et al. (1986) are adopted to use in the analysis and therefore E and E_t of the bilinear stress-strain relationships that used to calculate the present load-axial deformation relationships can be obtained from the following expression:

$$E(T) = (1.0 - 0.905 \cdot 10^{-6}) \cdot E_{RT} \qquad (4.3.d)$$

$$E_t(T) = \begin{cases} 40 & ;(RT \le T < 400) \\ (1 - \frac{0.9(T - 400)}{200}) \cdot 40 & ;(400 \le T < 600) \\ (1 - \frac{(T - 600)}{250}) \cdot 4 & ;(600 \le T < 850) \end{cases} \qquad (4.3.e)$$

where E_{RT} =2100 tf/cm^2.

$E_t(T)$ is the averaged tangent modulus at temperature T determined from the slope of the stress-strain relationships at $\varepsilon = 0.025$ in Furumura's relationships.

Fig. 4.3.4 illustrates the solved post-buckling relationships of heated columns based on the above proposed prediction and compared them with the numerical solutions at temperatures of RT, 400, 500, 600, 700, 800 $°C$, respectively. The column's cross-section is Box:350x350x16 in the numerical analyses. Three column slenderness ratios, 25.6, 38.6 and 51.2, are analyzed. It can be seen that increasing the column temperature and the column slenderness ratio decrease the residual resistant force of a column. It is because reduction in both the strength and the tangent modulus of the heated column causes reduction in the residual resistance of a column.

It is found that, for the columns at temperature of RT and 400°C, the load-axial responses calculated from Eq. 4.3.10 are stronger than the numerical ones when Δ/h is over 0.02. This discrepancy may result from the inaccurate assumption for strain distribution of the mid span sections of the column. Regardless of the fact that, after the column is largely deformed, bending straining comes to predominate in these sections over shortening straining, the increasing plastic shortening strain ε_o is always assumed to take place in the above prediction (see Figures 4.3.3(b) and (c)). That means the axial deformation determined form Eq. (4.3.10) is larger at least in a certain extent than the actual value. On the contrary, in the high temperature range, T > 500℃, the results calculated from the proposed equation, Eq. (4.3.10), are in good agreement with the numerical results. Furthermore, Eq. (4.3.10) is readily calculated. Eq. (4.3.10) seems therefore appropriate to estimate the load-axial relationships of the column at the elevated temperatures. The certainty of the prediction will be observed specifically in later sections.

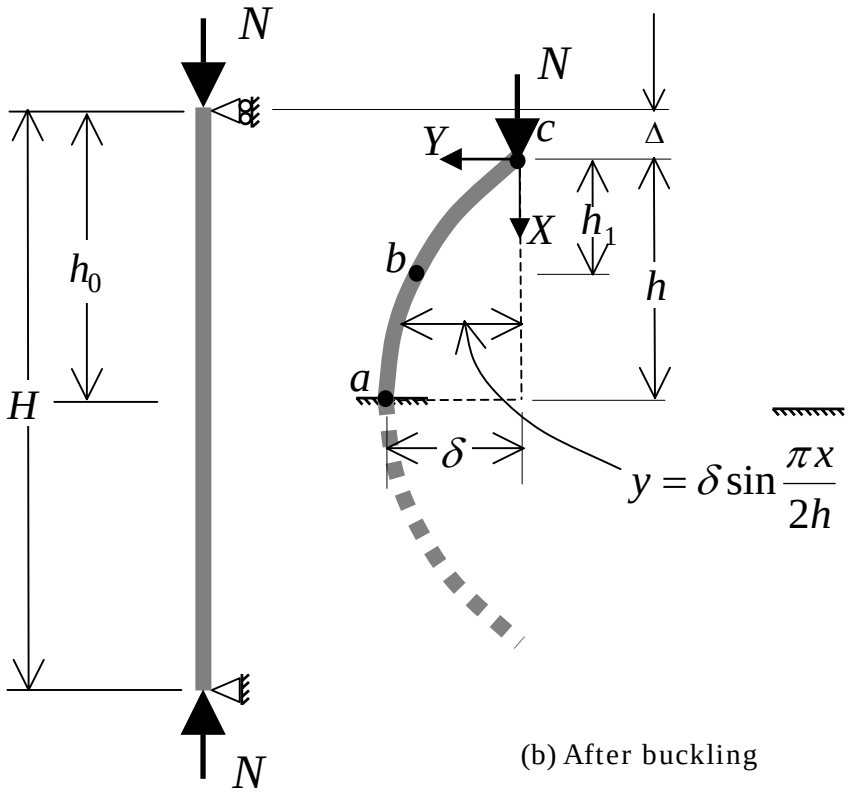

(a) Before buckling

Fig. 4.3.1 The simply supported column

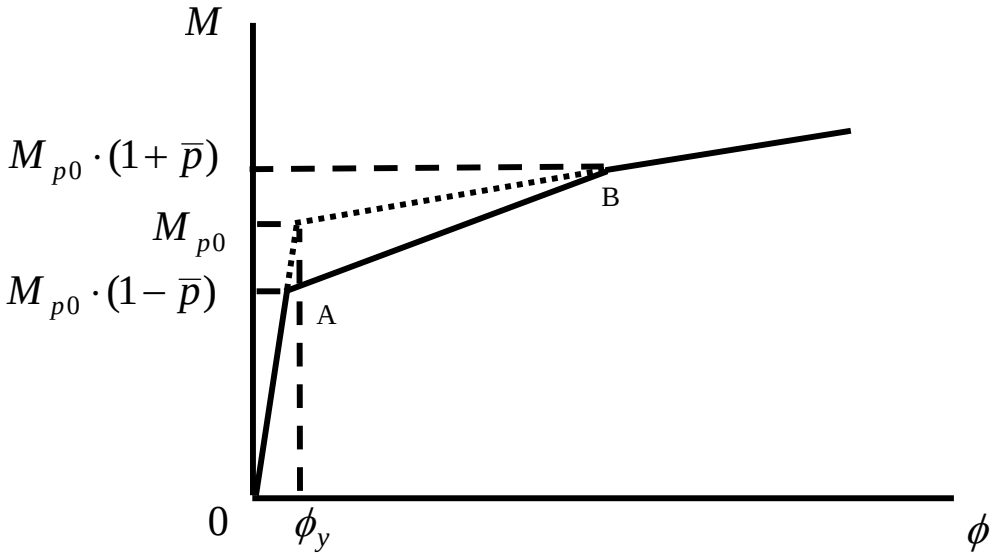

Fig. 4.3.2 Moment-curvature relationships of two-flange columns at Temperature T

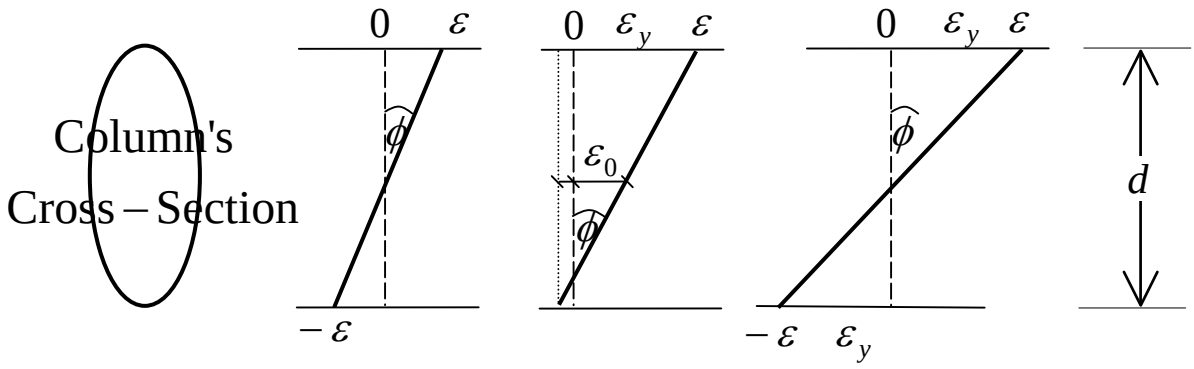

(a) Elastic State (b) Elasto-Plastic State (c) Plastic State

Averaged Strain $\varepsilon_0 \approx \frac{d}{2}\phi$

Fig. 4.3.3 The strain distribution of the column

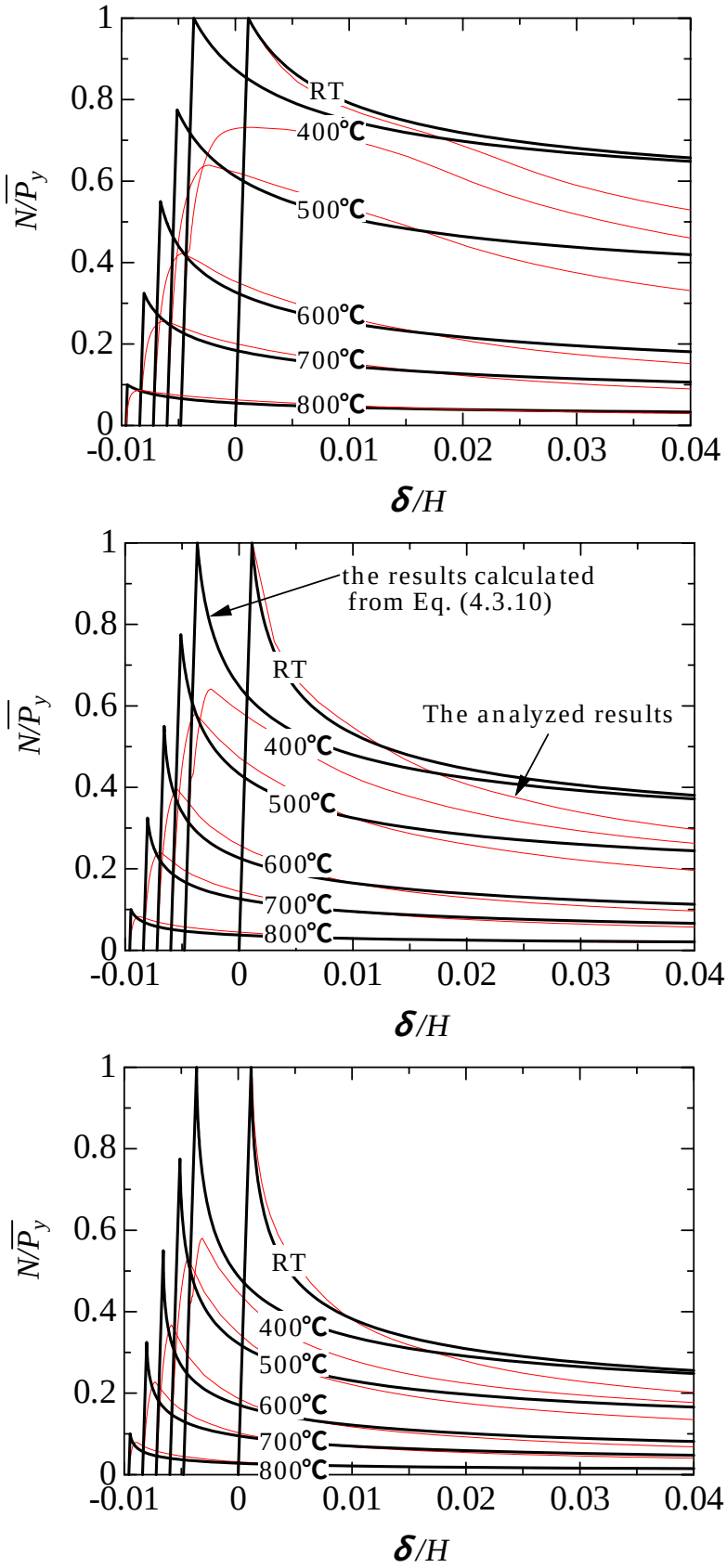

(a) λ_e = 25.6

(b) λ_e = 38.6

(c) λ_e = 51.2

Fig. 4.3.4 The load-axial deformation relationships at vary temperatures

4.4 The predicted ultimate temperature of a steel frame subjected to fire (The temperature when beams are fully plastified)

After a column buckles, a part of the load which cannot be supported by the buckled column is redistributed to other sound columns with the help of adjacent beams. The stress redistribution of the adjacent beams is herein discussed specifically. The external vertical force and the vertical components of forces carried by a buckled column and the adjacent beams are respectively shown in Fig. 4.4.1. The equilibrium of the vertical forces can then be expressed as follows:

$$P - Q(\Delta) - N(\lambda, \Delta, T) = 0 \tag{4.4.1}$$

where P is the external vertical force, Q is the shear strength of the adjacent beams, and N is the residual resistance of the heated buckled column..

Under elevated temperatures, after a column buckles, increase in temperature and axial displacement of the column are to cause decrease in its residual resistance. However, the shear strength of adjacent beams Q increases according to their increasing vertical displacement as the axial displacement of the heated column increases compatibly. We assume that the structure can retain its static equilibrium and stability until all of these beams become fully plastified. However, once the strength Q of the beams becomes maximized due to their full plastification, the system must fall necessarily into instability in view of the equilibrium equation (4.4.1), since this equation cannot hold with the maximized Q and the continuously decreasing N of the buckled column. Therefore the full plastification of the adjacent beams may accord to one of the ultimate states of a frame subjected to fire. In this section, the temperature of structure at which the beams become fully plastified will be determined.

Since, after the adjacent beams become fully plastified in a frame shown in Fig. 4.4.2, plastic hinges are formed at both ends of beams, the shear force carried by all the adjacent beams can be evaluated easily as follows:

$$Q_p = \frac{2nM_p^b}{l} \tag{4.4.2}$$

where M_p^b is the full plastic moment of the unheated beam, n is the number of

the beam placed in the outer span over the fire floor, and l is the outer span length. However, if the fire compartment is otherwise placed, this Q_p will be evaluated differently. To evaluate Q_p for various structural and compartment forms will be found in the next section. Regardless of the fact that the expression of Q_p depends on the structural configuration where the heated column and the surrounding beams are placed, it is important to notice that its expression and therefore its quantity are always identical to the aforementioned maximized thermal compressive force onto the buckled column.

When the beams are fully plastified, the equilibrium equation can be written as the following expression.

$$P - Q_p - N(\lambda, \Delta_p, T) = 0 \tag{4.4.3}$$

where Δ_p represents the deflection of the beams when they become fully plastified. Since this deformation coincides with the axial deformation of the buckled column, the frame is to collapse directly after this state is reached. We assume that Δ_p is the elastic transverse deflection of an anti-symmetrically bent beam when the maximum fiber strain in the so deformed beam attains $3\varepsilon_y$, since this magnitude of strain may be enough for the beam to form plastic hinges at its both ends. The resulting Δ_p is written as the following.

$$\Delta_p = \frac{\varepsilon_y l^2}{d} \tag{4.4.4}$$

In case of JIS SS400 steel, this Δ_p can be determined by the following expression.

$$\Delta_p = \frac{l^2}{875d} \tag{4.4.5}$$

where l and d are the span length and the depth of the restraining beam.

Substituting Eq. (4.4.5) into Eq. (4.4.3), the critical temperature can be calculated, at which the restraining beams become fully plastified and therefore the frame is to fall into overall instability. Among the factors in Eq.(4.4.3), the residual resistance of the column N is only the factor that depends on temperature, while the shear strength of restraining beams Q_p and the axial force P are constant

respectively even though the member temperature changes. Therefore, if the structural geometry and load conditions are given, Eq. (4.4.3) can be solved with respect to only an unknown temperature, which is the critical temperature asked in this section. The procedures to determine this temperature are described in the following.

First step for solution is to obtain the constants, i.e. the shear strength of beams Q_p, the initial axial force of the heated column P, the column slenderness ratio λ, and the limiting axial deformation of the column Δ_p, respectively depending on the given structural and thermal conditions. The next step is to find the temperature that nullifies Eq. (4.4.3). Since the equation is nonlinear, trial and error method is used as follows. A trial quantity of N is determined if λ, Δ_p, and a trial temperature T are given. This N is greater than $P-Q_p$ if the temperature T is too low. This indicates that, at this temperature, the frame retains stability and does not collapse at this member temperature T. An increase in temperature leads to a decrease of the resistance N. Therefore a simple iterative choose of T makes N approach readily to the quantity $P-Q_p$. This procedure is continued until N becomes close sufficiently to $P-Q_p$. The temperature so solved is the one at which the beams become fully plastified (as shown in Fig. 2.5.4(b)), which is to coincide with the ultimate temperature of the steel frame subjected to fire

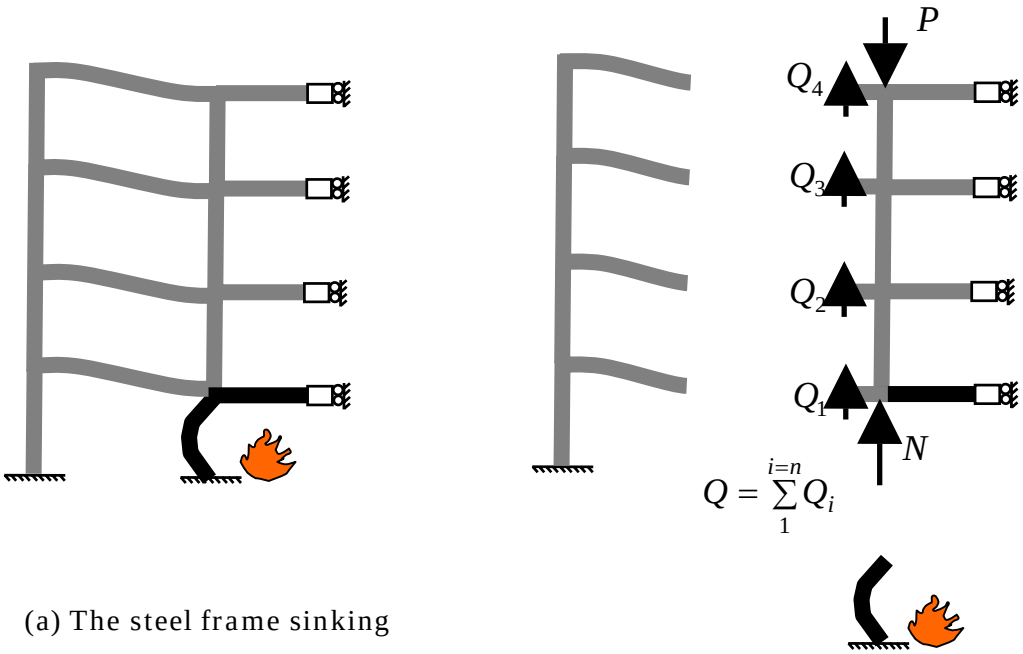

(a) The steel frame sinking due to the column buckle

(b) The equilibrium of the vertical forces acting on the steel frame

Fig. 4.4.1 A steel frame during fire after the column buckles

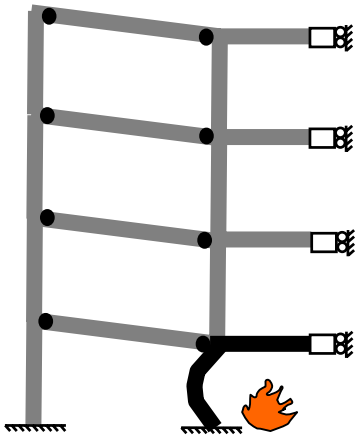

Fig. 4.4.2 A steel frame after the adjacent beams fully plastified

4.5 Evaluation of the ultimate temperature of frames and the buckling temperature of heated columns

In this section, the axially restraining effects of adjacent members on the column buckling temperature and the ultimate temperature of frames are investigated. Parametric analysis is carried out to study the effect of various column slenderness ratios and the axial forces of columns on the ultimate temperature of frames and the buckling temperature. The accuracy of the proposed predictions of Eq. (4.2.4) and Eq. (4.4.3) are verified specifically by comparing them with numerical results. For this purpose, the *alternate controlled analysis* method proposed in section 2.4 is adopted again to obtain numerical results. Herein, two conditions of fire compartment and two types of structure are considered and JIS SS400 steel is taken as the material.

4.5.1 Simple frames when fire occurs at an inner span

Fig. 4.5.1 shows a multi-storied frame and is adopted for study herein. It is because of symmetry of the structure that only the left half is illustrated in the figure, which is actually subjected to present numerical analysis.

To predict the buckling temperature of an interior column, Fig. 4.5.2(a) is used in that the plastic hinges are formed at the both ends of the adjacent beams which are provided by the thermal expansion of the heated columns. Instead, to predict the ultimate temperature of the frame, Fig. 4.5.2(b) is used, where both ends of the adjacent beams are plastified after the heated column buckled and shortened. Since, within the prediction, the latter state coincides with the one when the beams are fully plastified, the temperature according to this predicted state is referred to as *beam plastified temperature* herein.

In Fig. 4.5.2(a) and (b), the thermal compressive force acting on the heated column can be determined from the following expression:

$$Q_p = \frac{2nM_p^b}{l} \tag{4.5.1}$$

The buckling temperature of the column under thermal effect can be evaluated from the expression as follow:

$$\lambda_e = \sqrt{\frac{\pi^2 E_t (T_{cr,}\, \bar{p}\bar{\sigma}_y + \sigma_{th})}{\bar{p}\bar{\sigma}_y + \sigma_{th}}} \tag{4.5.2}$$

where $\sigma_{th} = Q_p / A$. And the beam strength restraining the buckling column can be obtained from the next expression

$$Q_p = \frac{2nM_p^b}{l} \tag{4.5.3}$$

Where M_p^b is the full plastic moment of the unheated beam, n is the number of the beam placed in the outer span over the heated story, and l is the outer span length. As pointed out, equations 4.5.1 and 4.5.3 are identical to each other. Using the above quantities, the beam plastified temperature can be determined from the

expression as follow:

$$P - Q_p - N(\lambda, \Delta_p, T) = 0 \qquad (4.5.4)$$

The definitions for the variables are described in section 4.4. From the above expressions, the buckling temperature under the thermal effect and the ultimate temperature of the structure can be predicted by Eq. (4.5.2) and Eq. (4.5.4), respectively. The effective slenderness ratio of interior columns is to be 0.5 as seen in chapter 3.

The analysis parameters are as follows:

1. Beam strength (the restraining members)
2. Column slenderness ratio
3. Axial force ratio of the interior column
4. Beam size and beam span length
5. Column size

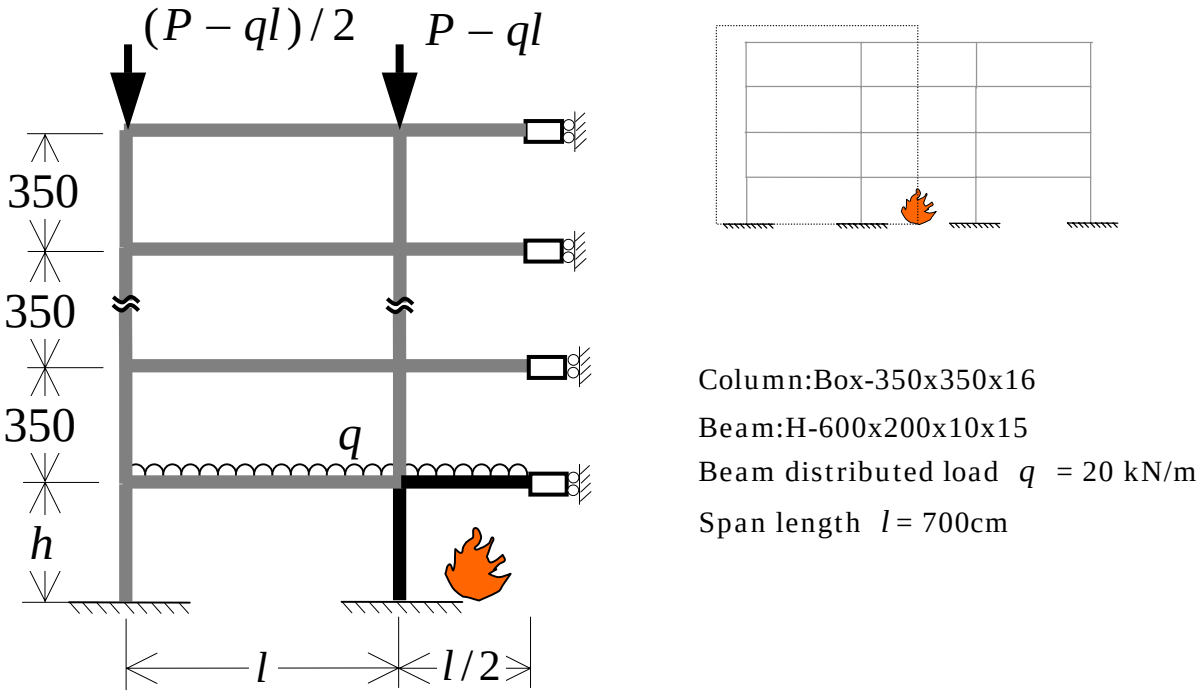

Fig. 4.5.1 The analysis model of a steel frame when fire occurs at an inner span

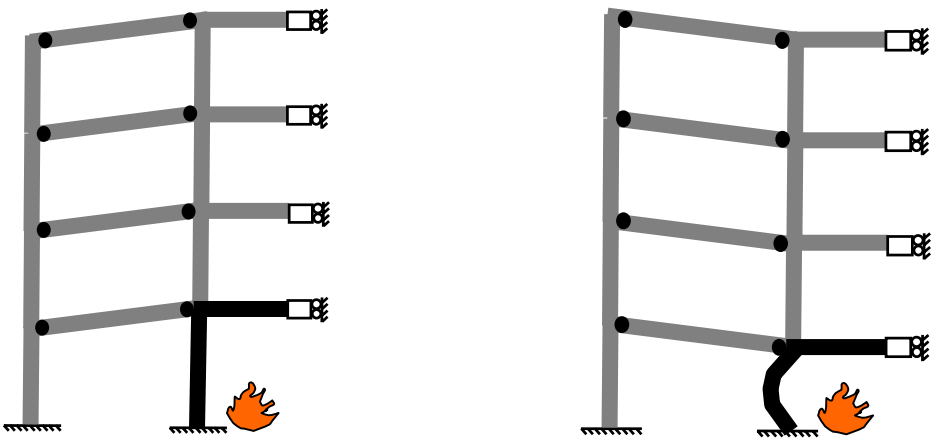

(a) Plastified surrounding beams due to the column's thermal expansion

(b) Plastified surrounding beams after the column buckled

Fig. 4.5.2 The steel frames after the adjacent beams fully plastified

Table 4.5.1 The analysis parameters of steel frames when fire occurs at inner span

Axial load ratios $\overline{p}$	0.2, 0.3, 0.4, 0.5
Slenderness ratios λ	25.6, 36.63, 51.3, 78.6, 102.6, 115.4, 128.2
Number of the story n	1-12

4.5.1.1 Effects of the beam strength (the restraining members)

The behavior of a structure subjected to fire has been summarized in section 2.5.2. In this section the study focuses on the effects of various analysis parameters and how to determine the ultimate temperature of the steel frame.

A series of numerical response analysis for a single storied through twelve storied frames are conducted and the results are summarized in Fig. 4.5.3 which shows the frames' ultimate temperature versus beam strength relations. In Fig. 4.5.3(a), (b), and (c) numerical results are shown of the frames with the effective slenderness ratio of the heated column of 20, 25, and 40, respectively.

As shown in the Fig. 4.5.3(b.1), the ultimate temperature of a single storied frame is almost the same as the aforementioned theoretical buckling temperature of 623℃ of the interior column which is shown as a horizontal solid line in the figure. For the two and three storied frames, the ultimate temperature becomes lower than the theoretical buckling temperature. It is because the larger thermal compressive forces are added to the interior columns due to the larger restraining effects of the beams in these cases. For the above three cases, the frames lose their stabilities immediately after the interior columns buckle and they never recover stabilities subsequently. The ultimate temperatures of these cases therefore coincide almost with the one when the interior columns buckle, which is marked by ○ in the figure.

On the other hand, the ultimate temperatures for the taller frames turn greater than the theoretical buckling temperature. The figure moreover indicates that the greater ultimate temperature is obtained, as the frame becomes the taller. Two conflicting roles are therefore inherent in the effects of Q_p. The restraining effect of Q_p adds thermal compressive stress and lowers the buckling temperature of the heated column as shown by the marks ○ in the figure. The stress redistribution effect of Q_p, on the contrary, works after the column buckles and adds stability to the frame. In fact, these taller frames remain still stable under higher temperatures after the interior columns buckle. They keep stabilities until the beams become fully plastified. The marks ● in the figure are in accordance with these temperatures which are now defined as the ultimate temperatures for these cases, since, as similar to the previous six storied case, too large further deformations are required until the plastified beams subsequently form catenary action and the frames then recover stabilities. For a single, two and three storied cases, however, the stress redistribution actions do not work effectively, since the quantities of Q_p are small, which results in the fact that the ultimate temperatures of these frames are lower than the buckling temperatures of the

interior columns.

The ultimate temperatures of the frame marked by $\times$ in the figure indicates that it fails locally without losing overall stability in that the heated center beam hangs down excessively near these temperatures. Since, under these temperatures lower slightly than 850°C, the material is to lose almost all strength as shown in Fig.2.2.1, any beam under these temperatures may collapse if it carries any load. This further indicates that the equally heated interior column must also lose its compressive strength at the same time, since both the column and the beam are of the same material. Regardless of this fact, the analysis results have shown that the frames in these cases do not lose their overall stabilities. As shown in the figure, the quantities Q_p for these cases are nearly equal to or greater than $0.4\overline{P}_y$. From the primary strength of materials, the strength of the beam therefore seems to be enough to redistribute the vertical load $0.4\overline{P}_y$ to the exterior column, which was initially carried by the interior column. The resulting solutions have therefore provided the evidence that this simple mechanical assessment is valid for these cases.

The predicted buckling and ultimate temperatures are also shown in the respective figures of Fig. 4.5.3. The buckling temperature of the column predicted by Eq. (4.5.2) is depicted by the gray broken line, while the black broken line indicates the frame's ultimate temperature predicted by Eq. (4.5.4). As seen in the respective figures, the numerical buckling temperature of the column is equal to the theoretical one when the beam strength is close to zero, while the numerically obtained ones lower below this temperature the more, as the beams become the stronger. On the other hand, the predicted beam plastified temperatures of the frames increase as the beams become stronger.

For a single and two storied cases, the predicted beam plastified temperatures are lower than the corresponding theoretical buckling temperatures. In theses cases the frame is considered to collapse directly after the heated columns buckle and therefore the ultimate temperature of this frame is to coincide with this buckling temperature, since the weak beams of this frame may not redistribute the force after the column buckles at this temperature. On the other hand, in case when the predicted beam plastified temperature is higher than the column buckling temperature, it is considered that, by means of the stress redistribution ability, the strong beams of this frame heightens the temperature over the column buckling temperature after the column buckles. Therefore the ultimate temperature of the frame in this case is to coincide with the beam plastified temperature. From above discussion, the ultimate temperature of structure can be evaluated from the

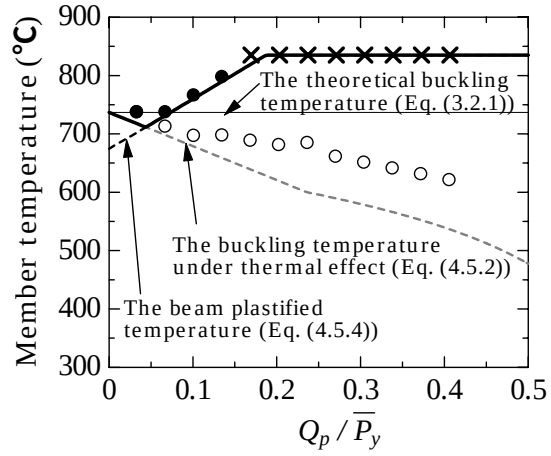

(a.1) $\overline{p}$ =0.2, λ_e = 18.3

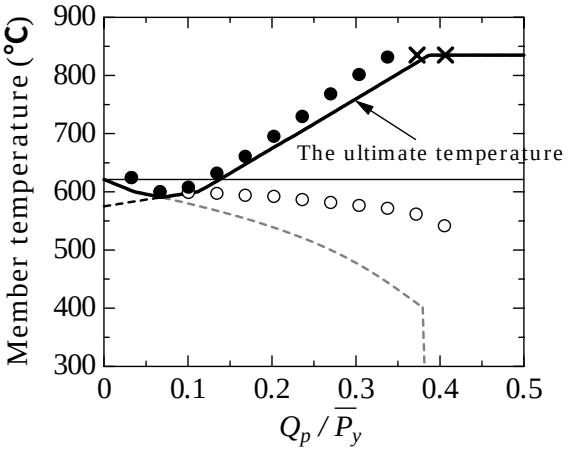

(b.1) $\overline{p}$ =0.4, λ_e = 18.3

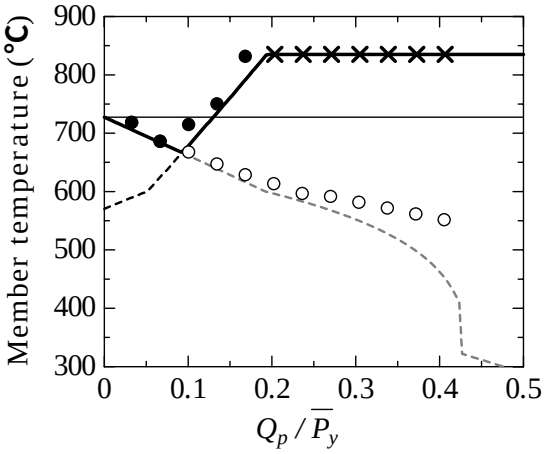

(a.2) $\overline{p}$ =0.2, λ_e = 38.5

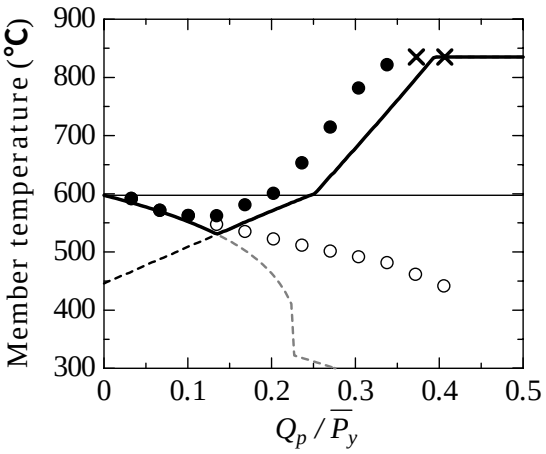

(b.2) $\overline{p}$ =0.4, λ_e = 38.5

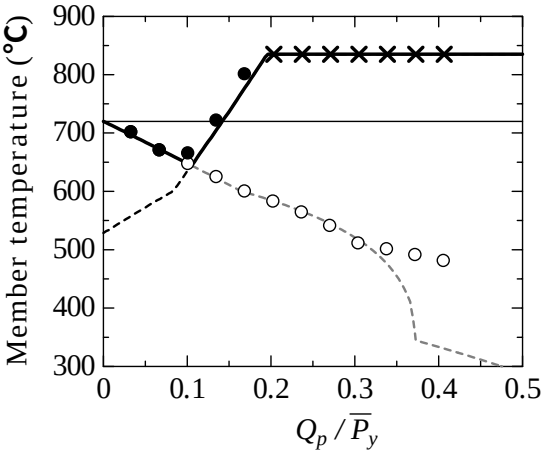

(a.3) $\overline{p}$ =0.2, λ_e = 51.3

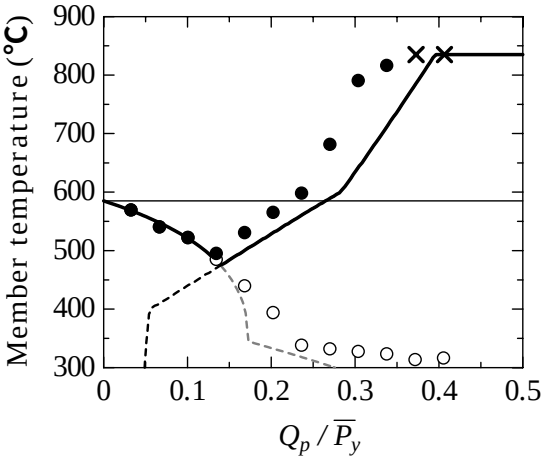

(b.3) $\overline{p}$ =0.4, λ_e = 51.3

Numerical results

○ Buckling temperature ● Ultimate temperature × Locally failure temperature

Fig. 4.5.3 The numerically analyzed buckling temperature and the ultimate temperature of the multi-storied frame - effect of the beam strength

higher temperature between the buckling temperature of the column and the beam platified temperature of the frame. The higher are depicted by thick solid lines in Fig. 4.5.3.

From comparison between the numerical results and the predicted ones, it is found that the predicted results are in good agreement fairly with, or somewhat lower than, the numerical results.

For frames with shorter columns, as seen in Figures (a.1) and (b.1), the predicted buckling temperatures become lower significantly than the numerical ones. The inaccuracy in these cases may be caused by assuming too large thermal compression Q (=Q_p) in the prediction. In fact, the columns in these cases are so short that the thermal elongations of these columns cannot make the beams plastified and therefore the actual effective Q in these cases may be smaller significantly than Q_p.

4.5.1.2 Effect of the column slenderness ratio

The plotted results shown in Fig. 4.5.4 and Fig. 4.5.5 are numerical results of four storied and six storied structures, where the effective slenderness ratio of the columns range from 12.5 to 153.8. Thin solid lines, gray broken lines, black broken lines, and thick solid lines in the figures are the theoretical buckling temperature, the predicted buckling temperature under thermal effect, the beam plastified temperature and the predicted ultimate temperature of the structure, respectively. The vertical axis shows the member temperature, and the horizontal axis shows the effective slenderness ratio of the column. As explained in section 3.4, not only the buckling temperatures but the post-buckling resistances of the columns decrease also for larger column slenderness ratios.

It is found that the buckling temperatures under thermal effect Eq. (4.5.2) are lower than the theoretical buckling temperature Eq. (3.2.1) and they become the lower for the longer columns, since the larger thermal forces are added to the longer heated columns. The predicted beam plastified temperature (the black broken line calculated from Eq. (4.5.4)) becomes lower similarly for the frame with longer columns, since the post-buckling strengths deteriorates more severely for longer columns as noted above. As seen in Fig. 4.5.4(d) for six storied frames with $\overline{p}$ = 0.5, the beam plastified temperature drops severely and reduces almost to zero for the frame with longer columns of $\lambda_e \geq 50$. It means that the post-buckling strength of a

longer column deteriorates too severely to perform the stress redistribution even at room temperatures.

The predicted buckling temperature is found to be lower than the numerical results for shorter columns as seen in Fig. 4.5.4, while, for longer columns, both are in good agreement. The assumed thermal compression Q is overestimated for shorter columns as noted earlier and this results in too lower predicted buckling temperature, while the assumption for Q is found to be appropriate for longer columns.

If a frame has shorter columns, it usually retains its stability after the heated columns buckle owing both to column's post-buckling strength and stress redistribution of the surrounding beams. They usually collapse at the temperature at which the beams are fully plastified. On the other hand, if a frame has longer columns with poorer post-buckling strengths, the beam plastified temperature often becomes lower than the predicted buckling temperature. The latter frame collapses immediately after column buckles, which accords with the prediction that, in such cases, the ultimate temperature with thick solid lines becomes equal to the buckling temperature. The predictions for these cases are in good agreement with the numerical results as shown in the figures. It can therefore be concluded that the ultimate temperature of frames can be evaluated from the higher temperature between the predicted buckling temperature under thermal effect and the beam platified temperature, which is indicated by the thick solid line in the figures.

4.5.1.3 Effect of the axial force ratio

From the results shown in Fig. 4.5.4 and Fig. 4.5.5, it is seen that larger axial force ratio of columns leads both to lower column buckling temperature and lower frame's ultimate temperature. It is noticed that, the temperature margin from the buckling up to ultimate temperatures in the numerical results expands larger for the frame with smaller axial force ratio. It is because, since small axial force ratio of the column indicates the force to be redistributed is small accordingly, the frame can withstand higher temperatures without losing stability as far as the restraining beams remains elastic. On the contrary, if axial force ratio of the column is large, the force to be redistributed becomes large and it makes the restraining beam plastified soon.

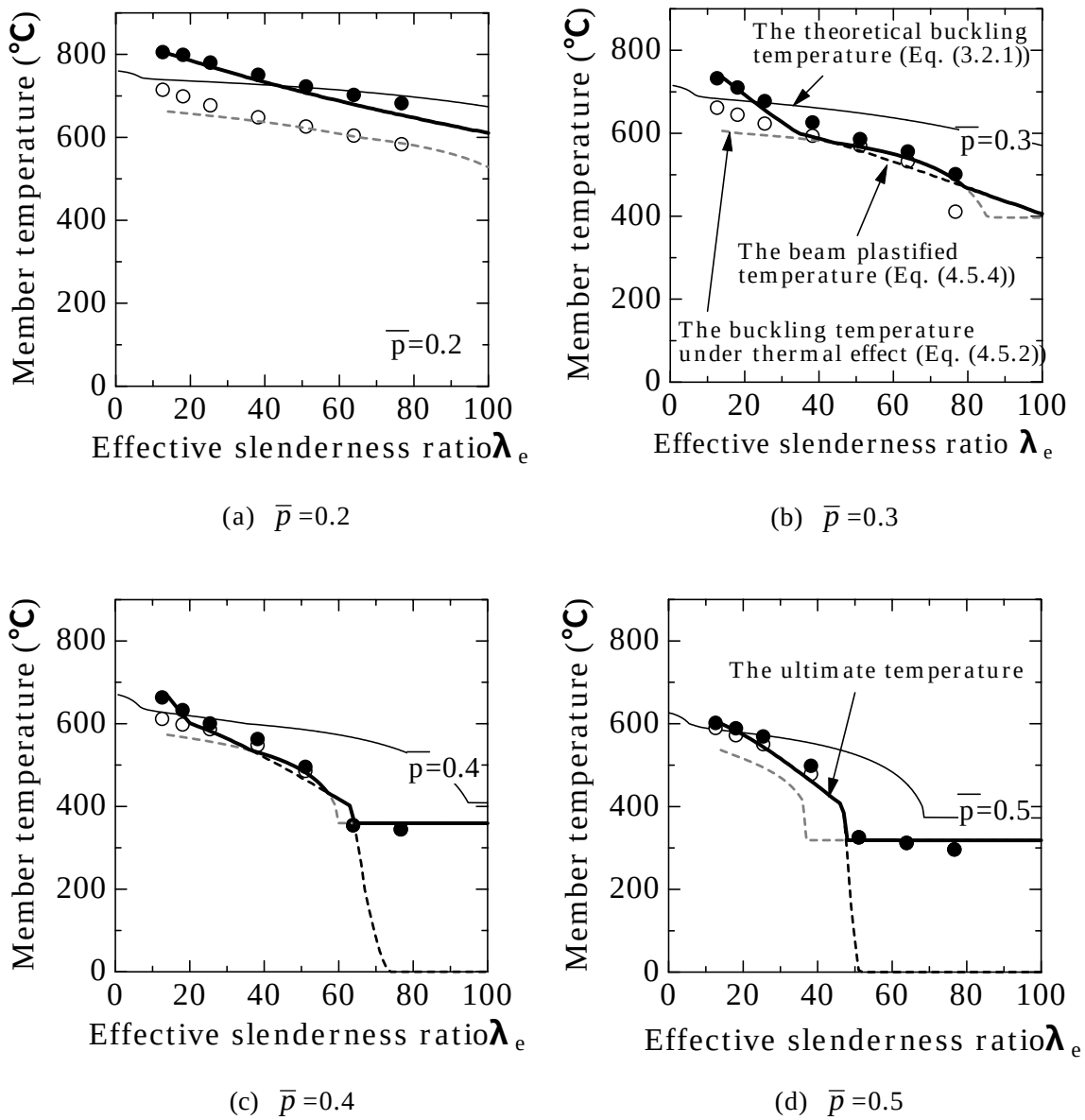

(a) $\bar{p}$ =0.2

(b) $\bar{p}$ =0.3

(c) $\bar{p}$ =0.4

(d) $\bar{p}$ =0.5

Fig. 4.5.4 The numerically analyzed buckling temperature and the ultimate temperature of four-storied frame - effect of the slenderness ratio and the axial load ratio

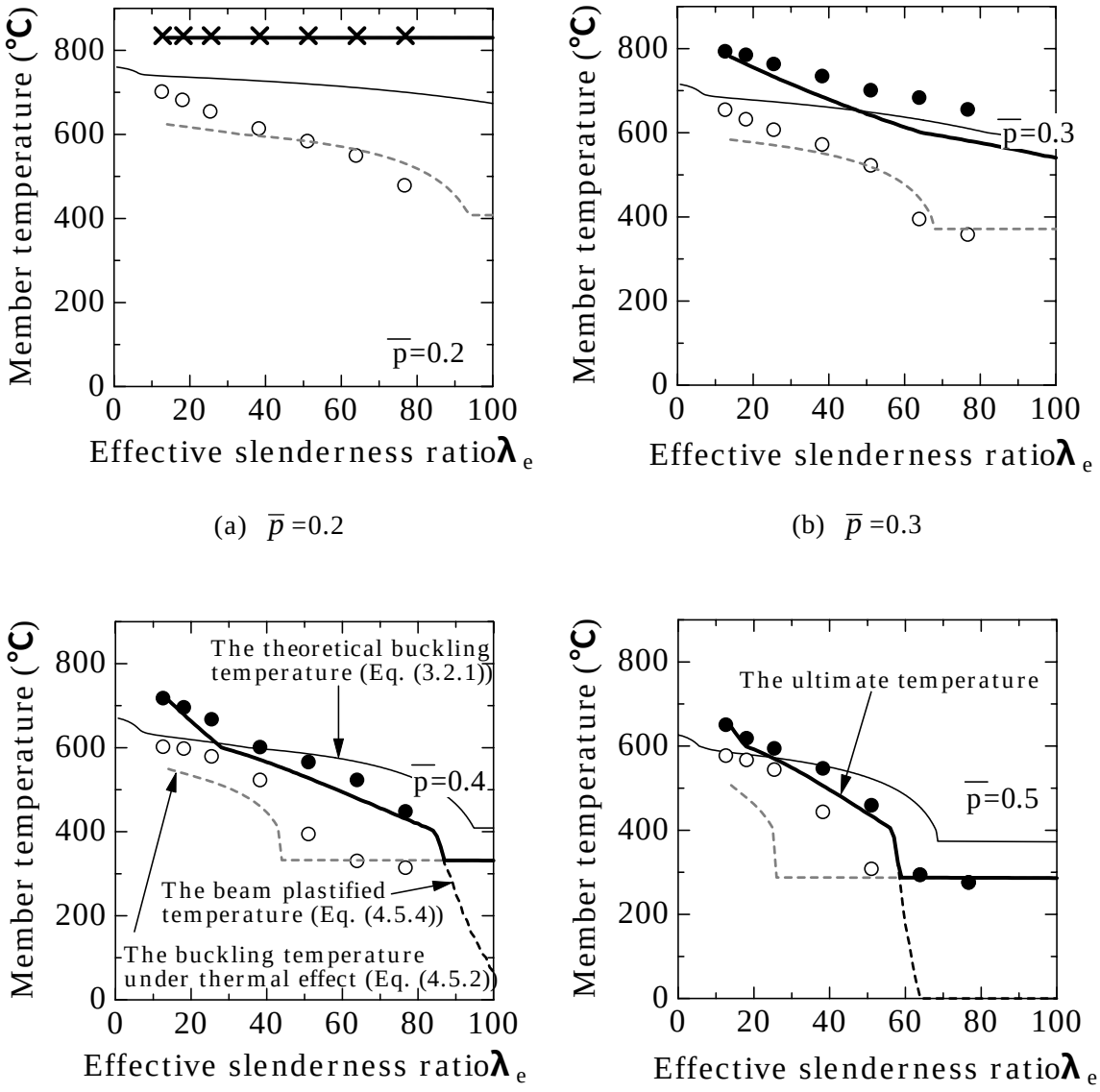

Fig. 4.5.5 The numerically analyzed buckling temperature and the ultimate temperature of six-storied frame - effect of the slenderness ratio and the axial load ratio

4.5.1.4 Effect of the beam size and beam span length

The analysis model shown in Fig. 4.5.1 is used to study the question. The Axial load ratio $\overline{p}$ and the column's slenderness ratio λ are to be 0.4 and 36.8, respectively. The analysis parameters are shown in Table 4.5.2.

Table 4.5.2 The analysis parameters of the steel frame when fire occurs at the inner span – effect of beam size and span length

Span length of the beam l(m)	5.25, 7, 10.5, 14
Beam size	H-700x250x13x24
Number of story n	2, 4

The numerical results are shown in Fig. 4.5.6. From Eq. (4.5.2), we find that an increase in the stress redistribution ability of adjacent beams is provided by increasing beam size and/or by decreasing beam span length. When comparing the numerical ultimate temperature of the four storied frame where beam size is H-700x250x13x24 and l = 10.5 m (plot d as shown in Fig. 4.5.6) with that of the five storied frame where beam size is H600x200x10x15 and l = 700 (the fifth plot from the left side as shown in Fig. 4.5.3(b.1)), the former is lower than the latter, although the beam strength of the former model is larger. It is noticed that the beam length of the former model is larger than that of the latter model. This is the cause of a drop of the ultimate temperature of the former frame. Since, in the prediction, an increase of the span length of the beam leads to an increase of Δ_p, the residual resistance of the post-buckling column N decreases accordingly. It can be concluded that an increase in beam size leads to an increase in the ultimate temperature of the steel frame, but the ultimate temperature decreases when the beam span length increases.

As seen in Fig. 4.5.6, the estimated ultimate temperatures are in good agreement with the numerical results and it can therefore be concluded that the ultimate temperature determined by the proposed equation (Eq. (4.5.4)) is appropriate.

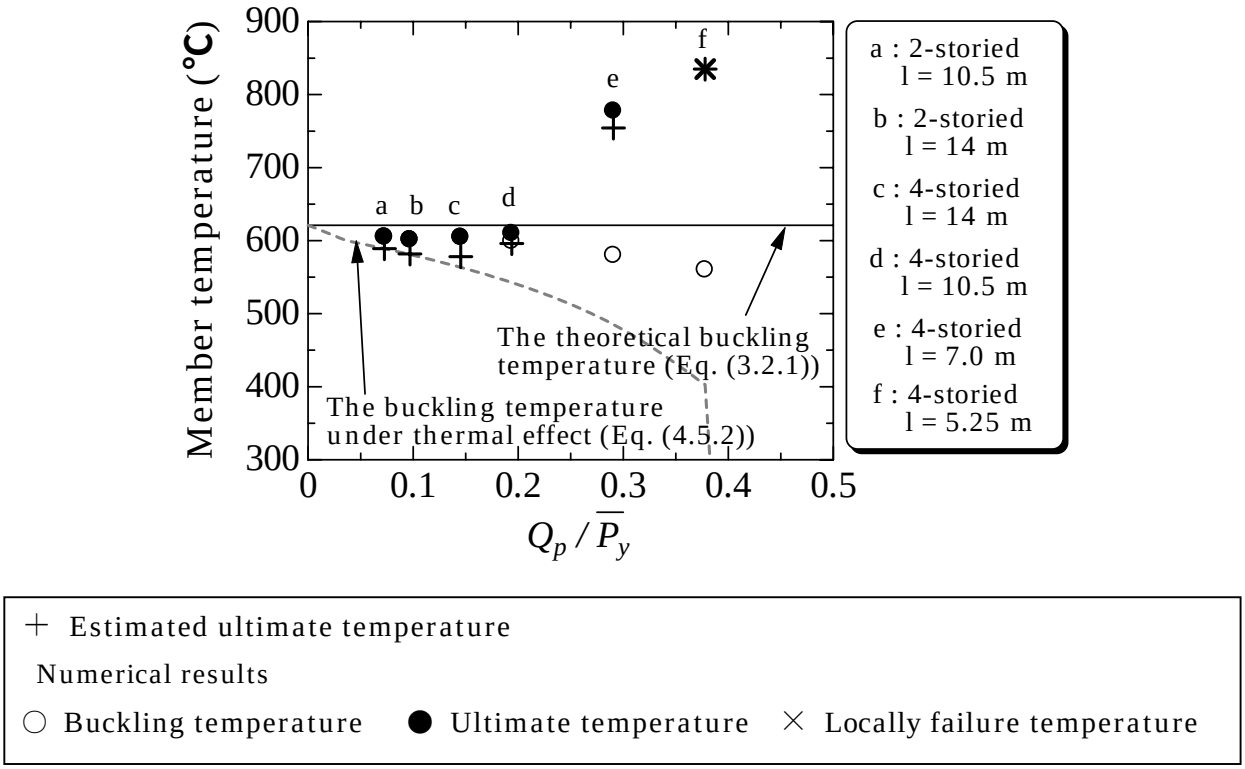

Fig. 4.5.6 The numerically analyzed buckling temperature and the ultimate temperature of the multi-storied frame - effect of the beam size and the beam length

4.5.1.5 Effect of the column size

The analysis model is a six storied frame as shown in Fig. 4.5.1 and the analysis parameters are shown in Table 4.5.3.

Table 4.5.3 The analysis parameters of the steel frame when fire occurs at inner span - effect of the column size

Axial load ratio $\overline{p}$	0.3, 0.5
Column length h	25.6, 36.63, 51.3, 78.6, 102.6, 115.4, 128.2
Column Size	Box-350x350x16 Box-250x250x23.6 Box-200x200x31.8 Box-150x150x58.2

Figs. 4.5.7 show the numerical bucking temperature and the ultimate temperature of the frames. Both the column's buckling temperature and the ultimate temperature drop as the effective slenderness ratio increases. Comparing these results with those shown in Fig. 4.5.5(a) and (c), it is noticed that, for the same effective slenderness ratio, the former buckling temperatures are found to be slightly higher than the latter. It is because the latter column's lengths are longer and therefore the additional thermal compressions become larger for the latter cases. However, the estimated bucking temperature determined from Eq. (4.2.2) is equal for both cases. On the other hand, the estimated ultimate temperature of the former frames are lower than the latter, since the smaller sectional depth of column in the former frames leads to the more decrease in the residual resistance of the post- buckling column.

As seen in Fig. 4.5.7, the estimated ultimate temperatures are in good agreement with the numerical results. It may be concluded that the ultimate temperature determined by the proposed equation (Eq. (4.5.4)) is appropriate.

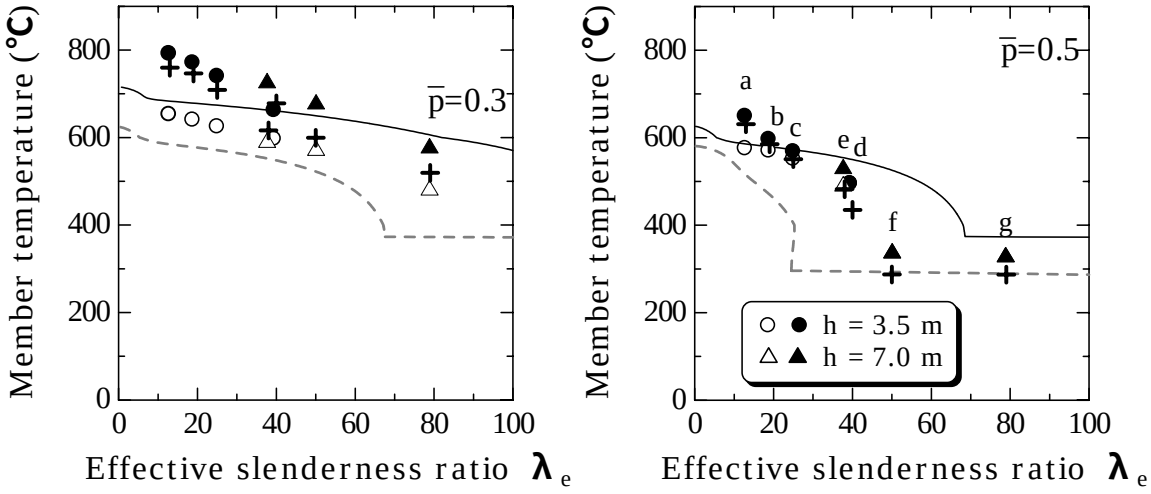

(a) $\bar{p}$ =0.2 (b) $\bar{p}$ =0.4

+ Estimated ultimate temperature

Numerical results

○ Buckling temperature ● Ultimate temperature × Locally failure temperature

a : Box-350x350x16, h = 3.5 m
b : Box-250x250x23.6, h = 3.5 m
c : Box-200x200x31.8, h = 3.5 m
d : Box-150x150x58.2, h = 3.5 m
e : Box-250x250x23.6, h = 7.0 m
f : Box-200x200x31.8, h = 7.0 m
g : Box-150x150x58.2, h = 7.0 m

Fig. 4.5.7 The numerically analyzed buckling temperature and the ultimate temperature of the six-storied frame - effect of the column size

4.5.2 Simple frames when fire occurs at an outer span

When fire occurs at one side or at the corner of the structure as shown in Fig. 4.5.8, both heated columns will vertically expand due to the thermal expansion as shown in Fig 4.5.9. In this case, the interior column is axially restrained by adjacent beams of the inner span upper of the fire floor. Therefore, the thermal compressive force is added to this heated column. However, the exterior column also expands due to the thermal expansion similarly. In this case, the thermal force may not be generated in the exterior column. For ordinary steel structures, the axial force acting on the exterior column is equal to or lowers than the force acting on the interior column. It is usually thermal effect why the interior column would buckle before the exterior column. After the interior column buckles, a part of the force which had formerly been carried by this column is redistributed to other sound columns (the heated exterior column and the inner unheated column). From this state, the behavior of the structure and the collapse of the structure can be separated to 2 modes.

1. The first mode: the interior column buckles instead of the exterior column and the adjacent beams restraining the buckling of the interior column are fully plastified.

After the column buckles, as shown in Fig. 4.5.10(a), the beams connected to the heated columns act as the restraining members. If the strength of these restraining beams is not strong enough, all these beams probably become fully plastified, as shown in Fig. 4.5.10(a). Subsequently, it leads to the collapse of the structure.

From the above description, the buckling temperature of the heated interior column T_{I1} can be evaluated from the following equation:

$$\lambda_e = \pi \sqrt{\frac{E_t(\bar{p}\bar{\sigma}_y + \sigma_{thI}, T_{I1})}{\bar{p}\bar{\sigma}_y + \sigma_{thI}}} \; ; \; \sigma_{thI} = \frac{2nM_p^b / l}{A} \qquad (4.5.5)$$

where σ_{thI} is the thermal compressive stress which is added to the interior column. The other notations have the same meaning as in Eq. (4.2.3) and Eq. (4.2.4). The effective slenderness ratio γ can be equal to 0.5.

On the other hand, the buckling temperature of the heated exterior column

T_{E1} can be calculated from the following expression:

$$\lambda_e = \pi \sqrt{\frac{E_t(\bar{p}\bar{\sigma}_y, T_{E1})}{\bar{p}\bar{\sigma}_y}} \tag{4.5.6}$$

As shown in Fig. 4.5.11(a), the beam plastified temperature T_{B1} can be obtained from the following equation.

$$P - Q_p - N(\lambda_e, \Delta_p, T_{B1}) = 0\,; \;\; Q_P = Q_{P1} + Q_{P2} = 2\left(\frac{2nM_p^b}{l}\right) \tag{4.5.7}$$

The meanings of the notations are found in section 4.4. From the above three member temperatures (T_{I1}, T_{E1}, and T_{B1}), this mode of collapse shown in Fig. 4.5.10(a) will occur, if the following condition is met.

$$T_{E1} > (T_{B1}, T_{I1}) \tag{4.5.8}$$

And the corresponding ultimate temperature T_U can be determined from

$$T_U = \max(T_{B1}, T_{I1}) \tag{4.5.9}$$

2. The second mode: both the exterior and interior columns buckle while the adjacent beams at the inner span become fully plastified

After the heated interior column buckles, a part of load that cannot be carried by the buckled column is also transferred to the heated exterior column. On the contrary from the first mode, in this case, the exterior column buckles before the restraining beams at the outer span become fully plastified. The mode of collapse is shown in Fig. 4.5.10(b). As seen in the figure, after both columns buckle, the beams at the inner span have to support the axial forces which have formerly been carried by both of buckled columns.

To make the determination easier, both buckled columns are assumed to be combined into a single buckled column. Its bucking temperature T_{C2} can be determined from the following expression.

$$\lambda_e = \pi \sqrt{\frac{E_t(\sigma_C + \sigma_{th2}, T_{I1})}{\sigma_C + \sigma_{th2}}}; \qquad (4.5.10)$$

$$\sigma_{th2} = \frac{2nM_p^b / l}{(A_{CI} + A_{CE})} \quad , \quad \sigma_C = \frac{P_I + P_E}{A_{CI} + A_{CE}}$$

where A_{CI} and A_{CE} represent cross sectional areas of the interior column and the exterior column, respectively. P_I and P_E are the initial axial compressive forces on the interior column and exterior column, respectively. The effective slenderness ratio γ is to be calculated from Eq. (3.3.8).

In view of Fig. 4.5.11(b), the beam plastified temperature T_{B2} can be estimated from the following equilibrium equation

$$(P_I + P_E) - Q_p - (N_I(\lambda_e, \Delta_p, T_{B2}) + N_E(\lambda_e, \Delta_p, T_{B2})) = 0; \; Q_P = \frac{2nM_p^b}{l} \qquad (4.5.11)$$

where N_I and N_E represent the resistances of the interior column and the exterior column that can be calculated from Eq. (4.3.10). This mode of collapse shown in Fig. 4.5.10(b) will occur if the inequality

$$T_{E1} < T_{B1} \qquad (4.5.12)$$

is met and the corresponding ultimate temperature T_U can be determined from

$$T_U = \max(T_{B2}, T_{C2}) \qquad (4.5.13)$$

For parametric studies, the frame shown in Fig. 4.5.12 is used, in which fire is assumed to occur inside the outer span. The analysis parameters are shown in Table. 4.5.4.

Table 4.5.4 The analysis parameters of the steel frame when fire occurs at an outer span

Axial load ratios $\overline{p}$	0.2, 0.3, 0.4, 0.5
Slenderness ratios λ	25.6, 36.6, 51.3, 78.6, 102.6
Axial load of exterior column	$P_E = P_I / 2$

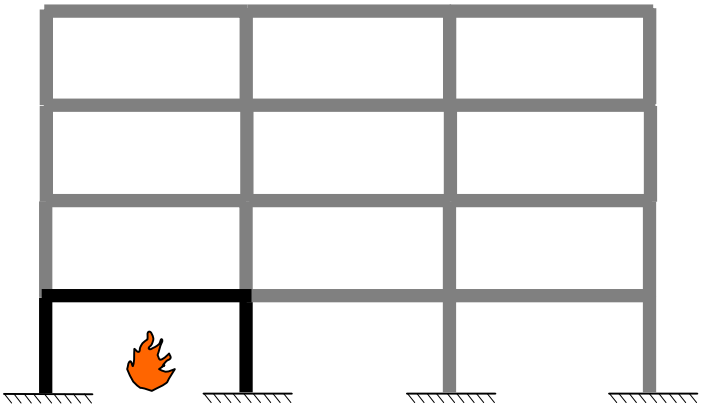

Fig. 4.5.8 A steel frame when fire occurs at outer span

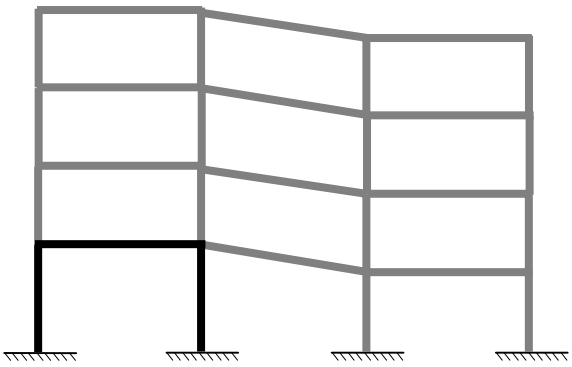

Fig. 4.5.9 The expansion of the heated column due to the thermal expansion

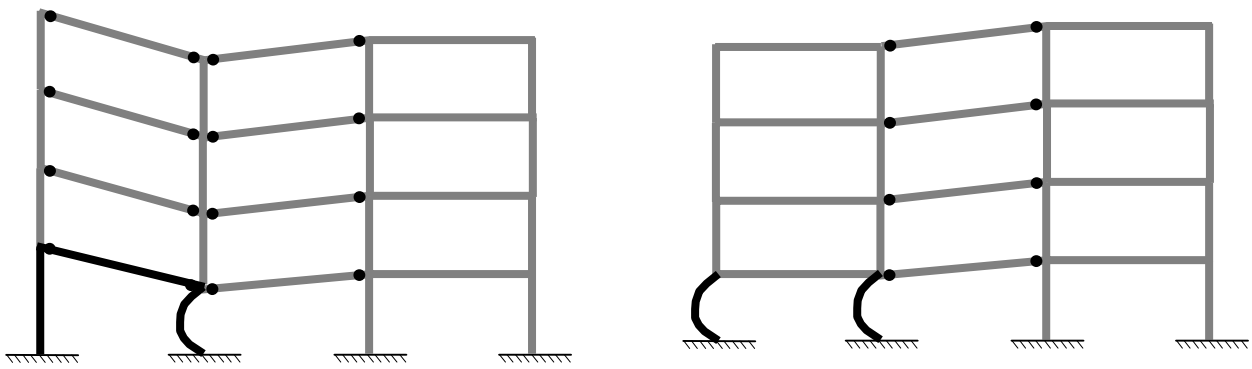

(a) Mode A　　(a) Mode B

Fig. 4.5.10 The failure mode of a steel frame when fire occurs at outer span

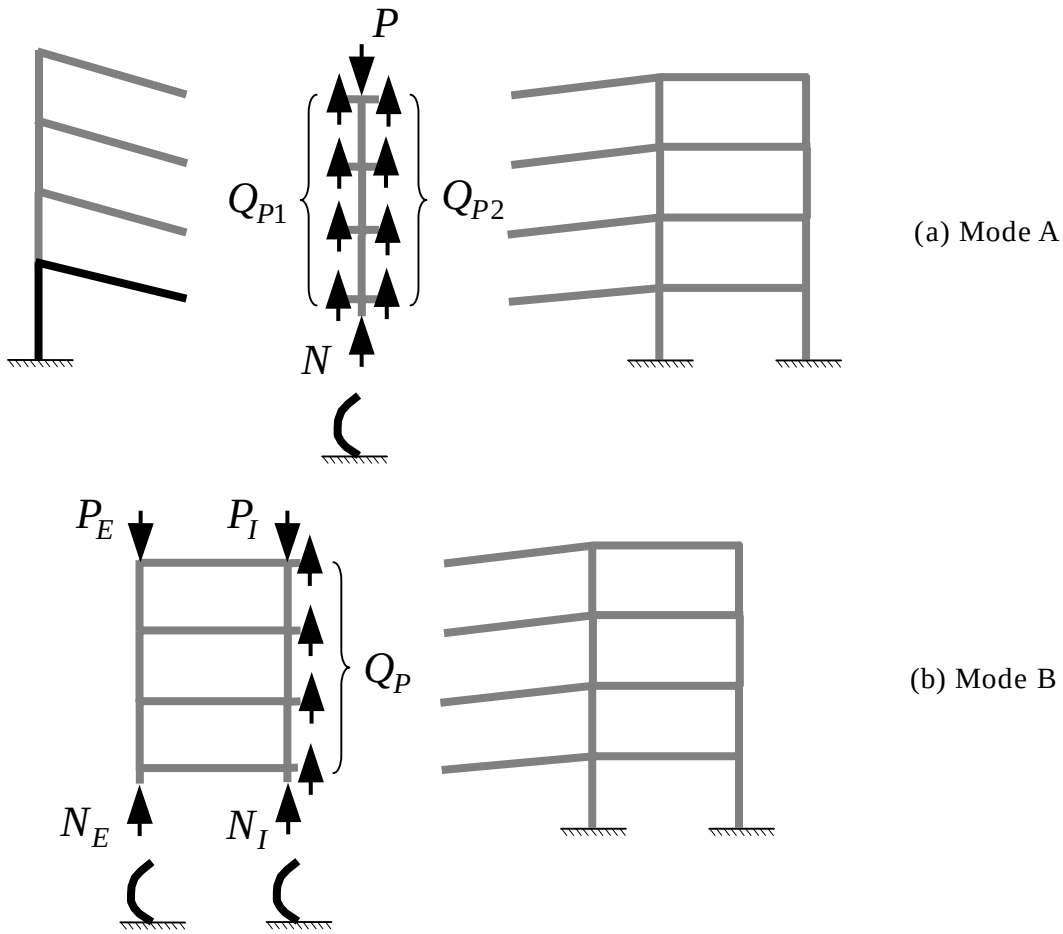

(a) Mode A

(b) Mode B

Fig. 4.5.11 An equilibrium of force of the failure structure

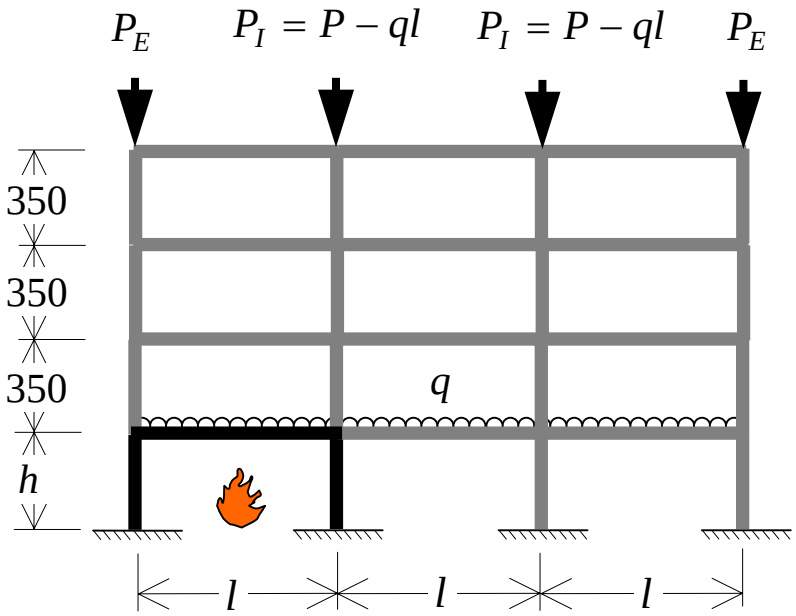

Column:Box-350x350x16

Beam: H-600x200x10x15

Beam distributed load q = 20 kN/m

Span length l = 700cm

Fig. 4.5.12 The analysis model of a multi-storied frame when fire occurs at outer span

4.5.2.1 The behavior of the steel frame when fire occurs at outer span

The change of states of deformation of the four-storied frame which is subject to fire inside the outer span is shown in Fig. 4.5.13. These are numerical results. The results are also summarized in Fig. 4.5.14. As shown in Fig. 4.5.14(b), both heated columns displace upward similarly due to their own thermal expansion. The axial compressive force in the interior column increases largely, while the increase is not found in the exterior column as shown in Fig. 4.5.14(a). These are of the thermal effects in that the interior column is restrained more heavily by the beams placed in the right-next inner span. When the member temperature reaches 575°C, the heated interior column buckles. As a result, a part of the force that has formerly been supported by the buckled interior column transfers to the heated exterior column. Thus, the structure still retains its stability, and the member temperature increases subsequently.

As shown in Fig. 4.5.14(a), change of the compressive force in the interior column turns from moderate increase to steep drop when it buckles. On the other hand, as shown in Fig. 4.5.14(b), the exterior column remains unbuckled when the interior column buckles and it continues to expand according to further temperature increase. It buckles at the temperature of 690°C which corresponds to state b in Fig. 4.5.13(b). At this temperature, the structure cannot keep its stable state anymore. We can continue the analysis of this unstable process of the frame by changing the control to *displacement controlled analysis*. It is found from the *displacement controlled analysis* that, although the adjacent beams in the right-next span attempt to redistribute the forces, they become fully plastified before the frame recovers stability. Finally, the structure is struck by an overall collapse as shown in Fig. 4.5.13(d).

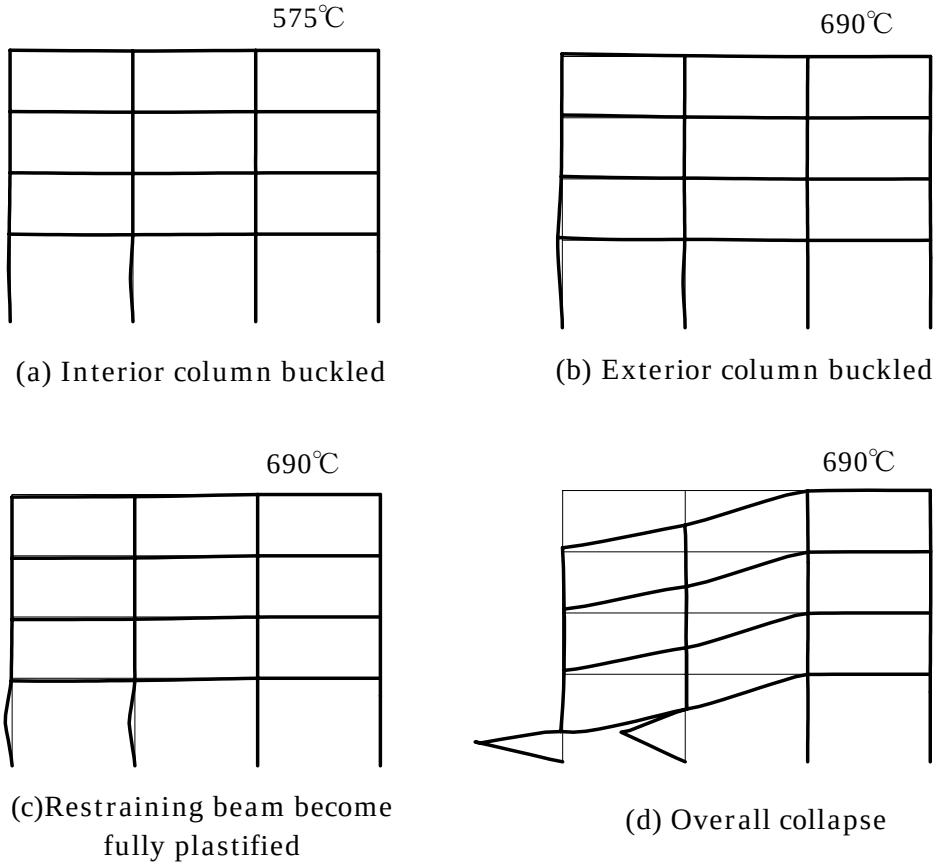

(a) Interior column buckled

(b) Exterior column buckled

(c)Restraining beam become fully plastified

(d) Overall collapse

Fig. 4.5.13 Change of states of deformation for the four-storied frame when fire occurs at outer span ($\overline{p}$ = 0.4, λ_e = 18.6)

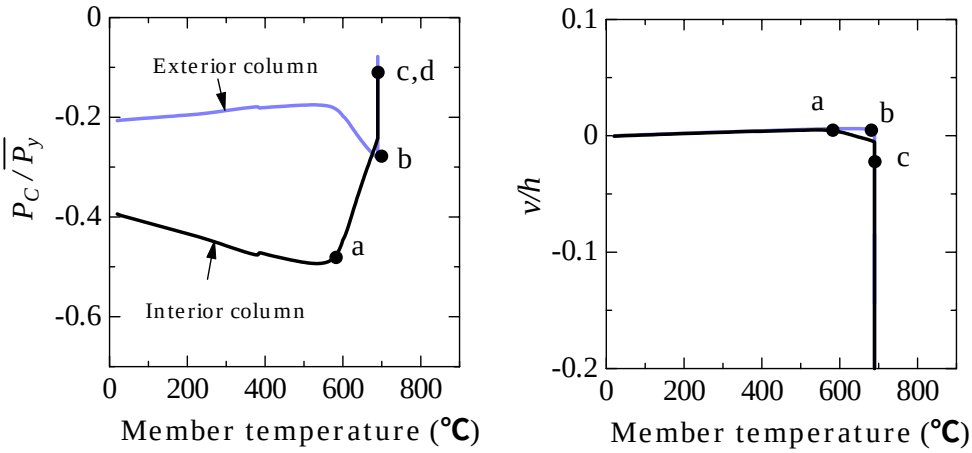

(a) Axial forces of the columns

(b) Vertical displacement of the head of the heated column

P_C : Axial forces of the columns

v : Vertical displacement of the head of the first floor interior column

Fig. 4.5.14 Summaries of analysis for the four-storied frame when fire occurs at outer span ($\overline{p}$ = 0.4, λ_e = 18.6)

4.5.2.2 Effect of the axial force ratio

Fig. 4.5.15 shows the numerical results for steel frames when fire occurs at outer span. From the results, the steel structure tends to collapse in the second mode B if $\overline{p}$ is smaller, which corresponds to the cases of $\overline{p}$ = 0.2 and 0.3 in the figure. It is likely because, in these cases, since the strength of the heated columns is much reduced at the attained high temperature, the weakened exterior column hardly carries the force to be redistributed after the interior column buckles.

On the contrary, for the case where $\overline{p}$ = 0.4 or 0.5, since the restraining adjacent beams have to redistribute larger forces, they are apt to fully plastified before the heated exterior column buckles, which may lead the frame to the first collapse mode A. Especially, in the case of large effective slenderness ratio, since the residual resistance of the buckled column drops severely, almost all the structures in these cases fail in the first mode A indicated by Fig. 4.5.10(a). It is however noticed that the frame with $\overline{p}$ = 0.4 and λ = 25.6 as well as the frame with $\overline{p}$ = 0.5 and λ = 25.6 collapse in the second mode B. In these cases with larger $\overline{p}$ s and smaller λ s, since the post-buckling strength of the column with smaller slenderness is not so lost and this provides smaller loadings to the adjacent beams during stress redistribution, the beams remain almost elastic until the exterior column buckles.

As shown in Fig. 4.5.15(a.1) and (b.1), the estimated beam plastified temperature T_{B1} given by Eq. (4.5.7) is higher than the buckling temperature of the exterior column T_{E1} given by Eq. (4.5.6). Therefore, the ultimate temperatures of the cases of $\overline{p}$ = 0.2 and 0.3 must fall into the mode B collapse. On the other hand, for the cases of $\overline{p}$ = 0.4 and 0.5, since T_{B1} becomes smaller than T_{E1}, the mode of collapses must fall into mode A and the ultimate temperature of the frame is therefore to be estimated from Eq. (4.5.9), which are shown in Fig. 4.5.15(c.1) and (d.1). From the comparison between the numerical results and the estimated ones, it is found that almost all the estimated ultimate temperatures are in good agreement with the corresponding numerical ones.

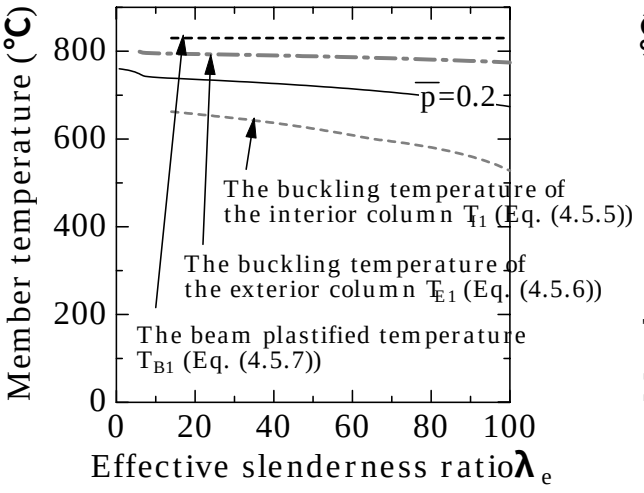

(a.1) $\bar{p}$ = 0.2 (Mode A)

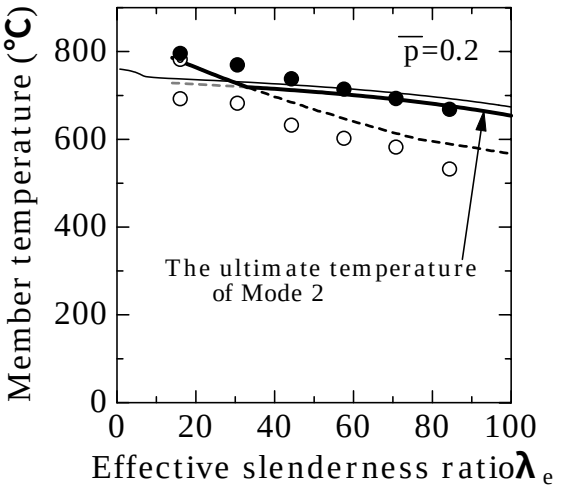

(a.2) $\bar{p}$ = 0.2 (Mode B)

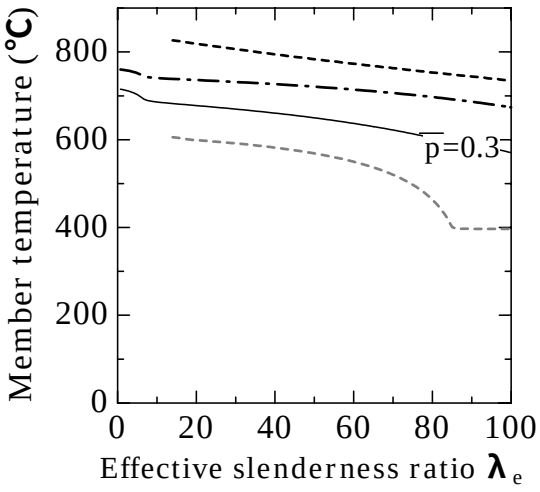

(b.1) $\bar{p}$ = 0.3 (Mode A)

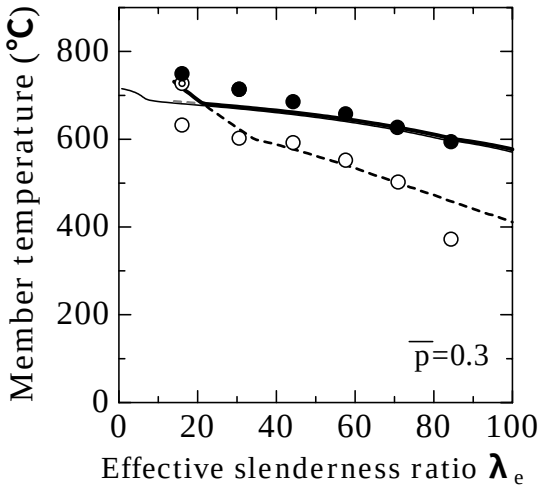

(b.2) $\bar{p}$ = 0.3 (Mode B)

Numerical results
○ Interior column buckling temperature ◎ Exterior column buckling temperature
● Ultimate temperature

Fig. 4.5.15 The numerically analyzed results for the four-storied frame when fire occurs at outer span

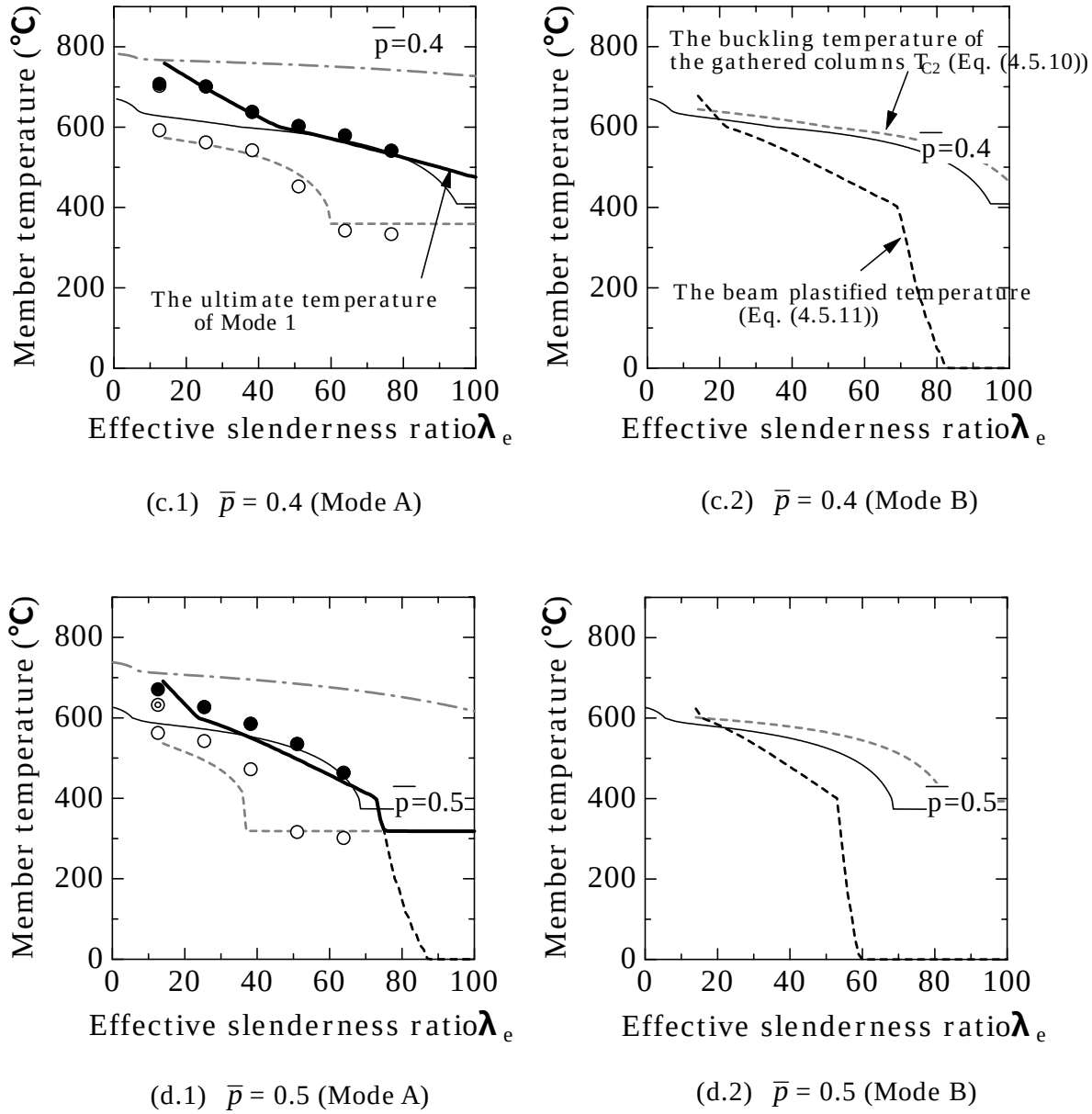

(c.1) $\bar{p}$ = 0.4 (Mode A)

(c.2) $\bar{p}$ = 0.4 (Mode B)

(d.1) $\bar{p}$ = 0.5 (Mode A)

(d.2) $\bar{p}$ = 0.5 (Mode B)

Fig. 4.5.15 The numerically analyzed results for the four-storied frame when fire occurs at outer span

4.5.3 Hatted frame

It is found in the previous discussion that a locally heated frame may fall into an overall instability ultimately unless it has sufficient stress redistribution abilities against the vertical load. It is noticed that if the stress redistribution ability of the frame is superior to the vertical load, the structure will only locally collapse at high temperature and it will not lose its stabilities at all. In Japan, bracing members are generally used to reinforce steel-frames to lessen the damage due to earthquakes. Bracing is a reinforcement of frames against horizontal forces. Similarly, any vertical reinforcement may help frames to improve stress redistribution abilities and therefore fire resistances. In this research, their ability against the vertical load is considered. As one of the ways to prevent a frame from such an overall instability, the effects of installing a hat truss are now examined. Different types to improve stability of a heated frame are found elsewhere (Ohi et al., 2003). However, as described above, increase in the vertical restraining effect also leads to increase in the thermal force added to the columns. Therefore, this point needs further to be clarified.

A hatted steel frame shown in Fig. 4.5.16 is regarded as the analysis model to investigate the behavior of the hatted frame subjected to fire. The connection of the hat truss is assumed to be a rigid joint. As seen in the figure, when the heated column expands due to thermal expansion, it becomes axially restrained by both hat truss (member B) and the adjacent members. In this case, the thermal force can be determined under the following two conditions.

1. The hat truss reaches the compressive yield strength, while the adjacent beams remain elastic.

Due to thermal expansion of the heated column, the compressive force of the hat truss member A reaches the compressive strength. Therefore, in this case, the thermal force can be determined from the following expression:

$$P_{th1} = \overline{P}_y^{Br} \tag{4.5.14}$$

where $\overline{P}_y^{Br}$ represents the yield strength of the hat truss at room temperature.

2. The adjacent beams become fully plastified and the hat truss buckles.

In this case, a part of the thermal force is determined from the condition that the axially restraining beams become fully plastified. In addition to this force, the axial restraint of the hat truss should be summed up to the thermal stress. However, when the restraining beam will become fully plastified, the vertical displacement is going to be very large and therefore the hat truss will buckle. Therefore, the thermal force induced by the hatted member accords with its post-buckling residual resistance. In this case, the thermal force added to heated column during fire can be determined from the following expression:

$$P_{th2} = Q_p + N_{Br}\left(\lambda_{Br}, (\Delta_p \cos\theta)/2, RT\right) \cdot \cos\theta \qquad (4.5.15)$$

where $Q_P = 2nM_p^b / l$. N_{Br} represents the residual resistance of the hat truss member after it buckles at room temperature. λ_{Br} is the effective length of the hat truss member A. θ is the slope of the hat truss as shown in Fig. 4.5.16.

The buckling temperature of the column under the thermal effect can be determined by the following equation.

$$\lambda_e = \pi \sqrt{\frac{E_t(\overline{p}\overline{\sigma}_y + \sigma_{th}, T_{cr})}{\overline{p}\overline{\sigma}_y + \sigma_{th}}} \qquad (4.5.16)$$

where $\sigma_{th} = \max(P_{th1}, P_{th2})/A$. Δ_p represents the deflection of the beams when the beams become fully plastified, which can be determined from Eq. (4.4.4)

The beam plastified temperature of the hatted frame is obtained as follows. After the heated column buckles, the structure will subsequently sink down locally. Therefore, member B of the hat truss turns from a compressive member to a tensile member and member A turns simultaneously from a tensile to compressive member after column buckles. Therefore, the redistributable force through the hat may be maximized when the compressive member A buckles. Fig. 4.5.18 shows the deformation of the structure after the adjacent beams become fully plastified and the compressive member A buckles. Therefore, the beam plastified temperature can be calculated from the following equilibrium equation:

$$P - (Q_p + N_{Br}(\lambda_{Br}, (\Delta_p \cos\theta)/2, RT) \cdot \cos\theta) - N(\lambda_e, \Delta_p, T)) = 0; \qquad (4.5.17)$$

$$Q_P = \frac{2nM_p^b}{l}$$

where N_{Br} represents the residual resistance of the truss member after it buckles at room temperature. λ_{Br} is the effective length of the truss member A.

To investigate the behavior of the hatted frame, the analysis for steel frames shown in Fig. 4.5.16 is conducted. The analysis parameters are shown in Table. 4.5.5.

Table4.5.5 The analysis parameters of the hatted frame.

Axial load ratios $\bar{p}$	0.4, 0.5
Slenderness ratios λ	25.6, 36.6, 51.3, 78.6, 102.6
Hat truss size	H-100x100x6x8 H-250x250x9x14
Number of story	4, 6

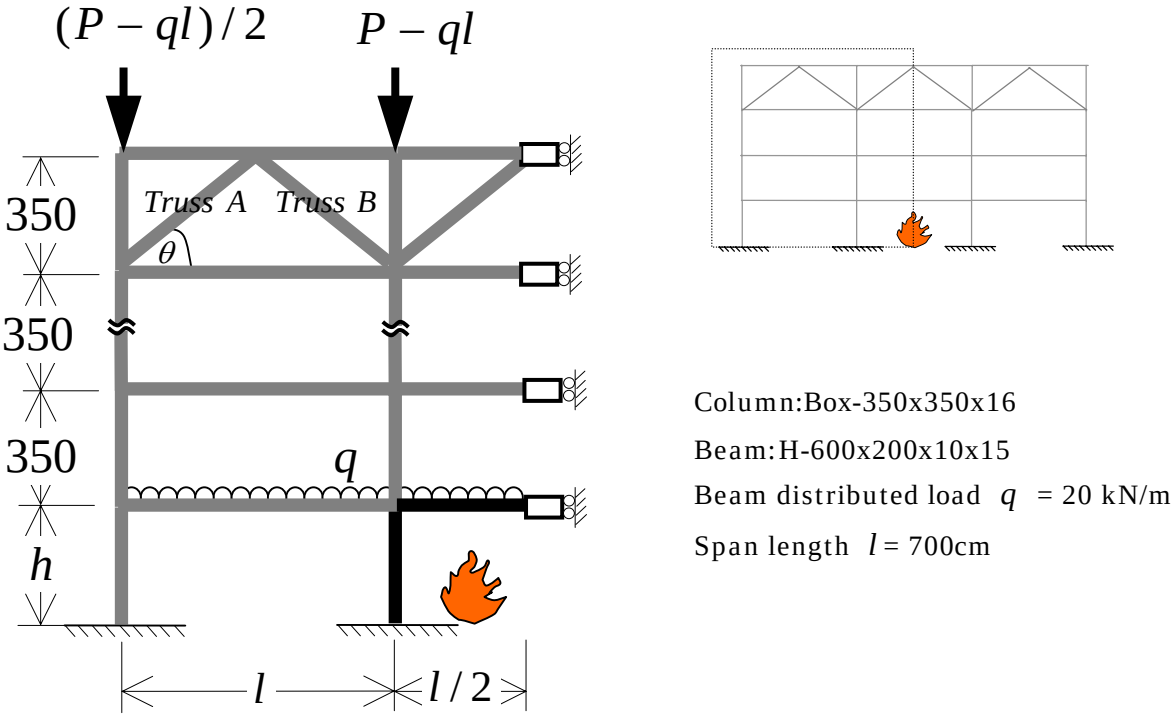

Fig. 4.5.16 The analysis model of a multi-storied hatted frame

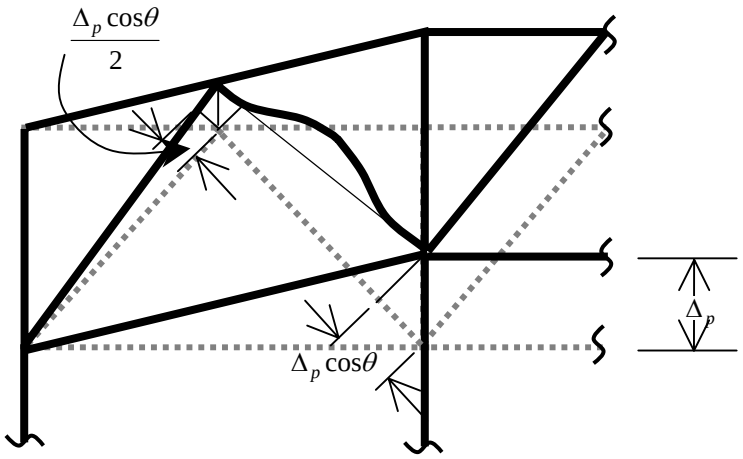

The contraction of a hat truss = $\frac{\Delta_p \cos\theta}{2}$

Fig.4.5.17 The contraction of a hat truss due to the expansion of the heated column

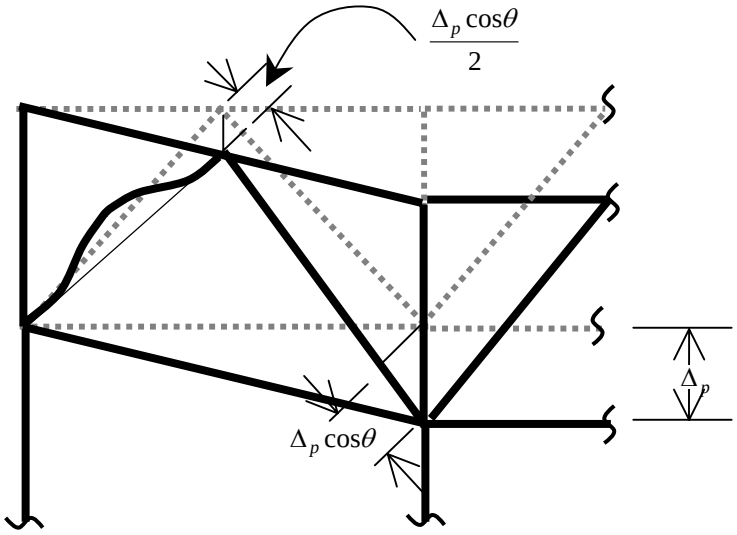

The contraction of a hat truss = $\frac{\Delta_p \cos\theta}{2}$

Fig.4.5.18 The contraction of a hat truss due to the expansion of the heated column

4.5.3.1 The behavior of the hatted frame during fire

Figures 4.5.19 shows the change of states of deformations for the six-storied hatted frame with a first floor interior column of $\overline{p}$ =0.4 and λ = 36.6, and with a diagonal member of H-250x250x9x14. Fig. 4.5.20 shows the axial force responses of the diagonal members.

The heated column displaces upward due to thermal expansion in earlier stages of heating. As seen in Fig. 4.5.20, the axial compressive force in member A shown by the black solid line increases linearly as temperature increases, while the axial force in truss B is tensile. The heated column buckles when the member temperature reaches 560°C. In this case, the structure still retains its stabilities although the heated column buckles. Subsequently, the axial forces of both diagonal members drop rapidly, as seen in the figure, because the structure starts to sink down. At the temperature 600°C, the axial force in both truss members reduce to 0. The force of member B changes subsequently to tension and the force of member A changes to compression.

The member temperature is increased up to the ultimate temperature 830°C (state B as shown in Fig. 4.5.19(b)). The mode of failure is excessive hanging deformation of the heated beam as shown in the figure, which is a local failure similar to the ordinary frames with $Q_P \geq 0.4\overline{P}_y$ (as described in section 4.5.1). This frame, therefore, does not fall into an overall instability. Although the interior column buckles at a lower temperature, the shortening of buckled column ceases subsequently, as if it were suspended by the hat truss. Carrying axial forces, the diagonal members help the beams to redistribute the vertical load after the interior column buckles.

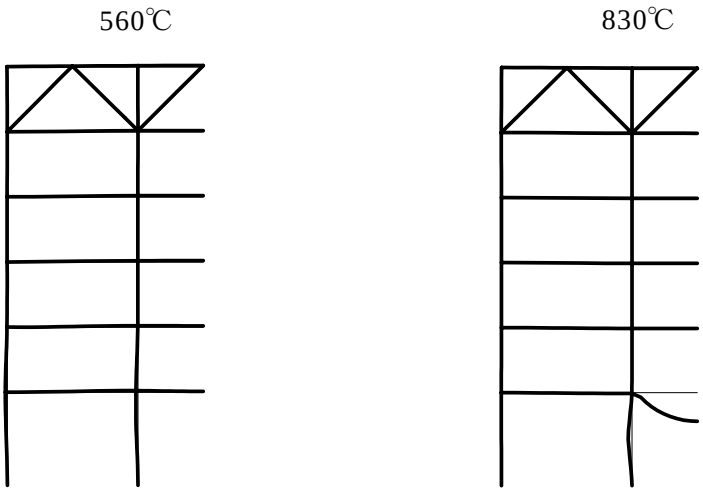

(a) Column Buckled (b) Locally ultimated

Fig. 4.5.19 Change of states of deformation for the six-storied hatted frame

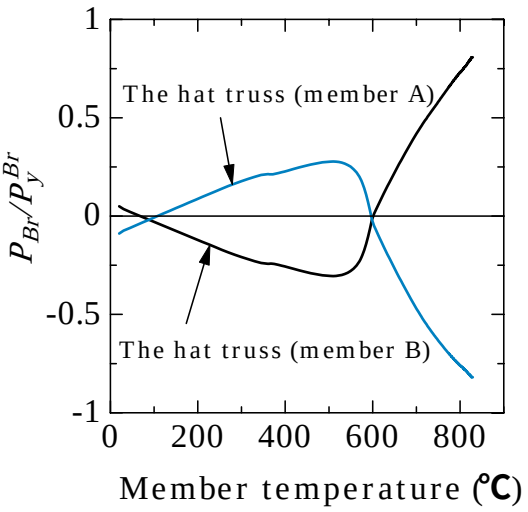

P_{Br} :Axial forces of the hat trusses $\overline{P}_y^{Br}$: Yield strength of the hat truss

Fig. 4.5.20 Summaries of analysis for the six-storied hatted frame

4.5.3.2 Effect of the Hat truss size

The figures 4.5.21 and 4.5.22 exhibit the numerical results for the hatted frame shown in Fig. 4.5.16. It can be clearly seen in the figure that an increase in the hat truss size is likely to cause a drop in the buckling temperature of the heated columns, while it causes a rise in the ultimate temperature. For the case of four-storied frame with $\overline{p}$ = 0.3 and the diagonal member size of H-250x250x9x14, the ultimate temperature rises up to 830°C and the corresponding failure mode results in the local collapse where the heated beam bows excessively. For the cases of the four-storied frames with a larger $\overline{p}$ =0.5, on the other hand, frame falls into an overall instability. However its ultimate temperatures increase by around 100°C compared to the results of the case of the frames with a smaller diagonal member size of H-100x100x6x8. Thus, it is concluded that additional installation of a hat truss is found to be quite efficient in that the truss helps beams to redistribute vertical forces and to improve the fire-resisting capacity of a frame when and after it undergoes buckling of heated columns under fire.

The predicted buckling and ultimate temperatures of the hatted frames are also shown in Fig. 4.5.22. The predicted buckling temperatures of the structure, that the hat truss size of H-100x100x6x8, are in good agreement with the numerical results. On the contrary, for the cases where the hat truss size is H-250x250x9x14, the predicted buckling temperatures are somewhat lower than the numerical results. It is because the heated columns in these cases buckle under weaker restraining forces than the assumed magnitudes which are used to formulate the buckling temperature. In fact, it is found in the numerical results for these cases that the heated column buckles while both the beams and the hat truss remain elastic. However, it is found that the estimated ultimate temperatures are almost in good agreement with the numerical results. It is therefore be concluded that the proposed expression, Eq. (4.5.16) and Eq, (4.5.17) can be used for estimation of the ultimate temperature of hatted frames.

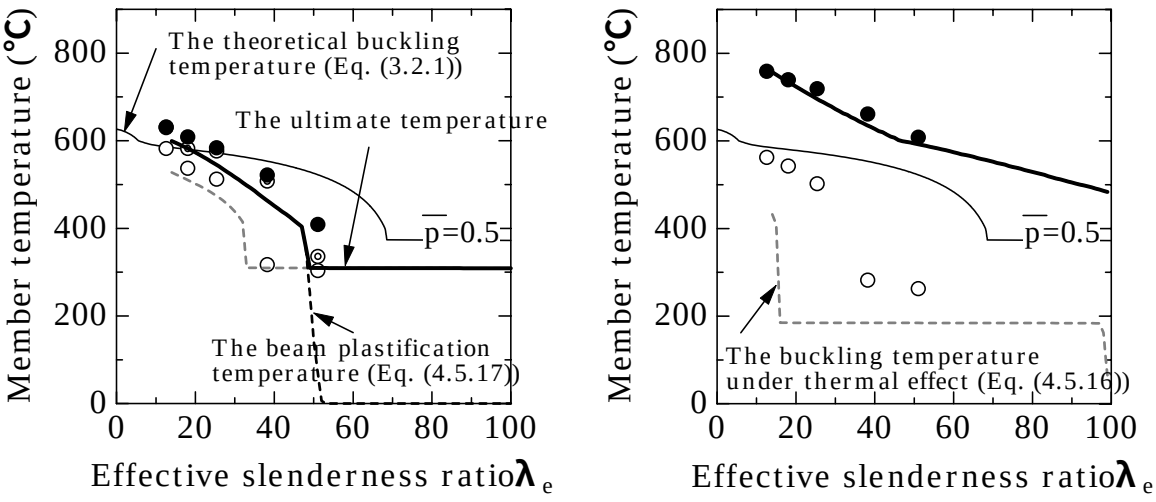

(a) The hat truss size: H-100x100x6x8 (b) The hat truss size: H-250x250x9x14

Fig. 4.5.21 The numerically analyzed results of the four-storied hatted frame ($\bar{p}$ = 0.5)
-Effect of the hat truss size

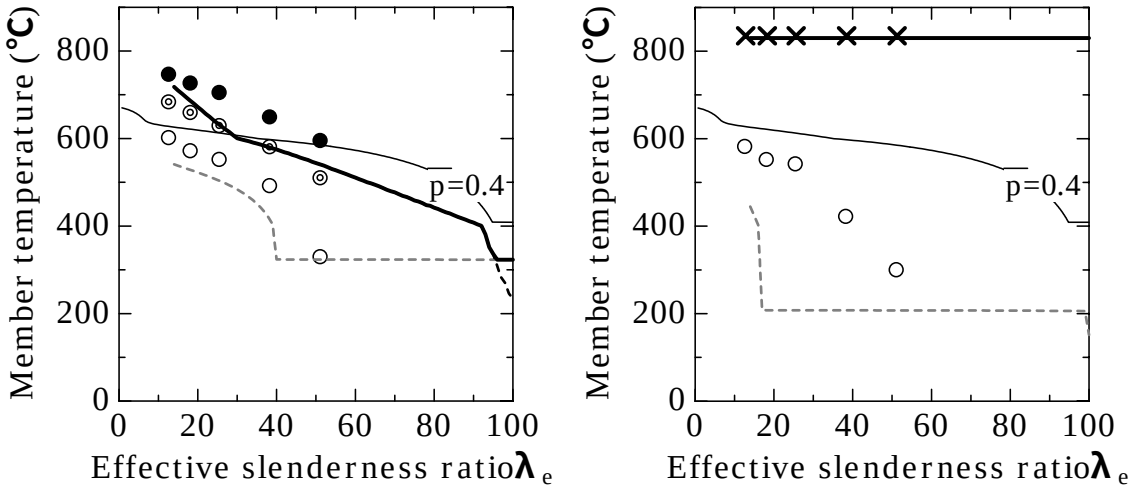

(a) The hat truss size: H-100x100x6x8 (b) The hat truss size: H-250x250x9x14

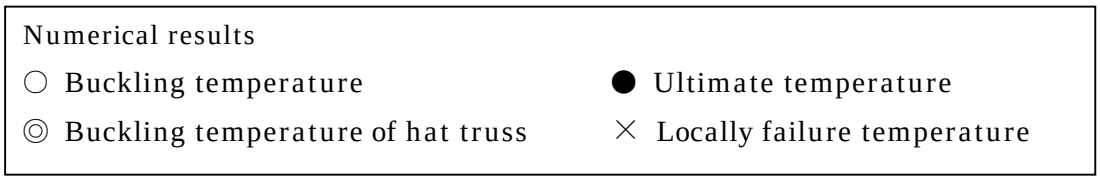

Fig. 4.5.22 The numerically analyzed results for the six-storied hatted frame ($\bar{p}$ = 0.4)
-Effect of the hat truss size

4.6 Conclusion

In this chapter, the effects of axially restraining members have been investigated. And the way to estimate the ultimate temperature of the steel frame subjected to fire was proposed. The following conclusions can be drawn:

◆ The effects of the axially restraining members have two mechanical roles. The first role is to restrain an expanded heated column. As a result of this action, the thermal compressive force is added to the heated column. This causes a drop in buckling temperature of heated columns. On the contrary, the second role is to redistribute a part of the compressive force of the buckled column to other sound columns. As a result of this action, the structure can retain its stability after the column buckles. It causes a rise of the ultimate temperature of a frame. However, if the second stress redistribution ability is not enough, it falls into instability immediately after the heated column buckles. The ultimate temperature for this frame is lower than the theoretical buckling temperature, since the buckling is affected by the first thermal effect.

◆ Based on the above observation, it is found that a higher ultimate temperature of a frame is obtained if it has higher stress redistribution capacity. A way to improve the fire-resistance capacity of a frame is to install a suitably proportioned hat truss. A hatted frame is found to have definitely an improved redundancy.

◆ Closed form formulae to predict both the buckling temperature of a heated column and the beam plastified temperature of a frame is presented herein. Conducting the numerical fire response analysis, the predicted temperatures are found to be in good agreement with the numerical results for various structural and heating conditions. The prediction to estimate the improved ultimate temperature of hatted frames is also proposed herein.

Chapter 5

Conclusions

5. Conclusions

Based on the results presented throughout this study the following conclusions can be drawn:

In chapter 2, the stabilities and behaviors of the steel structure after the column buckles are extensively investigated. To examine the behavior of the steel subjected to fire, the numerical method, which can analyze the structure in both stable state and unstable state, are developed in this study. Due to the fact that when the structure subjected to fire loses its stability, the static equilibrium solution does not exist, the analysis cannot be continued by the increase-in-temperature method (the *load controlled analysis*). In order to solve this problem, the *displacement controlled analysis* is adopted. This displacement analysis is the analysis that one degree-of-freedom of the unstable member's node is gripped, and it is moved in the direction that the unstable state is growing. The displacement analysis is carried out under the temperature that the structure loses its stability. By using the numerical method whereby the control of the analysis is switched between load and displacement methods, we can examine the behavior of the steel column subjected to fire until it overall collapses. By using this analysis method to analyze some examples of a steel structure subjected to fire, the following conclusions can be drawn:

● The main unstable condition of a steel structure subjected to fire is the "*snap-through*" process. This snap-through easily occurs in the structure when the residual resistance is low and the stiffness and the strength of the restraining members in the structure are low. That means that the structure's ability to remain stable while the surrounding members restrain the buckling column is intimately connected with the instabilities of the structure itself.

● The collapse of the structure is not decided solely by the buckling of the heated column. The ultimate temperature of the structure's collapse mode varies according to the stress redistribution ability of the surrounding members. If the stress redistribution ability of the surrounding members is low, the structure loses its stability and collapses suddenly after the column buckles. In this case, the ultimate temperature of this kind of structure is lower than the column buckling temperature (due to thermal stress). However, if the stress redistribution ability of the surrounding members is high, the structure still keeps its stability even though the column buckles. The ultimate temperature of this kind of structure is more than

the column buckling temperature.

In chapter 3, the buckling temperature of the column subjected to fire is extensively investigated. The following conclusions can be drawn:

● The rotationally restraining effect of the connecting members has an effect on the column's buckling temperature. However, the thermal expansion of the beams does not have a direct affect on the buckling temperature.

● The exterior column is not axially restrained by the adjacent members during the fire. The lower end of the heated column is rotationally restrained by the unheated connecting members, so its boundary condition can be assumed to be fixed end. On the other hand, for the upper end of the heated column's case, the rotationally restraining effect of the upper-story unheated column can be neglected due to the thermal expansion of the beam. The buckling temperature of the exterior column can be assumed to be the theoretical buckling temperature when the effective length is determined from the proposed equation.

● The interior column is strongly rotationally restrained by the adjacent members, so its effective length is equal to $0.5h$. However, it is also axially restrained by the adjacent members. As a result, it buckles at a temperature that is lower than the estimated buckling temperature. In this case, when considering the buckling temperature, the thermal effect should be included.

The axially restrainting effects of the surrounding members are described in chapter 4. Moreover, in this chapter, the way to estimate the ultimate temperature of steel frame subjected to fire is also proposed. The following conclusions can be drawn:

● The effects of the axially restraining members have two mechanical roles. The first role is to restrain an expanded heated column. As a result of this action, the thermal compressive force is added to the heated column. This causes a drop in buckling temperature of heated columns. On the contrary, the second role is to redistribute a part of the compressive force of the buckled column to other sound columns. As a result of this action, the structure can retain its stability after the column buckles. It causes a rise of the ultimate temperature of a frame. However, if the second stress redistribution ability is not enough, it falls into instability immediately after the heated column buckles. The ultimate temperature for this frame is lower than the theoretical buckling temperature, since the buckling is affected by the first thermal effect.

● Based on the above observation, it is found that a higher ultimate temperature of a frame is obtained if it has higher stress redistribution capacity. A way to improve the fire-resistance capacity of a frame is to install a suitably proportioned hat truss. A hatted frame is found to have definitely an improved redundancy.

● Closed form formulae to predict both the buckling temperature of a heated column and the beam plastified temperature of a frame is presented herein. Conducting the numerical fire response analysis, the predicted temperatures are found to be in good agreement with the numerical results for various structural and heating conditions. The prediction to estimate the improved ultimate temperature of hatted frames is also proposed herein.

REFERENCES

AIJ (1999), "Recommendation for resistant design of steel structures." *Architectural Institute of Japan*. (in Japanese)

Aasen, B. (1985) "An experimental study on steel columns behaviour at elevated temperatures" Res. Tep., Div. of Steel Struct., Norwegien Inst. Of Technol., Univ. of Trondheim, Norway.

Bailey, C.G (2000) "The influence of the thermal expansion of beams on the structural behaviour of columns in steel-framed structures during a fire." *Engineering Structures*, No. 22 (7), July.

Barthelemy, B. (1976) "Heating Calculation of structural steel members." *Journal of the Structural Division,* Vol. 102, No. 8, August, 1549-1558.

Bathe, K.J., Ramm E., and Wilson E.L. (1975) "Finite element formulations for large deformation dynamic analysis" *International Journal for Numerical Methods in Engineering*, Vol.9, 353-386.

Bazant, Z.P., and Zhou, Y. (2002) "Why did the world trade center collapse? Simple analysis." *Journal of Engineering Mechanics*, ASCE, Vol.128 (1), 1-6.

Burgess, I.W., Olawale, A.O., and Plank, R.J. (1992) "Failure of steel columns in fire" *Fire Safety Journal*, No.18 (2), 183-201.

Cheat, E. K. (1984) "Stress analysis of steel frame structures with non-rigid connections subjected to thermal gradient." *Trans. of A.I.J*, No. 346, December.

Cheng, W.C., and Mark, C. K. (1975) "Computer analysis of steel frame in fire." *Journal of the Structural Division*, ASCE, Vol. 101, No. ST4, April, 855-867.

Correia Rodrigues J.P., Neves, I.C., and Valente J.C. (2000) "Experimental reseach on the critical temperature of compressed steel elements with restrained thermal elongation." *Fire Safety Journal*, No.35 (2), 77-98.

Culver, C., Aggarwal, V., and Ossenbruggen, P. (1973) "Bucking of steel columns at elevated temperatures." *Journal of the Structural Division*, ASCE, Vol. 99, No. St4, April.

Culver, C., Aggarwal, V., and Ossenbruggen, P. (1973) "Steel column failure under thermal gradients." *Journal of the Structural Division*, ASCE, Vol. 99, No. St4, April.

Federal Emergency Management Agency (FEMA) (2002): World Trade Center Building Performance Study: Data Collection, Preliminary Observations

and Recommendations. Technical Report FEMA 403, Washington, DC, May.

Franssen J.M. (2000) “Failure temperature of a system comprising a restrained column submitted to fire.” *Fire Safety Journal*, No.34 (2), 191-207.

Franssen, J.M., Cooke, G.M.E., and Latham, D.J. (1995) “Numerical simulation of a full scale fire test on a loaded steel framework.” *Journal of Constructional Steel Research*, Vol.35 (3), 377-408.

Franssen, J.M., Schleich, J.B, Cojot, L.G., and Azpiazu, W. (1996) “A simple model for the fire resistance of axially-loaded members – Comparison with experimental results.” *Journal of Constructional Steel Research*, Vol.37 (3), 175-204.

Franssen, J.M., Schleich, J.B., and Cojot, L.G. (1995) “A simple model for the fire resistance of axially-loaded members according to Eurocode 3.” *Journal of Constructional Steel Research*, Vol.35 (1), 49-69.

Franssen, J.M., Talamona, D., Kruppa, J., and Cajot, L.G. (1998) “Stability of steel columns in case of fire: experimental evaluation.” *Journal of Structural Engineering*, Vol. 124, No. 2, February, 158-163.

Furumura, H., and Shinahara, Y. (1981) “Inelastic behavior of protected beams and frames in fire.” *Trans. of A.I.J.*, No. 300, February.

Furumura, R., Ave, T., Okabe, T., and Kim, W. J. (1986) “A uniaxial stress-strain formula of structure steel at high temperature and its application to thermal deformation analysis of steel frames” *Trans. of A.I.J*, Vol. 363, May, 110-117. (in Japanese)

Furumura, R., Migita, K., Ave, T., Okabe, T., and Kim, W. J. (1986) “Elasto-plastic creep thermal deformations behavior of plastic designed steel frames”, Trans. of A.I.J., No 368, October. (in Japanese)

Katoh, B., Akiyama, H., Inoue, K. (1975) “The post-buckling behavior of the compressive short steel column.” *Trans. of A.I.J.*, No. 229, March, 67-76. (in Japanese)

Kruppa, J. (1979) “Collapse temperature of steel structures.” *Journal of the Structural Division,* Vol. 105, No. 9, September, 1769-1788.

Kubota, H., and Wada, A. (1989) “Dynamic analysis method for the collapse problem.” *Journal of Structural and Construction Engineering*, No. 403, August, 97-103. (in Japanese)

Motegi, T., Yusa, S., Nishida, I., Okamura, Y., and Nakayama I. (2000) “Experimental study on buckling loads of steel columns under elevated temperature in Large Scale.” *Journal of Structural and Construction*

Engineering, No. 538, December, 187-194. (in Japanese)

Neves, C.I. (1995) "The critical temperature of steel columns with restrained thermal." *Fire Safety Journal*, No.24 (3), 211-227.

Paris, P.C. (1954) "Limit design of columns." *Journal of the Aeronautical sciences*, Vol. 21, January, 49.

Poh, K.W., and Bennetts, I.D. (1995) "Analysis of structural members under elevated temperature conditions." *Journal of Structural Engineering*, Vol. 121, No. 4, April, 664-675.

Poh, K.W., and Bennetts, I.D. (1995) "Behavior of steel columns at elevated temperatures." *Journal of Structural Engineering*, Vol. 121, No. 4, April, 676-684.

Seigel, L.G. (1974) "Performance requirements for fireproofing materials." *Journal of the Engineering Mechanics Division,* Vol. 100, No. 3, May/June, 489-495.

Stanzak, W.W., and Lie, T.T. (1973) "Fire resistance of unprotected steel columns." *Journal of the Structural Division,* Vol. 99, No. 5, May, 837-852.

Suzuki H., and Nakagawa, H. (1999) "Ultimate temperatures of steel beams subjected to fire." *Journal of steel construction*, Vol. 6(22), June, 118-126. (In Japanese)

Suzuki, H. (1995) "Ultimate temperatures of steel frames subject to fire." *Journal of Structural and Construction Engineering*, No. 477, November, 147-156. (in Japanese)

Suzuki, H., Iwai, A. (1993) "Evaluation of the ultimate behavior of steel wide-flange beam-columns" Journal of structural engineering, Vol.39B, March, 539-349. (in Japanese)

Suzuki, H., Kondo, A., Ishida, Y. (1992) "Ultimate temperature of steel frames subject to fire part II study on the effect of creep strain." *Summaries of Technical Papers of Annual Meeting*, Architectural Institute of Japan, Vol.A-2, August, 1371-1372. (in Japanese)

Suzuki, H., Maeda, K. (1988) "Analysis of the post-buckling behavior of steel columns." *Journal of Structural and Construction Engineering*, No. 387, May, 61-70. (in Japanese)

Tada, M., and Suito, A. (1993) "Dynamic analysis for buckling behavior of skeleton structures including Truss Members." *Journal of Structural and Construction Engineering*, No. 446, April, 51-56. (in Japanese)

Talamona, D., Franssen, J.M., Schleich, J.B., and Kruppa, J. (1997) "Stability of steel columns in case of fire: numerical modeling." *Journal of Structural*

Engineering, Vol. 123, No. 6, June, 713-719.

Usmani, A.S., Chung, Y.C., Torero J.L. “How did the WTC towers collapse: a new theory.” *Fire Safety Journal*, No. 38 (6), 501-533.

Wang, Y.C., Moore, D.B. (1994) “Effect of thermal restraint on column behaviour in frame.” *4th International Symposium on Fire Safety Science*, Ottawa, IAFSS, Kashiwagi T, editor, 1055—1066.

Wang, Y.C., Moore, D.B. (1994) “The effect of frame continuity on the critical temperature of steel columns.” Third Kenrensky Conference on Flobal Trends in Structural Engineering, Singapore, 681-686.

Washizu, K. (1975) “Variational methods in elasticity and plasticity”, Oxford, Pergamon Press.

LIST OF PUBLICATIONS

A-REFEREED PAPER

[1] Suzuki, H., Ruangtananurak, N., and Fujita, H (2002) “Stabilities of steel frames subjected to fire” *Journal of Structural and Construction Engineering*, No. 571, September, 161-168. (in Japanese)

B-PRESENTATION PAPERS

[1] Ruangtananurak, N., and Suzuki, H. (1999) “Frame buckling temperature with sideways” *Summaries of Technical Papers of Annual Meeting Architectural Institute of Japan*, Vol. A-2, 35-36. (in Japanese)

[2] Ruangtananurak, N., Fujita, H., and Suzuki, H. (2000) “Analysis of unstable behaviors of steel frames subject to fire” *Summaries of Technical Papers of Annual Meeting Architectural Institute of Japan*, Vol. A-2, 63-66. (in Japanese)

[3] Ozaki, F., Ruangtananurak, N., and Suzuki, H. (2002) “Buckling temperatures of the perimeter columns” *Summaries of Technical Papers of Annual Meeting Architectural Institute of Japan*, Vol. A-2, 39-40. (in Japanese)

[4] Ruangtananurak, N., Ozaki, F., and Suzuki, H. (2002) “Buckling temperatures of steel frames without lateral sway” *Summaries of Technical Papers of Annual Meeting Architectural Institute of Japan*, Vol. A-2, 41-42. (in Japanese)

[5] Fujita, H., Ruangtananurak, N., Koi, T., and Suzuki, H.(2002) “Stability of heated steel frames and improvement of their fire resistances” *Summaries of Technical Papers of Annual Meeting Architectural Institute of Japan*, Vol. A-2, 79-82. (in Japanese)

[6] Kijima, M., Ruangtananurak, N., and Suzuki, H. (2003) “Buckling temperature of steel columns and ultimate temperature of steel frames-theory” *Summaries of Technical Papers of Annual Meeting Architectural Institute of Japan*, Vol. A-2, 279-280. (in Japanese)

[7] Ruangtananurak, N., Kijima, M., and Suzuki, H. (2003) “Buckling temperature of steel columns and ultimate temperature of steel frames-analysis” *Summaries of Technical Papers of Annual Meeting Architectural Institute of Japan*, Vol. A-2, 281-282. (in Japanese)

Acknowledgements

The author of this dissertation would like to express deep and sincere gratitude to his academic advisor Professor Dr. Hiroyuki Suzuki of Institute of Engineering Mechanics and Systems, University of Tsukuba, for his wise guidance, suggestions, kind support and continuous encouragement to make this research well achieved.

Deep appreciation also goes to the committees of this thesis, Professor Dr. Hiroshi Imai, Professor Dr. Tetsuro Inoue, Associate Professor Dr. Yuuki Sakai, and Associate Professor Dr. Daigoro Isobe of Institute of Engineering Mechanics and Systems, University of Tsukuba, for their guidance, review, suggestions, kindness, valuable time and comments through the course of this investigation.

During the whole period of this study, the author certainly learned so much and got invaluable help from the members of the Suzuki laboratory family of his generation. For their kind cooperation and undocumented help, he would like to warmly thank all of them. In particular, he would like to extend his warm and sincere thanks to Dr. Hirofumi Nakagawa and Dr. Fuminobu Ozaki for various assistances including their advice about living and studying in Japan.

In addition, the author would like to extend his sincere thanks to the Ministry of Education, Culture, Sports, Science and Technology of Japan for financing the author's doctoral studies and giving him an exceptional opportunity to learn more about the people, culture and traditions of this country. To all the teachers at the International Student Center, University of Tsukuba, it is because of them the author has learnt a lot in many ways. A special note of thanks goes to them.

The author also wishes to thank all Thai students in Tsukuba and Japanese friends, for warmth, support, and encouragement. Their always being there makes life a lot more meaningful. It is also important to note that many people have helped the author, one way or the other, in writing this thesis. He takes this opportunity to thank them all.

Last but not the least, the most cordial appreciation is expressed to the author's beloved parents and family for their love and continual encouragement which have helped him to get through all difficulties and have made this research possible. This thesis is dedicated for all members of his family.

March 2004

Ruangtananurak Nara